New roles for cripto in the assembly and localisation of nodal signalling platforms

BLANCHET, Marie-Hélène

Abstract

The TGFβ family member Nodal is essential during development to allocate pluripotent cells to distinct germ layers and to establish the basic body plan. To establish a signaling gradient of the transcription factors Smad2 and Smad3, Nodal forms a complex with Activin receptors that is activated with the help of the glycosylphosphosphatidyl-inositol-anchored proteoglycans Cripto or Cryptic. To elucidate the underlying mechanism, we investigated whether Cripto regulates the proteolytic maturation and/or trafficking of Nodal precursor protein. We show that Cripto captures Nodal already during secretion, partly via the propeptide, and assembles a processing complex with the proprotein convertases Furin at the cell surface. Subsequently, Cripto mediates uptake of mature Nodal via a conclathrin, noncaveolar pathway to signaling endosomes. Our results suggest that Cripto is a receptor for proprotein convertases and couples Nodal processing and signaling in target cells.

UNIVERSITÉ DE GENÈVE

UNIVERSITE DE GENEVE   FACULTE DES SCIENCES

Section de chimie   Prof. D. Constam
Département de biochimie   Prof. J. Gruenberg

New Roles for Cripto in the Assembly and Localisation of Nodal Signalling Platforms

THESE

présentée à la Faculté des sciences de l'Université de Genève
pour obtenir le grade de Docteur ès sciences, mention interdisciplinaire

par
Marie-Hélène Blanchet
de
Cully (VD)

Thèse N° 3951

*Doctorat ès sciences
mention interdisciplinaire*

Thèse de *Madame Marie-Hélène BLANCHET*

intitulée :

" New Roles for Cripto in the Assembly and Localisation of Nodal Signalling Platforms "

La Faculté des sciences, sur le préavis de Messieurs D. CONSTAM, professeur et directeur de thèse (Ecole Polytechnique Fédérale de Lausanne – Faculté des Sciences de la vie - Institut Suisse de la Recherche Expérimentale sur le Cancer – Epalinges, Suisse), J. GRUENBERG, professeur ordinaire et co-directeur de thèse (Département de biochimie), Madame A. GRAPIN-BOTTON, professeur (Ecole Polytechnique Fédérale de Lausanne – Faculté des Sciences de la vie - Institut Suisse de la Recherche Expérimentale sur le Cancer – Epalinges, Suisse), Messieurs P. GÖNCZY, professeur (Ecole Polytechnique Fédérale de Lausanne – Faculté des Sciences de la vie - Institut Suisse de la Recherche Expérimentale sur le Cancer – Epalinges, Suisse), H. RIEZMAN, professeur ordinaire (Département de biochimie), et M. GONZALEZ-GAITAN, professeur ordinaire (Département de biochimie), autorise l'impression de la présente thèse, sans exprimer d'opinion sur les propositions qui y sont énoncées.

Genève, le 4 février 2008

Thèse - 3951 -

Le Doyen, Jean-Marc TRISCONE

2

REMERCIEMENTS

J'aimerais tout d'abord remercier le Prof. D. Constam de m'avoir donné l'opportunité de faire mon doctorat dans son laboratoire, pour les intéressantes discussions et pour sa confiance ainsi que son enthousiasme.

J'aimerais ensuite remercier le Prof. J. Gruenberg d'avoir accepté de codiriger cette thèse et d'avoir été disponible et engagé à maintes reprises tout au long de ces années.

J'aimerais remercier le Prof. P Gönzcy d'avoir accepté de faire partie de mon jury de demi-thèse ainsi que celui de ma thèse.

J'aimerais remercier le Prof. A. Grapin-Botton pour sa précieuse aide et son soutien durant ces quatre années de thèse.

J'aimerais remercier le Prof. M. Gonzalez-Gaìtan de m'avoir acceptée dans son cours EMBO sur l'endocytose à Dresden. Ce fut deux semaines intensives mais décisives pour la suite de mon travail.

J'aimerais remercier le Prof. H. Riezman d'avoir accepté de présider ma défence de thèse.

J'aimerais aussi remercier mes parents, et tout spécialement mon père, de m'avoir encouragée à suivre cette voie qui sera à jamais porteuse.

Finalement, j'aimerais remercier mon compagnon de vie et ami pour la douceur qu'il a su glisser dans ma vie les jours où les cieux étaient moins bleus.

Table of content

1 RESUME

1.1 Introduction

1.1.1 Nodal est une protéine clef dans l'embryogenèse précoce

Durant l'embryogenèse chez la souris, plusieurs étapes cruciales ont lieu pour façonner l'embryon et créer des lignées de tissus spécifiques. Après fertilisation, le zygote murin (cellule primordiale) se divise jusqu'au stade du blastocyste (environ 32 cellules). A ce stade, cet amas de cellules se compose de cellules et d'une cavité au centre. Adjacente à cette cavité, se loge la masse cellulaire interne (MCI) qui donne l'embryon proprement dit. Durant les prochaines divisions, l'expression de certains gènes se met en place pour définir les différents territoires de l'embryon. L'embryon se compose à la fin de la gastrulation d'un axe antéro-postérieur (axe A/P). L'axe A/P constitue la première marque morphologique de l'embryon. Suite à cette première ébauche architecturale, les lignées primordiales de cellules sont établies: l'endoderme, le mésoderme et l'ectoderme. Ces trois lignées façonnent l'embryon. Tandis que les tissus extra-embryonnaires permettent une attache ainsi que des échanges nutritifs avec la mère.

Tout au long de l'embryogenèse une connexion étroite entre les tissus embryonnaires et extra-embryonnaires a lieu. Nous nous focaliserons ici sur les mécanismes de la partie embryonnaire. Une protéine est essentielle durant les stades précoces de l'embryogenèse: Nodal. Nodal fait partie de la super-famille des ligands nommés 'Transforming growth factors-β' (TGF-β) qui comporte trois familles principales : celle des 'bone morphogenic factor' (BMP), le sous-groupe des TGF-β *per se* et le groupe de l'Activin/Inhibin. La structure de Nodal étant très différente des autres membres de cette super-famille, on classe Nodal dans une quatrième catégorie à part entière.

La voie de signalisation de Nodal est régulée par deux types de récepteurs à l'Activin : le récepteur de type I et celui de type II. L'activation du récepteur de type I par le récepteur de type II induit la phosphorylation d'effecteurs cytoplasmiques nommés Smad2 et Smad3. L'hétérodimère Smad2/4 ou Smad3/4 est ensuite transporté dans le noyau et induit la

régulation, positive ou négative, de différents gènes. Une inhibition peut de plus avoir lieu soit au niveau de l'activation du récepteur, soit de l'activité de l'hétérodimère. Cette régulation supplémentaire est effectuée par un inhibiteur appelé Smad7 au niveau du récepteur et Smad6 au niveau de l'inactivation de l'hétérodimère.

1.1.2 Nodal a besoin d'être clivé et requiert la présence d'un corécepteur pour envoyer un signal le long de la voie Smad2/3

Nodal est une protéine constituée d'un pro-domaine en N-terminal et d'un domaine mature en C-terminal. Un site de clivage ([RK]-X-X-[RK]) sépare ces deux domaines et permet à Nodal d'être pleinement actif le long de la voie de transduction Smad2/3. Les protéines qui coupent Nodal se nomment 'subtilisin-like proprotein convertases' (SPCs). Deux d'entre elles semblent jouer un rôle décisif pour l'activité de Nodal durant l'embryogenèse: Furin (ou SPC1) et Pace4 (ou SPC4). Etonnamment, il a été démontré que Nodal et ses convertases ne sont pas exprimées dans le même compartiment embryonnaire. Nodal est exprimé dans la partie embryonnaire tandis que ses convertases sont exprimées dans la partie extra-embryonnaire. Nodal est cependant actif dans le compartiment où il est exprimé. Ce constat impose donc que se sont les convertases qui migrent dans le compartiment embryonnaire où Nodal se trouve et sera par la suite activé. Nodal est libérée sous forme de dimère dans le milieu extracellulaire. Mais la façon dont Nodal et les protéines qui le coupe se rencontrent est encore hypothétique.

Par ailleurs, Nodal a besoin d'un corécepteur, Cripto, pour intensifier un signal relayé par les Smads. Des homologues de Cripto ont été trouvés dans différentes espèces dont le zebrafish et le xénope. Cripto fait partie de la famille des 'epidermal growth factor - Cripto1/FRL1/Cryptic' (EGF-CFC) protéines. Le CFC domaine est riche en cystéines. Le domaine C-terminal de cette protéine est composé d'un site d'ancrage aux membranes. Cette amarre se nomme 'glycosylphosphatidylinositol (GPI) anchor'. Par son ancrage à la membrane ce type de protéine accède à certains types de microdomaines présents sur la membrane cellulaire. Il a en effet été montré que les protéines ayant ce site d'amarrage sont capables d'accéder à des domaines riches en cholestérol et glycosphingolipides. Par la composition élevée en lipides saturés, ces domaines sont résistants à certains types de détergents (ex. Triton X-100). Sur la base de cette propriété, une technique de fractionnement

cellulaire a été mise au point. Cette technique permet de séparer les domaines constitués essentiellement de ces lipides, nommés 'rafts' ou radeaux, et les domaines pauvres en lipides.

1.1.3 Différentes voies d'internalisation permettent l'induction d'un signal

Pour envoyer un signal dans la cellule, non seulement certaines protéines doivent se situer dans des tissus particuliers, mais aussi certaines protéines doivent être internalisées par des domaines membranaires spécifiques et compétents pour l'induction de leur type de signal. La voie de signalisation utilisée par le sous-groupe des TGFβs est marquée par la présence de Clathrin sur ces organelles. La Clathrin crée un manteau en forme de nid d'abeille autour de la vésicule qui la rend facilement reconnaissable par microscopie électronique. Ces organelles entourées de Clathrin se nomment 'clathrin coated vesicles (CCV)'. Ce compartiment est connu pour sa capacité à induire un signal depuis ses vésicules. Au fil du temps, ces organelles vont se modifier et changer leurs caractéristiques allant de l'induction d'un signal à la dégradation. Dans cette voie d'endocytose, différents marqueurs permettent de visualiser les étapes de maturation vésiculaire à l'intérieur de la cellule. Ces marqueurs sont appelés les Rabs. Ces petites GTPases sont liés au côté cytoplasmique des membranes. Dans la progression de l'internalisation protéique, Rab5 est le premier marqueur. Rab5 se trouve à la membrane plasmique ainsi que sur les endosomes précoces. Par la suite, Rab4 marque le compartiment endosomal qui trie et recycle les protéines. Les protéines qui ne sont pas recyclées et renvoyées à la membrane plasmique progresseront dans les endosomes tardifs marqués par Rab7 pour finir le chemin dans les lysosomes où elles seront dégradées.

Lorsque les récepteurs des TGF-β sont destinés d'office à être dégradé par la cellule cible (sans même y produire un signal), les récepteurs suivent une autre voie. Cette internalisation membranaire est dotée de vésicules marquées par la Caveolin. Cette protéine forme un crochet dans la couche cytoplasmique de la membrane plasmique et permet à la membrane de s'invaginer formant par la suite une vésicule nommée caveolae. Une troisième voie de signalisation est caractérisée par son indépendance à la Clathrin et à la Caveolin. Cette voie est la moins connue et encore mal caractérisée. Elle semble contenir plusieurs sous-types d'internalisation définis par la présence de certains effecteurs. Cdc42 et Arf6 sont deux marqueurs qui définissent des compartiments riches en protéines comprenant un ancrage GPI. Cette voie se nomme 'GPI-APs enriched endosomal compartment' (GEECs) dans le cas de

Cdc42. Arf6 défini un nouveau compartiment tubulaire permettant aux protéines qui s'y trouvent d'être recyclée à la membrane plasmique. La formation de ces deux types de vésicules est dépendante de la Dynamin tandis que d'autre comme, la voie des GTPases Rho (une autre sous catégorie de vésicules Clathrin et Caveolin négative), ne l'est pas. De par leur récente découverte, ces types d'internalisation sont encore mal définis. Par ailleurs, les voies de signalisation qui ont été caractérisées jusqu'à présent semblaient ne pas être interconnectées. Il se trouve que récemment une connexion entre les caveolae et les endosomes précoces a été établie. Cette découverte suggère que le système d'internalisation est plus complexe que la vision linéaire émise au départ.

1.2 Résultats

Nodal est une protéine d'intérêt non seulement pour son rôle déterminant dans l'embryogenèse, mais aussi pour ses particularités biochimiques. La production d'un signal dépendant de Nodal semble être étroitement régulée. En effet, cette protéine semble être très instable une fois qu'elle est clivée et le processus de dégradation semble être très rapide. Le temps de demi-vie de la protéine active semble donc être très court. Lors de ce travail de doctorat, nous avons porté un accent particulier aux types de modifications présentes sur le précurseur de Nodal, à la localisation intracellulaire de la protéine et au rôle de son corécepteur Cripto.

NB : Pour des raisons encore peu claires, il est difficile d'exprimer la protéine Nodal dans des cellules. Nous travaillons essentiellement avec deux types de cellules capables d'exprimer Nodal : les cellules 293T et Cos1. Les cellules humaines 293T sont riches en SPCs. Tandis que les cellules de singe Cos1 sont fortement dépourvues de SPCs. Les cellules Cos1 sont plus grandes et nous permettent de mieux voir où se trouve notre protéine.

1.2.1   Nodal est une glycoprotéine qui ne passe pas par le Trans Golgi pour arriver à la membrane plasmique

Nodal est une glycoprotéine. Une glycoprotéine est synthétisée dans le reticulum endoplasmique (ER), puis acquière des modifications le long de son parcours depuis le ER

jusqu'au Trans Golgi. Chaque étape apporte des modifications spécifiques aux chaînes glycosylées. Nous nous sommes intéressés de prime abord à la nature de ses hydrates de carbone. Nous nous sommes aperçus que dans des extraits du milieu de conditionnement ou dans le lysat cellulaire, Nodal n'avait pas acquis les modifications terminales du Tans Golgi. Après traitement avec l'endoglysolidase-H et la N-glycosilase-F, la taille détectée de Nodal était en effet de plus petit poids moléculaire. Ces enzymes ont le même effet sur Cripto. Lorsque la localisation de Nodal et Cripto est examinée par immuno-fluorescence dans des cellules Cos1, Nodal et Cripto sont fortement localisés dans le ER. Cette localisation peu commune pourrait être due au fait que la surexpression de nos protéines crée une surcharge du système de production protéique et sature le ER. Cependant le fait que même les protéines secrétées sont sensibles à la N-glycosilase-F et la endoglysolidaseH semble indiquer qu'un autre mode de sécrétion est probable pour Nodal et Cripto.

Nous avons donc analysé nos données sous un autre angle. La brefeldin A (BFA) fusionne le ER avec l'appareil du Cis Golgi. Cette substance désorganise la topologie du Golgi et sa fonction. Le Cis et leTrans Golgi sont physiquement déconnectés. La BFA empêche donc les protéines d'acquérir leurs sucres terminaux dans le Trans Golgi. Nous avons analysé si Cripto et Nodal changent leur localisation membranaire en présence ou absence de cette drogue. La BFA n'a aucun effet sur la localisation de Cripto et de Nodal. Cripto est toujours présent à la membrane plasmique même après traitement à la BFA. Ceci est aussi le cas de Nodal.

Pour tester l'efficacité de cette drogue, nous avons utilisé un mutant de Cripto auquel il manque l'ancrage GPI en C-terminal. Ce mutant n'est donc pas attaché aux membranes et est fortement secrété dans le milieu extra-cellulaire. En présence de cette drogue, CriptoΔGPI n'est plus détecté à la membrane plasmique. Il semble donc que cette mutation affecte le transport non-conventionnel de Cripto à la surface cellulaire. L'attache membranaire GPI permet soit l'ancrage de Cripto dans des domaines membranaires spécifiques qui ne transitent pas par le Golgi ou la liaison à une ou d'autres molécules qui permettent à Cripto de dévier sa route en excluant un passage, normalement obligé pour les protéines sécrétées, par le Golgi. De plus, comme Nodal et Cripto semblent être affectés de la même manière par ce traitement, il est tentant de suggérer que leur sécrétion se fait ensemble et que le rôle de Cripto est de localiser Nodal dans des domaines spécifiques bien avant son apparition à la membrane plasmique. Nous avons donc testé si Nodal se localise à la membrane plasmique de la même

manière en présence et absence de Cripto. Cripto n'a aucun effet sur la présence de Nodal à la membrane plasmique. Il semble donc que la sécrétion de Nodal est indépendante de Cripto.

Exactement comment Nodal atteint la surface cellulaire n'est cependant pas encore résolu. Nodal est sécrété sous forme de précurseur. Nodal se compose d'un prodomaine de 27kD tandis que le domaine mature de Nodal ne fait que 12kD. Vu la taille du prodomaine, on pourrait s'attendre à ce qu'il ait un rôle dans la sécrétion. Cependant, le prodomaine semble différent dans son mode de sécrétion tandis que le domaine mature de Nodal a des propriétés similaires au précurseur. Il se pourrait donc que le domaine mature de Nodal soit responsable de sa sécrétion non-conventionnelle.

1.2.2 Cripto permet à Nodal d'accéder à des domaines membranaires propices pour l'activation du ligand

Le rôle de Cripto en tant que corécepteur n'étant pas encore clairement défini, nous nous sommes ensuite intéressé à l'interaction entre Nodal et son corécepteur Cripto. En effet, le fait que Nodal requière Cripto pour transmettre un signal le long de la voie des Smad est déjà un fait établi. Par contre, la nature de l'interaction entre Nodal et Cripto et le mécanisme sont encore à définir. Nodal est formé d'une partie N-terminale étant le prodomaine et d'une partie C-terminale étant le domaine mature capable d'induire un signal en présence de Cripto. Après co-immunoprécipitation, nous avons pu observer que toutes les formes de Nodal sont capables de se lier à Cripto. Cette expérience suggère que déjà avant son clivage, Nodal peut se lier à son corécepteur Cripto. Cette expérience nous laisse supposer que Cripto ne joue pas un rôle seulement dans l'activité de Nodal.

Nous avons donc regardé quelle était l'influence de Cripto sur Nodal dans sa localisation à la membrane plasmique. En présence de Cripto, seule la forme de Nodal résistante au clivage est alors stabilisée à la surface cellulaire. Ceci suggère que non seulement Cripto est requis pour la stabilisation de Nodal à la membrane plasmique mais que dès que la protéine est clivée, Nodal est balayé de la surface cellulaire. Ces résultats sont en accord avec nos anciennes données sur la stabilité du domaine mature de Nodal. Il serait donc plausible que Cripto présente Nodal aux protéases permettant la maturation de Nodal ainsi que l'induction de son signal. Une relation entre Cripto et les convertases clivant Nodal n'a à ce jour pas été établie. Utilisant la technique d'immuno-précipitation, nous avons pu identifier la présence d'une

liaison entre Cripto et Furin ainsi qu'entre Cripto et Pace4. Cette liaison suggère que Cripto non seulement présente Nodal a la surface cellulaire mais que Cripto sert aussi d'amarrage aux enzymes permettant la maturation et l'activité de Nodal. Il est donc possible que le corécepteur Cripto facilite l'interaction entre Nodal et ses convertases.

Nous nous sommes ensuite penchés sur la formation du complexe entre le ligand, le corécepteur et les protéases. Le fait que Nodal et les enzymes qui le coupent ne soient pas exprimés dans le même compartiment embryonnaire suggère que Nodal rencontre ses convertases après leur libération dans le milieu extracellulaire. Pour mieux s'accorder au modèle embryonnaire, nous avons procéder à un mélange de cellules contenant les protéases et d'autres pourvues du ligand, du corécepteur et les facteurs de transcription. Le même degré d'activation est produit lorsque les protéases rencontrent Nodal dans la même population cellulaire ou dans des cellules différentes. Le fait que Nodal ne rencontre ses protéines activatrices qu'une fois arrivé à la membrane cellulaire ne semble donc avoir aucun effet sur son niveau d'activation. Nous nous sommes intéressés en détail à la détection d'un complexe ligand/corécepteur/protéase. Après fixation des liaisons protéiques à la surface cellulaire, nous avons identifié le complexe formé par le précurseur de Nodal, Furin et Cripto à la surface cellulaire. Cripto semble donc jouer un rôle de pilier d'activation pour son ligand Nodal. Cependant, le lieu de cette activation n'est pas encore défini.

Nous nous sommes ensuite intéressés au compartiment de signalisation de Nodal. Plus précisément, dans quels domaines membranaires Cripto pourrait induire la formation d'un complexe avec ses protéases et ses récepteurs. La technique de fractionnement cellulaire permet d'identifier des domaines riches et pauvres en lipides. Après fractionnement de lysat cellulaire, Nodal était détecté dans la fraction riche en lipides uniquement en présence de Cripto. Nous avons donc continué à caractériser ces domaines en utilisant différents types de marqueurs d'endocytose. Récemment, une nouvelle voie d'endocytose a été identifiée. Elle est caractérisée par une composition lipidique élevée comme les 'rafts', un mouvement rapide de ses vésicules et la présence de Flotillin1. La Flotillin est aussi une protéine induisant une invagination membranaire comme la Caveolin. Pour ce faire, nous avons procédé à l'adjonction d'anticorps correspondant à notre protéine d'intérêt pendant 5min ou 10min dans le milieu de culture cellulaire à 37°C. Cette méthode nommée 'uptake experiment' en anglais est couramment utilisée dans le domaine de l'endocytose. Alors que la colocalisation entre la

Caveolin et Nodal est faible et peu affectée par la présence ou l'absence de Cripto, Nodal est fortement colocalisé avec la Flotillin en présence de Cripto. Cette colocalisation s'accentue entre 5 et 10 min d'internalisation pour atteindre ~30%. Etant donné la localisation de Nodal dans les 'rafts' en présence de Cripto, nous avons supposé que ces domaines pourraient avoir un rôle dans la signalisation de Nodal.

La Flotillin, tout comme la Caveolin, sont des protéines qui peuvent être modifiées. Par exemple, ces deux protéines sont modifiées par un groupement palmitique. Cette modification est une adjonction lipidique à la protéine. Certaines drogues inhibent les étapes nécessaires aux modifications. Dans ce cas présent, le 2 bromo-palmitate (2BP) inhibe la palmitoylation des protéines. Nous avons donc regardé la réaction de Nodal en présence de cette drogue. Premièrement, Nodal n'est plus capable d'induire un signal. De plus, Nodal reste bloqué à la membrane plasmique. En effet, en présence du 2BP, la forme précurseur reste non clivée et s'accumule dans le milieu extracellulaire même en présence des protéases. Ce résultat suggère que ces domaines sont déterminants pour le clivage de Nodal et forment un environnement adéquat au complexe (ligand/corécepteur/protéase) qui permet l'induction de son signal.

1.2.3 Cripto localise Nodal à la membrane périphérique des endosomes

En présence de Cripto, Nodal est capable d'induire fortement un signal grâce au récepteur de type I Alk4. Ce récepteur a besoin de SARA (Smad Anchor Receptor Activator), une protéine qui aide à la localisation et l'activation des effecteurs Smad à proximité du récepteur. Cette protéine est localisée à la membrane plasmique mais n'est active qu'à la surface d'endosomes. Il a déjà été démontré que les TGF-β sont internalisés par la voie dépendante à la Clathrin. De plus, une récente étude a démontré un lien entre les domaines positifs à la Flotillin et la voie classique des endosomes positifs pour Rab5 et Rab4. Notre attention s'est portée sur la présence ou non de Nodal dans les compartiments à des stades d'endocytose plus tardifs. Nous avons cette fois-ci procédé à l'adjonction pendant 40min d'anticorps correspondant à notre protéine d'intérêt. En absence de Cripto, Nodal est internalisé dans des vésicules internes aux endosomes. Ce type d'organelle se nomme un endosome multivésiculaire (ou multivesicular endosome (MVE) en anglais). La fonction de ces structures est déjà bien caractérisée. L'internalisation de protéines est suivie de leur dégradation après maturation de l'organelle en lysosomes. Etonnement, en présence de son corécepteur, Nodal est localisé sur

la membrane externe de l'endosome. Il semble que la présence de Cripto agrandit la taille des vésicules endosomales. Le rôle de Cripto serait donc d'empêcher l'invagination membranaire et donc l'internalisation de Nodal. La protéine Nodal serait donc stabilisée à la surface des endosomes et son signal serait prolongé dans les domaines adéquats à sa transmission. Contrairement à Nodal, l'Activin n'a pas besoin de Cripto pour se lier au recepteur Alk4 et induire un signal dans la voie des Smads. Nous avons donc regardé où était localisé l'Activin en absence de Cripto. Nous avons pu en effet voir que l'Activin est localisé à la périphérie des vésicules Rab4 même en l'absence de Cripto.

Par ailleurs, nous avons examiné certaines mutations chez Cripto et regardé si la localisation de Nodal était toujours sur le bord des vésicules. Nous avons testé des mutations provoquant une perte de fonction de Cripto. Toutes ces mutations ont déjà été testées in vivo et empêchent l'activité de Nodal. En accord avec ces résultats, la localisation de Nodal sur les membranes externes des endosomes était radicalement réduite en présence de ces mutants. En effet, Nodal se retrouvent séquestré à l'intérieur des vésicules en présence de ces différents mutants de Cripto. Pour quantifier l'effet de Cripto sur la localisation de Nodal, la distribution moyenne d'anticorps internalisé fût calculée en mesurant la plus courte distance du centre du marquage intra-vésiculaire jusqu'au pourtour de la vésicule. En moyenne, Cripto réduit la distance de Nodal au pourtour membranaire d'un facteur de 3.2. Après normalisation en tenant compte de la taille de l'endosome, ce facteur s'accentue et devient 4.2.

1.3 Conclusion

Nodal est une protéine essentielle à l'embryogenèse, plus particulièrement à la gastrulation. Pour effectuer un signal relayé par les effecteurs Smad2 et Smad3, Nodal doit s'assembler avec un corécepteur nommé Cripto. Cependant, Nodal est capable de se lier à ses récepteurs de type I et II en absence de Cripto. Notre étude s'est donc portée sur le mode de fonctionnement au niveau moléculaire du corécepteur Cripto. En effet, nos résultats ont démontré que Cripto a un rôle de stabilisation du ligand Nodal à la surface cellulaire, de formation du complexe ligand/corécepteur/récepteur, de localisation du complexe dans les domaines membranaires compétents pour l'induction d'un signal via Smad2. De plus, Cripto

est capable de localiser Nodal sur la membrane externe d'endosome et potentialise ainsi le signal induit par Nodal.

Nous avons pu en effet démontrer que Nodal et Cripto n'étaient pas sécrétés pas la voie conventionnelle ER-Golgi-membrane plasmique, mais que le ligand et le corécepteur cheminent directement du reticulum endoplasmique à la membrane plasmique. Ce type de sécrétion est encore mal connu, mais il semble que d'autres protéines ont la même capacité. Par exemple, le complexe majeur d'histocompatibilité suit une voie phagocytique similaire pour la présentation à la surface cellulaire d'antigène exogène. De plus dans l'adhésion axo-gliale, le complexe GPI-linked F3/Contactin et Caspr/Paranodin est insensible à la brefeldinA. Ce complexe est essentiel à la formation d'une jonction fonctionnelle aux paranodes se trouvant sur les axons. Dans le cas de Nodal, ce raccourci pourrait être possible grâce à une propriété du domaine mature de Nodal.

Nous avons ensuite défini le type de domaine membranaire sur lequel la formation du complexe ligand/corécepteur/protéase à lieu. Cripto semble rediriger Nodal dans des domaines riches en lipides. Nous avons pu identifier ces domaines comme étant des domaines marqués pas la protéine Flotillin. Il semble que ces sites spécifiques permettent le clivage de Nodal et la transmission du signal. En effet, en empêchant les modifications portées par la Flotillin d'avoir lieu, nous avons stabilisé le précurseur même en présence de protéases et anéanti l'activité de Nodal. Ce résultat s'inscrit dans le contexte de l' 'epidermal growth factor' (EGF). EGF est internalisé dans des voies différentes lorsqu'il est en forte ou faible concentration. Il semble donc probable que ce facteur de croissance ne produise pas le même signal suivant les domaines auxquels il est lié.

Nous avons démontré que Cripto et la liaison de Nodal à Cripto permettent la stabilisation du ligand sur la membrane externe des endosomes. Le ligand est maintenu sur la membrane vésiculaire et peut donc perpétuer son signal via la machinerie nécessaire à la production du signal. Il a en effet été démontré que SARA doit se trouver sur la membrane d'endosome pour pouvoir activement présenter Smad2 au récepteur. Par ailleurs, l'Activin est présente sur la membrane externe de ces mêmes vésicules même en absence de Cripto. Cette observation est en accord avec le fait que le signal induit par l'Activin ne nécessite pas Cripto. Cette idée de prolongation du temps de résidence à la périphérie membranaire est directement liée à une étude sur les récepteurs à l'Activin. Cette étude montre que le nombre de récepteurs ainsi que

16

leur temps d'activité à l'intérieur de la cellule détermine la durée du signal émis par le ligand. Et de ce fait, la durée du signal établit la réponse cellulaire ou plus concrètement quels gènes vont être exprimés. Récemment, la réponse au signal donné par Nodal a été expérimentée chez le zebrafish. Cette étude a montré que les cellule-cibles génèrent un signal en fonction de la dose maximale reçue durant une période donnée. La question qui reste maintenant à savoir est comment Cripto stabilise-t-il Nodal sur les membranes des endosomes. Deux hypothèses sont plausibles. Soit Cripto est capable d'interagir avec certaines molécules capables de modifier les propriétés membranaires (ex. invagination de membrane), soit Cripto séquestre Nodal dans des domaines membranaires portant le ligand hors d'atteinte de la machinerie de dégradation.

1.4   Activité de Nodal : un lien entre le développement et le cancer

Le fonctionnement des TGF-βs est complexe. Les TGF-βs sont sécrétés comme précurseur latent. Après clivage, le domaine mature de la protéine produit aussitôt un signal qui doit donc être sévèrement régulé. En effet, il semble qu'à faibles doses, Nodal est capable de contrôler le cycle cellulaire et la maintenance de l'information génétique. Par contre, lorsque l'expression de Nodal est ectopique, Nodal induit une réponse cellulaire aberrante. Il a été récemment démontré qu'une expression de Nodal était corrélée à une augmentation de l'agressivité des mélanomes. Nodal est impliqué non seulement dans le patterning de l'embryon, mais une surexpression menant à une activité anormale induit la formation de métastases. De plus en plus, l'établissement d'une relation entre une prolifération régulée (ex. la formation d'un embryon) et une prolifération incontrôlée (ex. la formation d'une masse cancéreuse) nous permet de mieux comprendre les mécanismes impliqués. En étudiant les voies de signalisation essentielles au développement embryonnaire, nous pourrons ensuite faire la comparaison avec le cancer et peut-être appliquer une thérapie adéquate pour empêcher la prolifération de cellules malignes.

NB : Pour de plus amples détails expérimentaux, illustrations, références et points techniques, veuillez vous référer au texte en anglais.

2 Abbreviation list

AP: adaptor protein
A/P axis: antero-posterior axis
AVE: anterior visceral enodoerm
BFA: brefeldin A
BMP: bone morphogenetic proteins
2BP: 2-bromo-palmitate
CMK: chloromethylcetone
CCV: clatherin coated vesicles (also called: clathrin coated pits)
Dally: Division abnormally delayed
Dly: Dally-like
dpc: days post coitum
DRMs: detergent-resistant membranes
DVE: distal visceral endoderm
ECM: extracellular matrix
EC: ectoplacental cone
ECV: endosomal carrier vesicles
EMT: epithelial-mesenchymal transition
ER: endoplasmic reticulum
ESCRT: endosomal sorting complex required for transport
ExE: extraembryonic ectoderm
GAG: glycosaminoglycan
GEEC: GPI-anchored protein enriched endosomal compartment
GDF: growth and differentiation factors
GDNF: glial-cell-derived neurotrophic factor
GFP: green fluorescent protein
GPI: glycosylphosphatidylinositol
GPI-AP: glycosylphosphatidylinositol-anchored protein
Hh: Hedgehog
HSPG: heparin sulphate proteoglycan
ICM: inner cell mass
LPM: lateral plate mesoderm
LSE: left-side specific enhancer
MVB: multivesiclular body
MVE: multivesicular endosome
P/D axis: proximo-distal axis
PrE: primitive endoderm
PS: primitive streak
SARA: Smad anchor for receptor activation
Smurf: Smad ubiquitination regulatory factor
SPC: subtilisin-like proprotein convertase
TE: trophectoderm
TGF-β: transforming growth factor-β
TGN: Trans Golgi network
Ub: ubiquitin
VE: visceral endoderm
Wg: Wingless

3 SUMMARY

The transforming growth factor (TGF) β family member Nodal plays important roles in embryo patterning and establishment of the body plan during gastrulation. Nodal is secreted as a precursor protein, which is then proteolytically cleaved by members of the subtilisin-like proprotein convertase (SPCs) family (Beck et al., 2002). It has been shown that Nodal can act across several cell diameters and, together with the glycosylphosphatidylinositol (GPI)-anchored protein Cripto, Nodal coordinates multiple cell fate decisions (Xu et al., 1999), (Chen and Schier, 2001).

In *Drosophila*, it has been shown that Dally and Dally-like, two coreceptors for Dpp, are required for Dpp transport (Fujise et al., 2003; Belenkaya et al., 2004). Similar to Dally and Dally-like, Cripto is anchored to the outer leaflet of the plasma membrane via a GPI anchor. With the help of the GPI-anchored Cripto or Cryptic, Nodal forms a complex with Activin receptors that are activated. The aim of this project was to elucidate the cellular mechanisms, which regulate Nodal signalling and trafficking.

Nodal signalling is regulated by the rate of precursor cleavage and rapid turnover of the mature protein (Le Good et al., 2005). Current models in the existing literature suggest that Nodal is recruited by Cripto to the plasma membrane, after cleavage by the SPCs, and that Cripto-binding is necessary to stimulate Nodal receptors. To elucidate the underlying mechanism in more detail, we investigated whether Cripto regulates the proteolytic maturation and/or trafficking of Nodal precursor protein. We show that Cripto captures Nodal already during secretion, partly via the propeptide, and assembles a processing complex with the proprotein convertases Furin at the cell surface. We also studied whether Cripto stabilises Nodal precursor on the plasma membrane and recruits the proproteins convertases to specific membrane domains favourable for signal transduction. Indeed, data suggest that Cripto mediates uptake of mature Nodal via a non-clathrin, non-caveolar pathway to early endosomes. In addition, Cripto tethers Nodal to the limiting membrane of endosome where the signalling machinery is present. Our results suggest that Cripto is a receptor for proprotein convertases which couples Nodal processing and signalling in cells.

4 INTRODUCTION

4.1 Establishment of the basic body plan during gastrulation

Following fertilisation, a set of mitotic division evolves determinants of the zygote. Smaller daughter cells, termed blastomers, are formed. After a set of divisions, the embryo is composed of 8 cells enclosed in a layer of glycoproteins (the zona pellucida). Then a unique feature in the mammalian phylum occurs: compaction. In this process, cells rearrange spaces between them. At the 16 cell stage, the morula is made of two layers, an inner and an external layer. The outer blastomers of the morula develop tight junctions that seal off the inside of the sphere and divide the plasma membrane into apical and basolateral domains (Fleming and Pickering, 1985; Pratt et al., 1982). The descendents of the external cells become trophectoderm (TE) cells (Johnson and Ziomek, 1981). Cells from this population will form extraembryonic structures (chorion, placenta), and do not contribute to the embryonic tissues (Papaioannou, 1982; Searle et al., 1976). The inner cells generate the inner cell mass (ICM), which will mainly give rise to the embryo and the placenta. By 3.0 days post coitum (dpc), the polarised outer trophoblast cells pump fluid into the morula to create a cavity called blastocoel. Meanwhile, inner cells break their contacts with outer cells and are pushed to one side by the liquid pressure (reviewed in Pelton et al., 1998). These cell movements will result in the formation of a cell mass filled with fluid. At the preimplantation stage, the mammalian embryo is called blastocyst (**Fig. 1**) (Pedersen and Spindle, 1980). By 4.5 dpc, the primitive endoderm (PrE), a second extraembryonic lineage, appears on the surface of the ICM that faces the blastocoelic cavity. Shortly after, some cells from the PrE detach from the ICM and acquire epithelial character. Some associate with the ICM to become embryonic visceral endoderm (VE) while others associate with the extraembryonic ectoderm becoming the extraembryonic visceral endoderm (reviewed in Zernicka-Goetz, 2002).

The VE is an extraembryonic endoderm component that derives from the primitive endoderm. Once these extraembryonic lineages have been set aside, the remainder of the ICM proliferates and, under the influence of signals from the VE, undergoes a process of cavitation to form a cup-shaped structure composed of an 'outer' layer of visceral endoderm and an 'inner' layer of ectoderm surrounding the proamniotic cavity. This so-called egg cylinder is a result of the cavitation process, and its cylindrical morphology is a characteristic of rodent

embryos. The primitive ectoderm, also known as epiblast, gives rise to the fetus, amnion, the allantois and the extraembryonic mesoderm. The proximal portion of the egg cylinder comprises the extraembryonic ectoderm (ExE), a derivative of polar TE cells (**Fig. 1**). The ExE gives rise to the chorionic component of the placenta, which provides the vascular interface with the mother and the embryo for nutrient and gas exchange. It also forms the ectoplacental cone (ec), which invades the uterus during the nidation process to connect the embryo to the mother (reviewed in Lu et al., 2001).
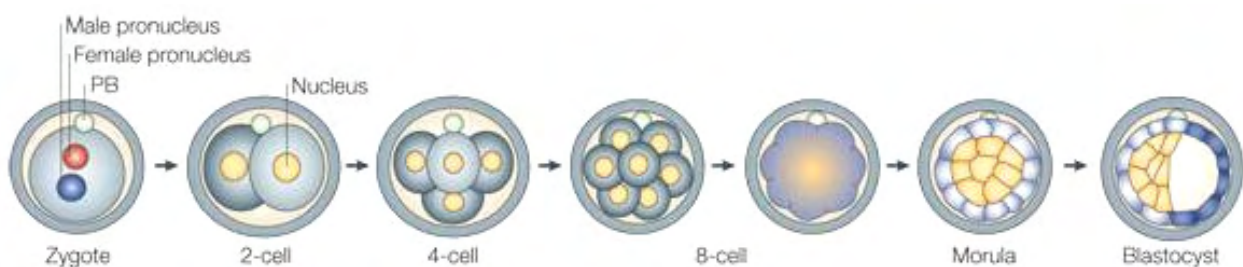
Figure 1. Cellular organisation from the zygote to the blastocyst
In the zygote, the female and male pronuclei are labelled red and blue respectively in addition to the second polar body (PB). Pronuclei fuse and the first cell further divides. At the 8-cell stage the cells are called blastomeres. They are initially round, but then they flatten at the compaction stage and undergo apical–basal polarization (shown by blue to yellow gradient). However, at the morula stage (16 cells), the embryo consists of inside (light yellow) and outside cells (light blue). At the blastocyst stage, inner cells form the inner cell mass (yellow), which is surrounded by polar TE (light blue) whereas the mural TE (darker blue) surrounds the cavity. Source: Zernicka-Goetz, 2002.

After day 5.5 dpc, the primary body axis is specified by signals from distal VE (DVE) cells. Labelling with a lipophilic dye in culture showed that DVE cells move to one side of the epiblast, which thus becomes defined as anterior (Thomas and Beddington, 1996). The conversion of proximo-distal (P/D) to antero-posterior (A/P) polarity which is associated with the anterior movement of the DVE thus already occurs before gastrulation (**Fig. 2**). At this stage the DVE cells migrate asymmetrically towards the prospective anterior side of the egg cylinder to form the anterior VE (AVE) (see below) (reviewed in Beddington and Robertson, 1998).

24
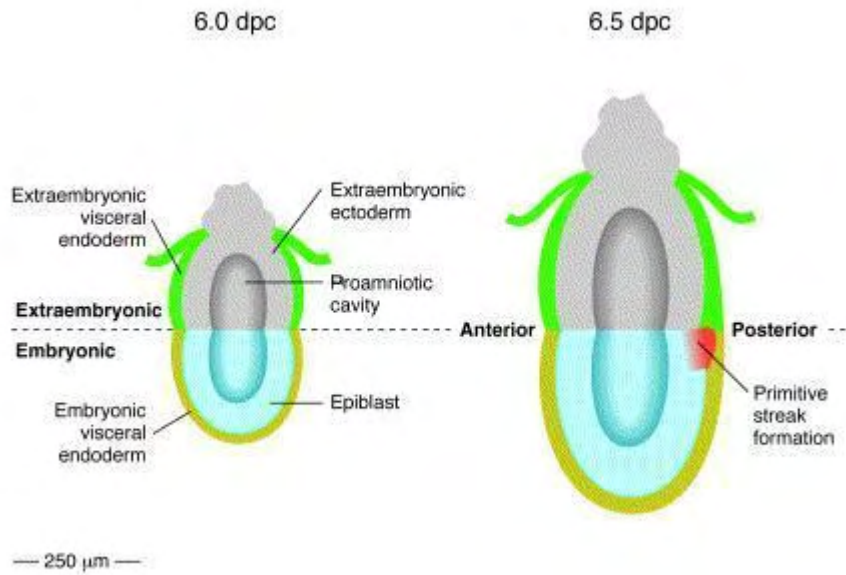
Figure 2. Formation of the primitive streak leads to the establishment of the antero-posterior axis
During gastrulation (6.0–7.5 days post coitum (dpc)) cells at posterior pole of the egg cylinder are induced to form the PS. The different cell types of the epiblast (blue), embryonic visceral endoderm (yellow), extraembryonic visceral endoderm (green) and extraembryonic ectoderm (grey) are shown. The PS is first evident at 6.5 dpc. This structure defines the A/P axis. Its formation is associated with the delamination of mesoderm (red) at the embryonic–extraembryonic junction. The site of streak formation defines the posterior margin of the embryo. The streak elongates to the tip of the cylinder. Source: Beddington and Robertson, 1998.

Gastrulation occurs in all animals. During this process, the epiblast is converted into three primary germ layers: ectoderm, mesoderm and definitive endoderm. In the mouse, this critical step begins at 6.5 dpc, when cells along the proximal rim of the epiblast start to ingress to form a transient embryonic structure termed primitive streak (PS) (reviewed in Bellairs, 1986). The PS marks the prospective posterior pole of the embryo and constitutes the first morphological sign of the A/P polarity within the embryo proper. Cells entering the PS undergo an epithelial-mesenchymal transition (EMT) (reviewed in Thiery and Sleeman, 2006). In this process, epiblast cells loose their polarised epithelial morphology, loose cell-cell contacts and undergo a massive cytoskeletal reorganisation to become motile mesenchyme cells. Mesenchymal cells detach from the PS and spread distally and anteriorly as a layer of cells between the epiblast and the visceral endoderm. By 7.5 dpc, a complete layer of mesoderm is formed between the ectoderm and the endoderm (Tam and Beddington, 1987).

By mid-streak stage, precursors of the definitive endoderm delaminate from the anterior PS and intercalate with the visceral endoderm cells. Definitive endoderm cells rapidly proliferate and spread so that by the end of gastrulation, they almost completely replace visceral endoderm cells. In addition, the epiblast cells outside the PS progressively differentiate into ectoderm cells. By then, the three first cell lineages (endoderm, mesoderm and ectoderm) are established (reviewed in Lu et al., 2001). The future lineages issued from the two first groups of cells give rise to differentiated cell types of the embryo itself and extraembryonic structures (**Fig. 3**). Growth factors, such as transforming growth factor β (TGF-β), play key roles in these processes.

Nature Reviews | Genetics
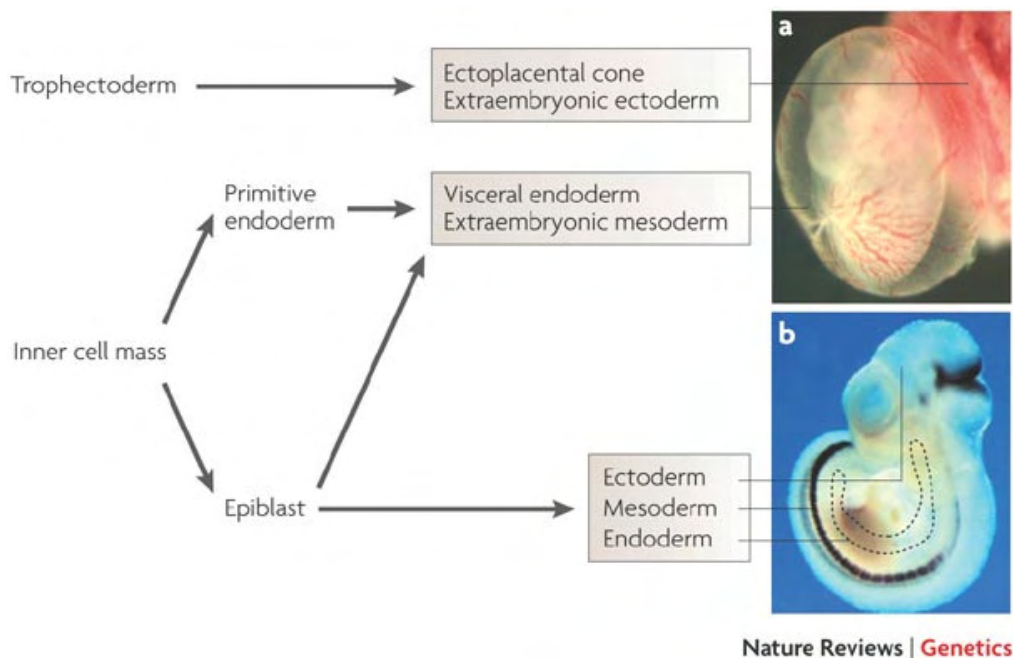
Figure 3. The fate of ICM and trophectoderm cells
At the morula stage, cells in the outer layer of the cellular mass become the TE. Further on, these cells form the extraembryonic ectoderm (ExE) and ectoplacental cone (ec) that make part of the placenta. Cells on the inside express genes that are characteristic of pluripotent cells and form the inner cell mass (ICM) of the blastocyst, from which the epiblast derives. The ICM gives rise to the primitive endoderm, which produces the visceral endoderm lining the extraembryonic yolk sac. The epiblast consists of a population of pluripotent cells from which all the fetal tissues will form (endoderm, mesoderm, ectoderm). In addition, the epiblast forms extraembryonic structures such as the extraembryonic mesoderm of the yolk sac, the allantois and the amnion. Cells that are allocated to the mesoderm are distributed to four main tissue compartments: the axial mesoderm (notochord); the paraxial mesoderm, which forms the somites and subsequently the vertebral column and skeletal muscle; the lateral plate mesoderm (circulatory system and gut wall); and the extraembryonic mesoderm (yolk sac vasculature and blood). The definitive endoderm forms the epithelium of the gut tube, lungs and organs including the liver, pancreas and thyroid. Source: Tam and Loebel, 2007.

26

4.2 Proteins of the TGF-β superfamily share similar protein sequences in their C-terminal domains

The TGF-β superfamily has attracted much attention because of their ability, from nematodes to mammals, to control multiple cellular functions required for embryonic development and adult tissue homeostasis (reviewed in Massague and Wotton, 2000). Indeed, TGF-βs are probably the most ancestral active cytokines characterised at the molecular level in both Protostome and Deuterostome lineage (reviewed in Massague et al., 1987). The initial discovery of Decapentaplegic (Dpp) in *Drosophila melanogaster* stressed the early origin of this superfamily (Padgett et al., 1987). The largest subfamily of TGF-β comprises widely distributed members within the animal kingdom (**Fig. 4**). Bone morphogenetic proteins (BMPs) can be divided in two main groups which show approximately 50% identity: the BMP2/4 group and the BMP5-8 group. On the basis of conserved structural features and sequence homologies, the TGF-β members are subdivided into different TGF-β isoforms. In addition, two smaller groups are attached to this family: the activin/inhibin group and Nodal related-proteins (reviewed in Heldin et al., 1997).

4.2.1 The BMP group

BMPs were originally discovered for their ability to induce bone formation (Wozney et al., 1988). In mammals, over 15 BMPs have been isolated. BMPs are involved in numerous early to late developmental events such as dorsoventral pattern formation, mesoderm induction, tissue and organ development as well as limb formation (reviewed in Hogan, 1996). BMPs can be further divided in two groups which show approximately 50% identity: BMP2/4 and BMPs5-8. The BMP2/4 group includes the first described invertebrate BMP, Dpp (Wozney et al., 1988). These proteins are key regulators of dorso-ventrsl axis specifications form vertebrates to insects (reviewed in Lemaire and Yasuo, 1998).

4.2.2 The TGF-β group

TGF-β subfamily members are pleiotropic multifunctional proteins (reviewed in Keah and Hearn, 2005). Five isoforms have been characterised in higher vertebrates (TGF-β 1-5). They are involved in development, tissue repair and remodelling, haematopoiesis and they increase the production and secretion of extrcellular matrix (ECM) proteins and protease inhibitors (Herpin et al., 2004). They also play numerous roles in the function and development of the

immune system and generally show immuno-suppressive and anti-inflammatory activities (Boivin et al., 1995).
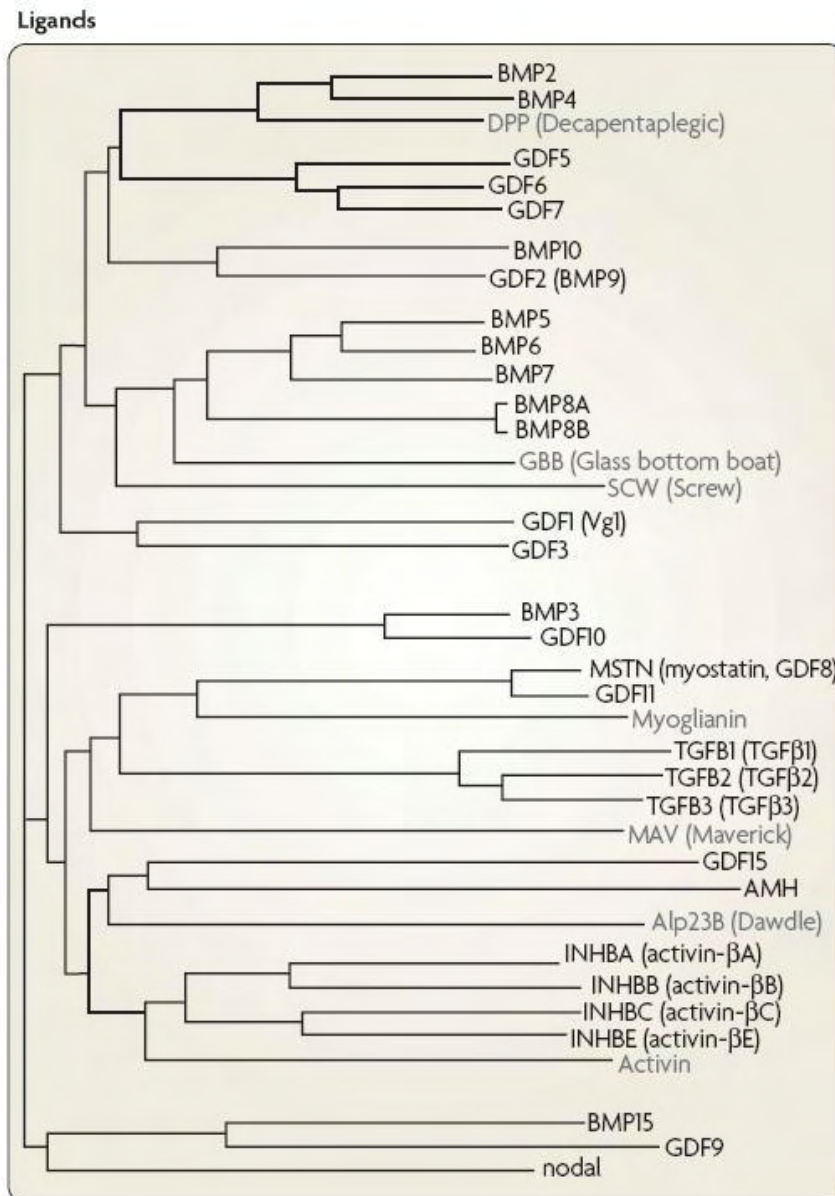
Ligands

4.2.3 The activin/inhibin group

The activins and inhibins were first identified as gonadally produced feedback regulators of pituitary follicle stimulating hormone secretion in vertebrates (reviewed in Risbridger et al., 2001). They are also involved in paracrine and autocrine regulation of growth and differentiation (reviewed in McDowell and Gurdon, 1999; Ramis et al., 2007). Activins comprise homo- and hetero-dimers of various Inhibin-β subunits, while Inhibins consist of a heterodimer of an Inhibin-β subunit with an Inhibin-α subunit.

4.2.4 The Nodal-related protein group

Nodal occupies a separate branch on the phylogenetic tree of the TGF-β superfamily (Herpin et al., 2004). Nodal has been found in invertebrate deuterostomes, such as ascidians and sea urchins, but so far, is missing in protostomes (reviewed in Chea et al., 2005). A single Nodal gene is found in the mouse and in the human species (Vallier et al., 2004; Zhou et al., 1993). In zebrafish, Nodal has three related proteins: Cyclops (which acts at short distance), Squint (which acts at long distance) and Southpaw (reviewed in Schier, 2003). In *Xenopus laevis*, 6 Nodal related proteins have been identified, including *Xenopus* nodal related (Xnr) 1, 2, 3, 4, 5 and 6. Finally, Nodal related protein has been found up to cephalochordates. In Amphioxus, the homolog is termed AmphiNodal (Yu et al., 2002). However, no Nodal related gene has been identified in *Drosophila melanogaster* and *Caenorhabditis elegans*.

TGF-β related proteins are secreted as precursor peptides forming homo- or hetero- dimers (Cheifetz et al., 1987; Cheifetz et al., 1988). Each monomer is synthesized as a large pre-pro-protein: a N-terminal pro-domain and a C-terminal mature peptide. After cleavage of the signal peptide, the precursor is N-glycosylated. The pro-domain is then proteolytically cleaved at the consensus site [RK]-X-X-[RK] by subtilisin-like proprotein convertases (SPC). In addition to the mature biologically active peptide, the pro-domain is supposed to be under selective constraints due to its putative accessory function (reviewed in Sinha et al., 1998), but its precise role is poorly understood.

4.3 TGF-β superfamily members signal through a common cascade

Aside from structural similarities, TGF-β members share several common features in their downstream signalling mechanisms. With the exception of glial-cell-derived neurotrophic factor (GDNF), a distant member of the TGF-β superfamily, the large majority of TGF-β family members transmit a signal through heteromeric complexes of type I and II serine/threonine kinase receptors (reviewed in ten Dijke et al., 1996). TGF-β superfamily members can bind to and transduce signals through the activated receptor type I kinases ALK1 to ALK6. BMP, TGF-β, and Activin signal through different sets of receptors. Nodal shares the receptor Alk4 with Activin. In addition, Nodal can signal through Alk7, but this type I receptor apparently is not used for Nodal signalling and cannot compensate for Alk4 in

the early embryo (Reissmann et al., 2001; reviewed in Wang and Tsang, 2007; Yeo and Whitman, 2001b). Moreover, two type II receptors can be used by Nodal: ActRIIa (Acvr2a) and ActRIIb. Ligand binding induces the formation of a tetrameric complex in which two type II receptors transphosphorylate two type I receptors on their cytoplasmic GS box (SGSGSGLP) (Wrana et al., 1994). Activated type I receptors in turn activate specific receptor substrate (Smads) organised in multisubunit complexes that translocate into the nucleus to regulate transcription of target genes. A key feature of the type I receptor is the L45 loop. The sequence of this loop determines specific TGF-β signalling activity and specifies the choice of Smad proteins by these receptors in the cell (Chen et al., 1998).

Smads can be divided into three distinct classes: Receptor-regulated (R-Smads), Common-partner (Co-Smads), Inhibitory (I-Smads) Smads (**Fig. 5**). The R-Smads are Smads-1, -2, -3, -5 and 8/9 for vertebrates and Mad (Mother against Dpp) for *Drosophila* (reviewed in Miyazono et al., 2000; reviewed in Raftery and Sutherland, 1999). R-Smads are directly phosphorylated by the type I receptors on two conserved serines at the COOH-terminus. Smad anchor for receptor activation (SARA) was the first protein identified for Smad2 recruitment to the type I TGF-β receptor (Tsukazaki et al., 1998). Phosphorylation induces the release from the receptor complex as well as from SARA. Furthermore, it was later shown that coexpression of Hepatocyte growth factor-regulated tyrosine kinase substrate (Hrs has recently been renamed as Hgs) and SARA both augments the response in an activity assay for Smad2 (Miura et al., 2000). The localisation of SARA in early endosome is required for efficient TGF-β/Smad2/3 signalling (Itoh et al., 2002; Panopoulou et al., 2002; Penheiter et al., 2002; Tsukazaki et al., 1998). Thus, SARA is also used as a marker for endosomal activity. Phosphorylation stimulates R-Smads to accumulate in the nucleus as heteromeric complexes with a second class of Smads, the Co-Smads, which are the human/mouse Smad 4 and *Drosophila* Medea (reviewed in Derynck et al., 1998; reviewed in Massague and Wotton, 2000). R-Smads and Smad4 share two conserved domains: the N-terminal Mad Homology 1 (MH1) domain and the C-terminal MH2 domain.

In the nucleus, the Smads associate with DNA binding partners and various transcriptional co-activators or co-repressors, positively or negatively regulating gene expression. In addition, a third class of Smads regulates the cascade: the I-Smads (Smad-6 and -7). They seem to function in several different ways. They were originally shown to compete with R-Smads for binding to activated type I receptors and thus to inhibit the phosphorylation of R-Smads

(reviewed in Shi and Massague, 2003). Subsequently, the I-Smads were found to recruit E3-ubiquitin ligases, known as Smad ubiquitination regulatory factor 1 (Smurf1) and Smurf2, to the activated type I receptor, resulting in receptor ubiquitination and degradation, and termination of signalling (Ebisawa et al., 2001). Recently, Smad7 has been shown to recruit a complex of GADD34 and the catalytic subunit of protein phosphatase 1 to the activated TGF-β type I receptor to dephosphorylate and inactivate it (Shi et al., 2004). Furthermore, the I-Smads might also have a nuclear role because Smad6 has been shown to recruit the corepressor CtBP to repress BMP-induced transcription (Lin et al., 2003). The TGF-β superfamily specificity is directed by R-Smads. Smads 2 and 3 mediate signalling of the TGF-β/activin branch (including TGF-β *sensu stricto*, Activins and Nodals), whereas Smads 1, 5, and 8/9 act in the BMP branch (BMPs) (reviewed in Miyazawa et al., 2002).
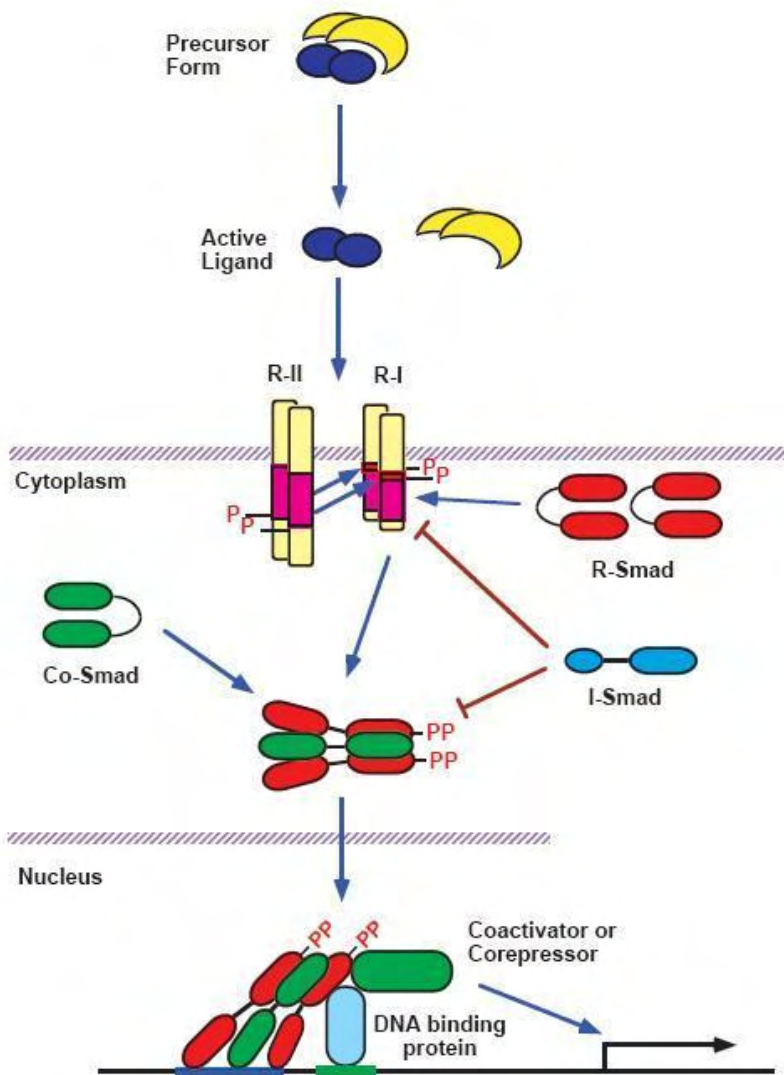
Figure 5. TGF-β signal transduction by Smad transcription factors
Activated receptors propagate a signal inside the cell through the phosphorylation of receptor-regulated Smads (R-Smads: Smad1, Smad2, Smad3, Smad5 and Smad8). Access of the R-Smads to the type I receptors is facilitated by auxiliary proteins such as SARA. ALK1, ALK2, ALK3 and ALK6 phosphorylate Smad1, Smad5 and Smad8, whereas ALK4, ALK5 and ALK7 phosphorylate Smad2 and Smad3. Many members of the TGF-β superfamily of ligands elicit multiple diverse cellular responses. Activated R-Smads form heteromeric complexes with Smad4. These complexes accumulate in the nucleus, where they control gene expression in a cell-type-specific and ligand dose-dependent manner through interactions with transcription factors, coactivators and corepressors. These proteins shuttle between the cytoplasm and nucleus both in uninduced cells (as monomers) and during active TGF-β signalling, when Smad2 and Smad3 (red), presented to the receptors (pink) by SARA, become phosphorylated and form heteromeric complexes with Smad4 (green). Inhibitory Smads (I-Smads) form a distinct subclass of Smads that act in an opposing manner to R-Smads and antagonise signalling. Smad6 and Smad7 (blue) are inhibitory factors, but seem to act differently to inhibit the cascade. Source: Miyazono et al., 2000.

Like other TGF-βs, Nodal consists of a prodomain and a mature region (Zhou et al., 1993). Nodal protein is formed by the binding of two monomeric subunits that are linked by a disulfide bond on the mature part of the protein. Whereas the prodomain sequences vary considerably among different TGF-β family members, the mature region is highly conserved and contains the entire structural features characteristic of the TGF-β family. Seven cysteine residues within the carboxyl terminal region are invariant in members of the family. Six of these cysteines are closely grouped to form three disulfide bonds within each monomer that generate a rigid structure, called a cystine knot, similar to the structure found in neurotrophic factors (NGF, BDNF, NT3) (reviewed in McDonald and Hendrickson, 1993; Schlunegger and Grutter, 1992; reviewed in Sun and Davies, 1995). The remaining cysteine residue in each monomer forms an additional disulfide bond that links two monomers into a dimer. The dimer is also stabilised by hydrophobic interactions that exist between the two monomer subunits (reviewed in Lin et al., 2006). Nodal is secreted as a precursor protein, which is then proteolytically cleaved by members of the SPC family (Beck et al., 2002; Constam and Robertson, 1999). It is now established that processing is essential to efficiently stimulate Nodal signalling through the Smad2/3 pathway. However, how this processing step is regulated, and its subcellular localisation remained unknown.

4.4   Nodal is responsible for early embryonic patterning

In amphibian embryos, the dorsal lip of the blastopore has the ability to induce a secondary axis when grafted ectopically. This cell mass was named the Spemann's organizer. A structure with axis-inducing abilities was also found in the chick and named Hensen's node. In the mouse, this population of cells has the ability to induce a partial secondary axis when grafted ectopically (Beddington, 1994). However, the secondary axis results in the formation of a truncated axis suggesting that the mammalian node is not the direct equivalent of the amphibian and chick organisers. In the early-streak stage mouse embryo, cells that are fated to form the axial mesoderm composed of notochordal and prechordal mesoderm are localised to a region of the proximal-posterior epiblast (Lawson et al., 1991; Tam et al., 1997). Compared to the node of late streak stage embryos, this region can induce a more complete secondary axis and thus is now referred to as the Early Gastrula Organizer (Kinder et al., 2001). Cells within the organizer in all species show similar tissue fates and are the primary source of the

axial mesoderm and prechordal plate tisse, which comprises a structure composed of both mesodermal and endodermal cells.

Aside from its role in axis and germ layer formation, Nodal already has an earlier function in the implanted blastocyst, where it is essential to expand a pool of pluripotent progenitors in the ICM (Mesnard et al., 2006). Thus, in Nodal mutants, the ICM precociously differentiates into neural tissue (Camus et al., 2006). Furthermore, Nodal is required for the specification of DVE and A/P axis formation (Brennan et al., 2001; Varlet et al., 1997; Conlon et al., 1991; Conlon et al., 1994). *Nodal* is initially expressed in the ICM and the primitive endoderm of the implanted blastocyst (4.5dpc) (Mesnard et al., 2006). Thereafter, Nodal is expressed throughout the epiblast and overlying embryonic VE until E5.5 (**Fig. 6**) (Brennan et al., 2001; Mesnard et al., 2006).
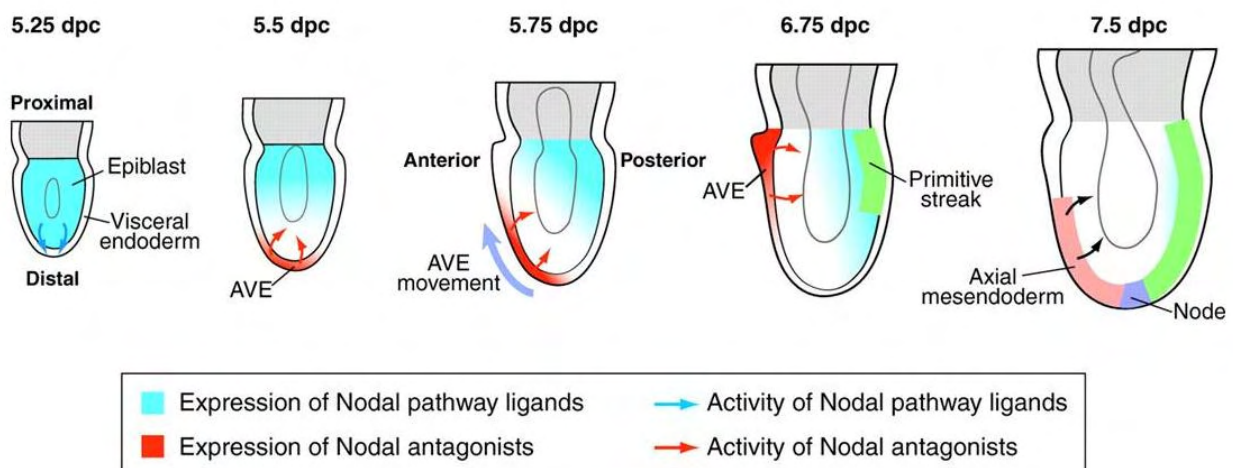
Figure 6. Nodal signalling in the early mouse embryo, and the role of AVE in anterior neural patterning
Blue shading indicates regions expressing *Nodal*; red shading indicates regions expressing the Nodal antagonists Lefty1 and Cer1. Shortly after implantation, *Nodal* is expressed throughout the epiblast at 5.25 dpc, and by 5.5 dpc induces formation of the anterior visceral endoderm (AVE, shown in red) at the distal end of the egg cylinder. Nodal signalling is also required for the movement of the AVE (purple arrow) to the anterior side (5.75 dpc) where the expression of Nodal antagonists (*Lefty1, Cer1*). Expression of Nodal antagonists by the AVE is essential for the specification of anterior neural identity in the adjacent epiblast. After full extension of the streak (7.5 dpc), the node (purple) appears at the posterior end of axial mesendoderm (pink) by the anterior primitive streak (the primitive streak is shown in green). In turn, the axial mesendoderm produces signalling factors (black arrows) that are essential for forebrain maintenance and ventral neural tube patterning. Source: Shen, 2007.

The formation and directional movement of the DVE directs Nodal expression pattern. This has been attributed to the fact that the DVE produces the Nodal feedback antagonists Lefty1 and Cerberus-1 (Cer1). Their expression is initiated by Nodal specifically in the DVE

(Srinivas et al., 2004). After the DVE migration to the anterior side of the embryo, this specialised group of cells becomes the AVE. The AVE continues to produce Nodal antagonists, Lefty1 and Cer1, which interfere with autoinductive Nodal signalling in the adjacent epiblast and thus limit PS formation to the opposite side at the prospective posterior pole (reviewed in Perea-Gomez et al., 2001). By contrast, in absence of Nodal, no DVE is formed and the P/D axis is not patterned (Brennan et al., 2001).

The Nodal signalling pathway is integral to pattern formation and differentiation during the pre-gastrulation and gastrulation stages of chordate development because it regulates an entire set of genes that are involved in early mouse embryogenesis (reviewed in Tam and Loebel, 2007). Nodal signalling also patterns the neural plate (Gritsman et al., 2000; Zhou et al., 1993). In addition, Nodal is essential for maintaining the molecular pattern in the murine extraembryonic ectoderm (Guzman-Ayala et al., 2004). Altogether, Nodal dictates the molecular identity of all cells within the early conceptus (reviewed in Schier, 2003). The roles of Nodal signalling and antagonism in mesoderm and endoderm induction, PS formation and left-right specification appear to be particularly well-conserved during evolution. The read-outs for Nodal signalling activity have been the phosphorylation of the downstream effector Smad2 and the induction of mesodermal or endodermal genes.

Activated type I receptor phosphorylates and thereby activates cytoplasmic Smad3 (in the epiblast) and Smad2 (in the epiblast and visceral endoderm), leading to their interaction with Smad4 and the subsequent formation of transcriptional complexes in the nucleus (Dunn et al., 2004). At the transcriptional level, Nodal function is mediated by the activities of transcription factor FoxH1 and the Mixer subclass of homeoproteins (Kunwar et al., 2003). These factors are needed to induce endoderm downstream of Nodal. Endoderm is induced by high doses of Nodal exceeding the signalling thresholds required for mesoderm formation (Dunn et al., 2004). Known targets of the Nodal pathway include *Cripto, Lefty1, Cerberus1* and *Nodal* itself. Nodal is positively autoregulated through the asymmetric enhancer (ASE) located in the first intron and by an upstream left-side specific enhancer (LSE) (Norris et al., 2002; Saijoh et al., 2005). A comparison of Nodal and Smad2 mutants reveals that Nodal is able to signal through a Smad2-independent pathway (Brennan et al., 2001). In particular, Nodal was able to induce the expression of Bmp4 and Eomesodermin in the ExE of Smad2 mutant embryos (Dunn et al., 2004).

4.5   Regulation of Nodal precursor processing

In order to efficiently activate the Smad2/3 pathway, Nodal has to be cleaved. Nodal is processed by the subtilisin-like proprotein convertases Furin (or SPC1) and Pace4 (or SPC4) (Beck et al., 2002; Constam and Robertson, 1999). Interestingly, at early stages (5.75-6.5dpc), Furin and Pace4 are specifically expressed in the extraembryonic ectoderm, rather than in cells expressing Nodal (**Fig. 7**), suggesting that Nodal may be cleaved after secretion.

Figure 7. The expression patterns of Nodal and Cripto are complementary to those of Furin and Pace4
At the onset of gastrulation, Nodal is expressed in the epiblast and visceral endoderm, whereas Furin and Pace4 transcripts are confined to the extraembryonic ectoderm (exe) and the ecoplacenal come (ec). Thus, if Nodal precursor protein is directly cleaved by these convertases, such an interaction must occur after secretion. The following model is currently investigated: a local source of Furin and Pace4 in the ExE activates Nodal in adjacent tissue to specify AVE and to induce expression of Cripto. Source: Beck et al., 2002; Mesnard et al., 2006.

In keeping with this model, soluble forms of Furin and Pace4 can process Nodal *in vitro*, whereas intracellular cleavage has never been observed (Beck et al., 2002). Given that the source of Nodal convertases is localised, one might predict that Nodal is not uniformly activated, but instead may be more efficiently cleaved in the proximal epiblast than in distal regions. However, when and where Nodal encounters its proprotein convertases is still unknown.

4.6 The EGF-CFC family is involved in several signalling pathways during development

Genetic studies in zebrafish and mouse have shown that Nodal signalling also critically depends on proteins of the epidermal growth factor-Cripto1/FRL1/Cryptic (EGF-CFC) family, represented in zebrafish by a single protein termed One-eyed pinhead (Oep) (Sakuma et al., 2002; reviewed in Schier, 2003; reviewed in Schier and Shen, 2000). In line with this view, Cripto$^{-/-}$ mice arrest development around day 7.5 due to their inability to form endoderm (Ding et al., 1998; Liguori et al., 1996). Furthermore, in the absence of Cripto, the DVE forms but does not translocate (Ding et al., 1998; Kimura et al., 2001). Later in embryogenesis, Nodal functions through Cryptic in the establishment of the left-right (L/R) asymmetry of the visceral situs (Shen et al., 1997; Yan et al., 1999).

Upon its discovery in teratoma, Cripto initially has also been termed teratocarcinoma-derived growth factor-1 (TDGF-1) (reviewed in Saloman et al., 2000). In the meantime, orthologous genes have been identified in human (Cr-1) (Dono et al., 1993), chicken (CFC) (Colas and Schoenwolf, 2000), zebrafish (Oep) (Zhang et al., 1998) and *Xenopus* (FRL1) (Kinoshita et al., 1995). EGF-CFC family members are composed of an N-terminal signal peptide, a modified EGF-like region, a conserved cysteine-rich domain (CFC motif) and a short hydrophobic C-terminus that contains a signal sequence for adding a GPI anchor (Minchiotti et al., 2001). Removing the COOH-terminal residues where the GPI linkage occurs generates soluble forms (Minchiotti et al., 2000) that were thought to mediate cell non-autonomous activity (Chu et al., 2005; Yan et al., 2002). However, a recent study clearly shows that deletion of the GPI signal sequence abolishes the ability of Cripto to stimulate Nodal signalling (Watanabe et al., 2007). This apparent paradox indicates that Cripto may be released together with its GPI anchor (Watanabe et al., 2007).

Cripto contains a consensus O-linked fucosylation site on a threonine residue within the EGF-like motif. It was previously thought that the fucosylation itself was required for the activity of Cripto (Schiffer et al., 2001). However, more recent work shows that the amino acid itself, rather than the fucose modification is required for Nodal signalling (Shi et al., 2007).

The first evidence that EGF-CFC proteins are required in the Nodal pathway came from studies in zebrafish showing that maternal-zygotic oep mutants mimicked the Cyclops/Squint double mutants, and that this defect can be rescued by constitutively active, ligand-independent mutant type I activin receptor (Gritsman et al., 1999). The same study also hypothesised that Oep may act as a coreceptor in signal receiving cells to increase Nodal binding to signalling receptors. In keeping with this model, coimmunoprecipitation analysis in *Xenopus* embryos subsequently revealed that murine Nodal produced in the context of the heterologous propeptide of Bmp10 was able to bind Cripto, and that Cripto apparently mediates the assembly of a complex with ALK4 and ActRIIa (Yeo and Whitman, 2001b). These authors also showed that Cripto binds ALK4 via the CFC domain. In addition, Cripto can also interact with Alk7 and thereby enhance the ability to mediate Nodal signalling (Reissmann et al., 2001). Similar results were obtained for Cryptic (Chen and Shen, 2004).

However, the Reissman study and subsequent receptor binding assays in 293T human embryonic kidney cells clearly showed that Nodal can bind both ActRII and ALK4 independently of Cripto and Cryptic, and that this binding is only marginally increased by Cripto (Chen and Shen, 2004). Likewise, binding of zebrafish Squint to ALK4 in Xenopus embryos was clearly Cripto-independent (Cheng et al., 2004). Moreover, while early receptor binding assays focused on processed Nodal (Reissmann et al., 2001; Yeo and Whitman, 2001b), the Constam lab recently could show that ALK4 and ActRIIb bind both cleaved and uncleaved Nodal irrespective of whether or not Cripto is present (Ben-Haim et al., 2006). Finally, close examination of the data in the Shen laboratory (Chen and Shen, 2004) raised the possibility that Cripto might primarily interact with unprocessed Nodal precursor. Prompted by these observations, we decided to revisit the question by which mechanism(s) Cripto might potentiate Nodal signalling. In particular, we hypothesized that EGF-CFC proteins may play a role in Nodal processing.

4.7 Cripto is a target of Nodal feedback inhibitors

It was initially proposed that Lefty antagonises Nodal signalling through competitive binding to the type II receptors (Sakuma et al., 2002). However, these results have not been confirmed. Instead, Lefty is now thought to directly compete with Nodal for Cripto (Chen and Shen, 2004; Cheng et al., 2004). In addition, both Lefty1 and Cer1 have been proposed to

directly bind Nodal, thereby inhibiting its access to signalling receptors (Chen and Shen, 2004; Piccolo et al., 1999).

4.8   Cripto can activate alternative pathways

Aside from stimulating Nodal/Alk4/Smad2/3 signalling, and independently of Nodal, Cripto can also activate the ras/raf/MAPK signalling pathway (reviewed in Bianco et al., 2004; De Santis et al., 1997; Kannan et al., 1997). Interestingly, this signalling pathway can even be activated by a soluble, GPI-truncated recombinant Cripto (Bianco et al., 2002; Kannan et al., 1997) through direct binding to Glypican-1, a membrane-associated heparansulphate proteoglycan (HSPG) (Bianco et al., 2003). However, it remains to be determined to what extent this pathway is used during gastrulation, and/or to mediate known effects on cell motility (Warga and Kane, 2003), cell invasion (Normanno et al., 2004), cardiac lineage specification and differentiation (Parisi et al., 2003; Xu et al., 1999).

In addition, to its role in embryonic development, Cripto can induce cellular transformation and tumorigenesis (reviewed in Bianco et al., 2004; reviewed in Salomon et al., 1999). When transfected into immortalised mouse NOG-8 mammary epithelial cells, Cripto induced anchorage-independent growth and colony formation in soft agar (Ciardiello 1991). Recent studies analysing markers of EMT suggest that Cripto is also involved in mammary gland hyperplasia and tumorigenesis (Strizzi et al., 2004). During EMT, intercellular contacts between epithelial cells are lost due to a decrease of E-cadherin expression and disruption of the adherens junction complex (Boyer et al., 2000). E-cadherin was significantly decreased in tissue extracts from the mammary tumor lesions that expressed Cripto. In addition, overexpression of Cripto leads to an increase of vimentin, a characteristic marker of cells undergoing EMT (Ackland et al., 2003; Casaroli-Marano et al., 1999; Dandachi et al., 2001).

In addition to MAP kinase signalling, Cripto can activate the PI3-K/AKT/GSK-3β pathway (Ebert et al., 1999), and interactions between Cr-1 signalling pathway and the Wnt/β-catenin/Lef-1 signalling pathway have been described. Specifically, microarray analysis revealed that Cr-1 is a primary target gene in the Wnt/β-catenin signalling pathway during embryonic development (Morkel et al., 2003). More recently, FRL1 and mouse Cripto have been implicated as coreceptors for Wnt-11 since they can be coimmunoprecipitated with Wnt-

11 in *Xenopus* embryo (Tao et al., 2005). This provides a new link between the EGF-CFC proteins and non-canonical Wnt signalling. Furthermore, in Xenopus, Wnt11 also interacts with glypican-4, suggesting that both glypican-4 and FRL1 are involved in regulating Wnt signalling (Ohkawara et al., 2003).

4.9   GPI-anchors allow localisation to specific membrane domains

EGF-CFC proteins are linked to the plasma membrane by a GPI anchor. Proteins of the secretory pathway can be attached to membrane structures by various mechanisms. GPI anchors have a common core structure in all species studied so far (reviewed in Ferguson, 1999; reviewed in Ikezawa, 2002), but can also acquire diverse modifications during maturation. In animal cells, GPI-anchored proteins (GPI-APs) are important in development, and several GPI-anchored cell-adhesion proteins are essential during early embryogenesis, including Gas1 and Ran-2 (Kawagoe et al., 1996; Mullor and Ruiz i Altaba, 2002; Salzer et al., 1998). GPI membrane anchoring allows proteins to be recruited to specific membrane microdomains at the cell surface (Varma and Mayor, 1998).

GPI-APs are synthesised as precursors with two cleavable ends. A hydrophobic amino-terminal signal sequence, which targets the protein to the lumen of the endoplasmic reticulum (ER), is immediately cleaved during translocation (reviewed in Udenfriend and Kodukula, 1995). The presence of a so-called ω signal sequence in the C-terminal region then leads to a second cleavage, followed by addition of the GPI moiety by GPI transamidase. The GPI moiety is already formed before its attachment to the COOH end of the nascent target protein. The GPI-anchoring consists of a hydrophobic region separated from the GPI-attachment site (ω-site) by a hydrophobic spacer region (**Fig. 8**) (reviewed in Mayor and Riezman, 2004). GPI anchors are not all uniform, but instead can be remodelled. Three mannose groups adjacent of the ω-site can be modified by the attachment of sugars or phosphoethanolamine. The lipid anchor can as well be rearranged by acylation, fatty-acid exchange and even lipid-backbone removal. These modifications may be essential for specific properties of the GPI-APs in the membrane, such as mobility in the lipid bilayer or trafficking.
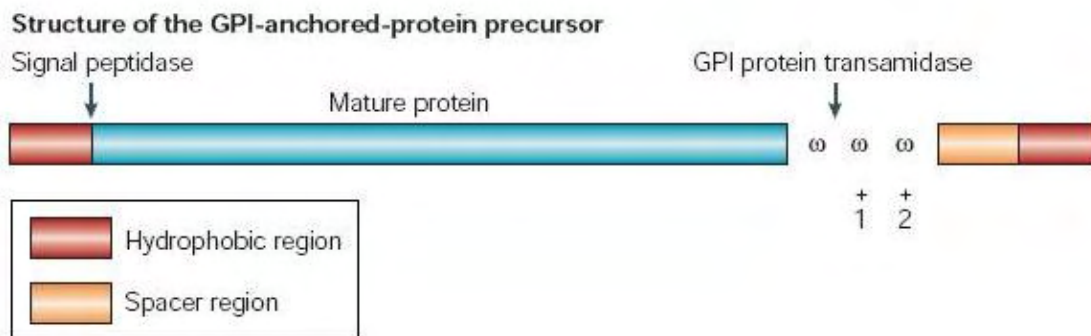
Structure of the GPI-anchored-protein precursor

Figure 8. Structure of GPI-anchored proteins and the position of a specific ω-site for GPI attachment
GPI-anchored proteins are synthesized as precursors with a cleavable, hydrophobic N-terminal signal sequence that targets the protein to the lumen of the ER. A cleavable, C-terminal signal sequence directs GPI anchoring. The GPI-anchoring signal consists of a hydrophobic region separated from the GPI-attachment site (ω-site) by a hydrophilic spacer region. The conserved core consists of ethanolamine phosphate in an amide linkage to the carboxyl terminus of the protein, three mannose residues, glucosamine and phosphatidylinositol. It can be modified and is subjected to various remodelling reactions of the lipid moiety. Due to their specific attachment to membranes, GPI-anchored proteins are embedded in the extracellular or lumenal leaflet of membranes through their glycolipid moieties and are not directly accessible from the cytosolic face of membranes. Source: Mayor and Riezman, 2004.

An extremely interesting feature of the GPI-anchoring of proteins is that this mode of attachment confers specific associations with detergent-insoluble/detergent-resistant membranes (DRMs) (Brown, 1994). The GPI-anchor is required for protein trafficking, but in addition seems important in conformational change enough that antibodies cannot recognise the protein (reviewed in Butikofer et al., 2001). Sorting between GPI-APs and other proteins in yeast already occurs upon exit from the ER (Muniz et al., 2001). There seem to be two distinct steps required for cargo sorting and packaging into vesicles; one that determines the vesicle population that will be used, and a second step that concentrates the cargo into the budding vesicles (Malkus et al., 2002; Miller et al., 2002). In fact, GPI-APs cannot directly interact with cytosolic components that recognise sorting signals. Thus, they may have to interact with specific transmembrane proteins in the lipid bilayer that mediate sorting into vesicles. It seems that the GPI-anchor is critical for the selective targeting of GPI-APs to particular internalisation routes. Van der Goot and coworkers have shown that different residence times of GPI-APs in lipid rafts regulate their sorting in the endocytic pathway (Fivaz et al., 2002). Clustering of cell-surface GPI-anchored proteins can trigger transmembrane signal transduction (Varma and Mayor, 1998). It has been reported that GPI-

APs were targeted to cholesterol and sphingosine-rich microdomains. These domains, also called lipid rafts, are detergent resistant (reviewed in Hooper, 1999).

Once they have reached the cell surface, GPI-APs similar to other cell surface proteins are subjected to internalisation, downregulation and degradation. GPI-APs are found in various endosomes, which implies potential existence of several internalisation pathways (reviewed in Chatterjee and Mayor, 2001; Fivaz et al., 2002; Mayor et al., 1998; Sabharanjak et al., 2002). Four known pathways can be considered for GPI-APs internalisation: caveolae, clathrin-coated pits (Rab5 positive vesicles), GPI-AP enriched endososmal compartments (GEECs) and Arf6 (see below). Several markers can indeed label different endocytic pathways.

4.10 Endocytosis can be mediated by several intracellular pathways

Protein uptake is characterised by the internalisation of molecules from the cell surface into internal membrane compartments. Endocytosis occurs by multiple mechanisms (**Fig. 9**). Two broad categories require actin filaments for their internalisation: phagocytosis or cell eating (uptake of large particles) and pinocytosis or cell drinking (uptake of fluid and solutes) (reviewed in Conner and Schmid, 2003). Phagocytosis is typically restricted to specialised mammalian cells (ex. macrophages), whereas pinocytosis occurs in all cells (reviewed in Aderem and Underhill, 1999). With pinocytosis, cells continually form small small vesicles called pinosomes. In macropinocytosis, large ruffles in the membrane engulf mass quantities of fluid in vesicles known as macropinosomes. Other types of vesicular trafficking require exclusively membrane invagination rather than membrane protrusion and membrane invagination. They can be divided into four basic mechanisms: clathrin-mediated endocytosis, caveolae-mediated endocytosis, and clathrin- and caveolae- independent endocytosis and macropinocytosis.

4.10.1 Clathrin-mediated endocytosis
The best characterised endocytic route involves clathrin-mediated uptake, which is responsible for the internalisation of various nutrients, pathogens, antigens, growth factors and receptors (reviewed in Schmid, 1997). Clathrin-coated vesicles (CCV) are formed by the assembly of cytosolic coat proteins, the main assembly unit being clathrin (reviewed in Brodsky et al., 2001). In addition, clathrin vesicle formation requires other main coat

constituants, the Adaptor Proteins (APs) (reviewed in Robinson, 2004). Only AP2 is involved in endocytic CCV formation, whereas the AP1, 3 and 4 complexes target vesicles to other organelles.
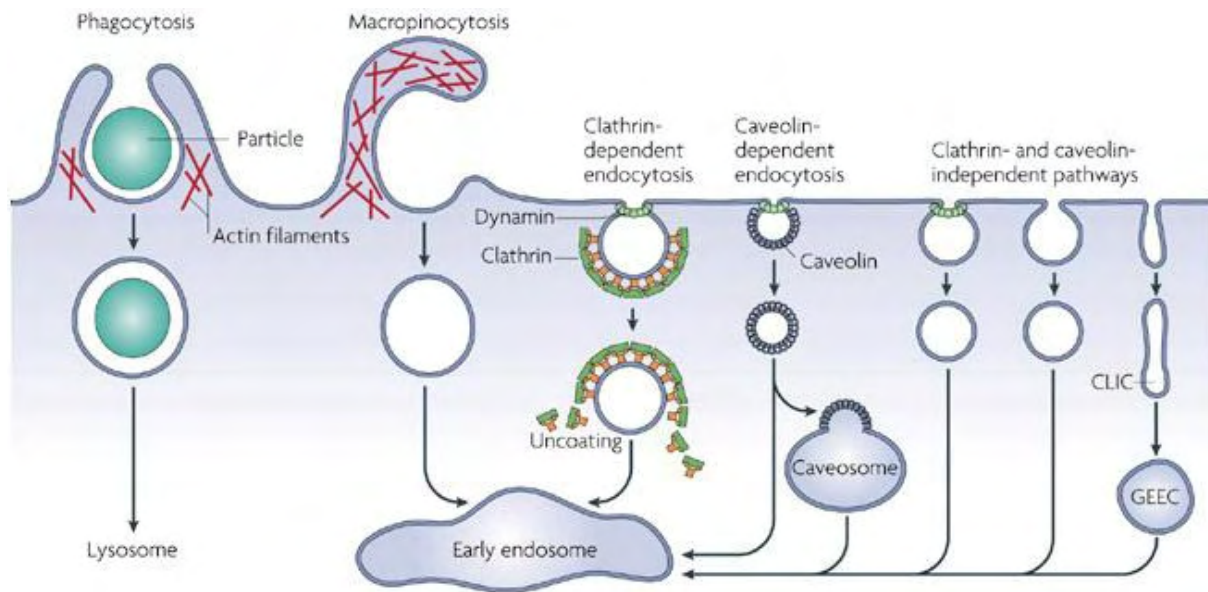
Figure 9. Multiple endocytic routes can internalise extracellular proteins
The plasma membrane is the interface between cells and their environment. 'Endocytosis' encompasses several diverse mechanisms by which cells internalize macromolecules and particles into transport vesicles derived from the plasma membrane. It controls entry into the cell and has a crucial role in development, the immune response, neurotransmission, intercellular communication, signal transduction, and cellular and organismal homeostasis. The endocytic pathways differ with regard to the size of the endocytic vesicle, the nature of the cargo (ligands, receptors and lipids) and the mechanism of vesicle formation. Compared with the other endocytic pathways, the size of the vesicles formed by phagocytosis and macropinocytosis is much larger and actin filaments trigger vesicle formation. Most internalised cargoes are delivered to the early endosome via vesicular (clathrin- or caveolin-coated vesicles) or tubular intermediates (known as clathrin- and dynamin-independent carriers (CLICs)) that are derived from the plasma membrane. Some pathways may first traffic to intermediate compartments, such as the caveosome or the GEECs, *en route* to the early endosome. In addition, Dynamin is not always required for vesicular internalisation processes. Source: Mayor and Pagano, 2007.

4.10.2 Caveolae-mediated endocytosis

Characteristic plasma membrane invaginations known as caveolae demarcate cholesterol and sphingolipid-rich microdomains (reviewed in Anderson, 1998). The shape and structural organisation of caveolae are conferred by Caveolin-1 or Caveolin-3, dimeric proteins that bind cholesterol insert into the inner leaflet of the plasma membrane, and self-associate to form a striated caveolin coat on the surface of the membrane invaginations (Li et al., 1996). To insert into the plasma membrane, Caveolins must be palmitoylated in the C-terminal segment (Dietzen et al., 1995). Caveolae are also thought to be involved in intracellular

cholesterol trafficking (reviewed in Ikonen, 1997; reviewed in Ikonen, 2008). Surprinsingly, caveolin-1 null mice have no overt phenotype (reviewed in Razani et al., 2002). The cells of these mice are devoid of morphologically detectable caveolae, establishing its structural importance (Razani et al., 2001a). Caveolin-null mice show a hyperproliferative response, but the mice seem not to be hyper-susceptible to tumors (reviewed in Razani et al., 2001b). Thus other pathways or other caveolar isoforms can replace the caveolar pathway in these mutant mice. However, endothelial cells that lack caveolin are defective in their ability to bind and internalise serum albumin. Despite that, the levels of albumin in serum and interstitial spaces in caveolin-null mice are normal (Drab et al., 2001).

After internalisation, caveolae can fuse to form caveosomes, i.e. caveolae-derived vesicles containing caveolin-1 (reviewed in Pelkmans and Helenius, 2002; Pelkmans et al., 2001). Caveosomes are a neutral compartment devoid of degradation capacity. They are distributed throughout the cytoplasm. Interestingly, caveosomes lack connection to the plasma membrane and thus are not directly connected to the extracellular space. The endocytic role of caveolae has remained elusive (reviewed in Parton, 2003). It is still unclear what is the final outcome of caveolae-dependent endocytosis (reviewed in Felberbaum-Corti et al., 2003). Uptake in caveolae may lead to different endocytic routes; one leading to caveosomes and another to a degradative compartment. Furthermore, caveosomes could be involved in signalling as it was shown that they communicate with early endosomes. Indeed, Rab5 targets caveolar vesicles to early endosome (Pelkmans et al., 2004).

4.10.3 Clathrin- and caveolae- independent endocytosis

While several types of vesicles are classified in this category, we will focus here on two pathways: the Cdc42-regulated pathway and the Arf6-regulated pathway (reviewed in Mayor and Pagano, 2007). Both pathways are positive for the scaffold protein Flotillin-1 (Glebov et al., 2006). So far, the presence of Flotillin has been found in two vesicular compartments independent of Clathrin and Caveolin: the Cdc42-regulated one and the one dependent on Arf6 function (reviewed in Mayor and Pagano, 2007). Both the Cdc42 pathway (Sabharanjak et al., 2002) and the Arf6 pathway (Naslavsky et al., 2004) are enriched in GPI-APs and do not required Dynamin for membrane scission. The relationship between these two pathways is not very clear and has to be further analysed.

The first compartment is called GEEC, because it was first identified as being enriched for GPI-APs (Sabharanjak et al., 2002). The defining feature of this pathway is the requirement for the small-molecule GTPase Cdc42. Cdc42 is a member of the Rho family of small GTPases. GEECs are pinocytic compartments distinct from the classical endocytic route, since specific proteins that orchestrate the classical route (ex. Rab5) are not involved in their regulation. GEECs are tubular acidic endosomes that are clathrin- and caveolin- independent. The second one is dependent on the small GTPase Arf6 and is identified as an early tubular recycling compartment (reviewed in D'Souza-Schorey and Chavrier, 2006). The Arf6-labelled compartment was first defined by the presence of major histocompatibility complex I (MHC I) (Naslavsky et al., 2003). More recently, it was shown that Arf6 compartment was involved in the trafficking of CD59, a GPI-AP (Naslavsky et al., 2004). Arf6 stimulates the formation of phosphatidylinositol 4,5 bisphosphate by activating phosphatidylinositol 2-phosphate-5-kinase. Arf6 induces the internalisation of GPI-APs in Hela cells. Surprisingly, Arf6 does not affect the endocytosis of GPI-APs in all cell types (Kalia et al., 2006).

4.10.4 Macropinocytosis

Macropinocytosis accompanies the membrane ruffling that is induced in many cell types upon stimulation by growth factors (reviewed in Amyere et al., 2002). Like phagocytosis, the signalling cascades that induce macropinocytosis involve Rho-family GTPases, which trigger the actin-driven formation of membrane protrusions (reviewed in Ridley, 2006). However, unlike phagocytosis, these protrusions extend in the extracellular space near the plasma membrane to further fuse with the cell membrane. This generates large endocytic vesicles, called macropinosomes, that sample large volumes of the extracellular milieu. The nature and the signals that are driven by this process have not extensively been studied, but it is known that transient induction of macropinocytosis in cells has a role in the downregulation of activated signalling molecules (Sallusto et al., 1995). In addition, macropinocytosis appears to regulate the transport of the major histocompatibility complex II (MHC II) in immature dendritic cells (reviewed in Mellman and Steinman, 2001).

The survival and physiology of neurons are regulated by growth factors of the neurotrophin (NT) family. NT signalling occurs through the Trk receptor tyrosine kinase after binding the specific ligands NGF (TrkA), BDNF (TrkB), and NT3 (TrkC). Trk activation had been seen at membrane ruffles where macopinocytosis occurs (Jullien et al., 2003). Pincher, a pinocytic

chaperone, mediates the marcoendocytosis of some of these ligands (Shao et al., 2002; Valdez et al., 2005). In addition, membrane ruffling requires Rac, a Rho-GTPase (Valdez et al., 2007). Another characteristic for Trk endosomal signalling is the formation of long-lived endosomes. Trk endosomal signalling persists all the way from the nerve terminal to the soma (Ye et al., 2003). Regulation of the signalling pathway occurs via GAIP-interacting protein C terminus (GIPC). GIPC is recruited by APPL to Trk endosomes and regulates TrkA signalling and trafficking to the early endosome in the juxanuclear region (Varsano et al., 2006). Interestingly, APPL was recently found to bind Rab5 on signalling endosomes (Miaczynska et al., 2004). Indeed, macropinocytosis markers colocalise with early endosomal markers (Falcone et al., 2006).

Different possible entry routes thus exist to regulate the internalisation of molecules. The endocytic pathways differ with regard to the size of the endocytic vesicle, the nature of the cargo (ligands, receptors and lipids) and the mechanism of vesicle formation. Each route has its own properties for cargo trafficking. However, cargo can often be internalised through several endocytic pathways in some instances to reach distinct destinations. For example, uptake of TGF-β receptors via CCVs is necessary for signalling, whereas uptake in caveolin-positive vesicles leads to degradation (Di Guglielmo et al., 2003). Other signalling molecules such as T cell receptors rely on uptake in specific membrane domains containing lipid rafts (Viola et al., 1999).

4.11 Lipid rafts concentrate receptors and activate ligand binding

The lipid raft hypothesis was postulated after the discovery that cholesterol and sphingolipids are enriched in specific regions of the exoplasmic leaflet of the plasma membrane (reviewed in Brown and London, 1998; reviewed in Simons and Ikonen, 1997; reviewed in Simons and van Meer, 1988). The raft concept has long been controversial, largely because it has been difficult to methodologically prove the existence that rafts exist in living cells (reviewed in Rajendran and Simons, 2005). The lack of standardised methodology has led to some confusion in the current nomenclature between rafts, DRMs and caveolae (**Fig. 10**). However, the organisation and the dynamic of these domains are likely to be cholesterol-dependent submicron-sized domains (Nohe et al., 2006; reviewed in van der Goot and Harder, 2001). It

is interesting to mention that raft isolation using the technique of DRMs flotation is dependent on the type of detergent used during cell fractionation (Schuck et al., 2003).

Suggested raft nomenclature

	I. Rafts	II. Clustered rafts	III. DRMs	IV. Caveolae
Components	• Glycosphingolipids • Cholesterol • Lipid-modified proteins containing saturated acyl chains: – GPI-anchored proteins – Doubly acylated Src-type kinases • Transmembrane proteins	• Rafts clustered by: – Antibody – Lectin – Adjacent cell proteins – Physiological crosslinking proteins	• Rafts remaining insoluble after treatment on ice with detergent‡§: Triton X-100 (most popular), Brij-58, CHAPS, NP-40	• Raft proteins and lipids • Caveolins
Properties	• 50 nanometres in diameter • Mobile (~10^{-8} cm^{-2} sec^{-1}) • Liquid-ordered phase	• Large, often hundreds of nanometres to micrometres in size • Often bound to cytoskeleton	• Float to low density in sucrose or Optiprep™ density gradients	• Morphological 'cave-like' invaginations on the cell surface
Comments	• Native rafts are only detected in living cells	• Clustering is used both artificially and physiologically to trigger signalling cascades	• Non-native (aggregated) raft • Variable effects depending on: – Detergent type – Detergent:lipid ratio – Cell type	• Raft subcategory • Highly specialized

* DRM, detergent-resistant membrane; DIG, detergent-insoluble glycolipid-rich domain; DIC, detergent-insoluble complex; LDM, low-density membrane; DIM, detergent-insoluble material; GEM, glycolipid-enriched membrane; TIFF, Triton X-100 insoluble floating fraction.
‡Care should be taken when choosing solubilization conditions for co-immunoprecipitation experiments, as these popular detergents do not solubilize rafts on ice. Co-localization of proteins in rafts or DRMs could be mistaken for direct protein–protein interactions if rafts are not completely solubilized.
§Rafts can be solubilized in octyl glucoside or in the detergents listed above at raised temperatures.

Figure 10. Raft nomenclature based on specific properties
The lack of standardised methodology has led to confusion in the current nomenclature between rafts, clustered or not, detergent-resistant membranes and caveolae. Here some advantages and disadvantages of specific methods used to study rafts are summarised. Based on these considerations, Simons and coworkers propose a more standardised nomenclature. Source: Simons and Toomre, 2000.

Only a subset of lipid rafts is found in cell surface invaginations called caveolae (reviewed in Kurzchalia and Parton, 1999; reviewed in Nabi and Le, 2003; reviewed in Nichols, 2003). Caveolae are formed from lipid rafts by oligomerisation of caveolins – hairpin-like palmitoylated membrane proteins (reviewed in Parton, 1996; reviewed in Smart et al., 1999). The distribution of lipid rafts over the cell depends on the cell type (Levis et al., 1976; Renkonen et al., 1971; reviewed in Schuck and Simons, 2004). Interestingly, lipid rafts are present mainly on the basolateral side of epithelial cells (Vogel et al., 1998). Rafts are most abundant at the plasma membrane, but can also be found in the biosynthetic and endocytic pathways (reviewed in Rajendran and Simons, 2005). Lipid raft trafficking does not end with surface delivery. Rafts are continuously endocytosed (reviewed in Mukherjee and Maxfield, 2000). Recently, it has been shown that caveolae can communicate with early endosomes (Pelkmans et al., 2004). From early endososmes, lipid rafts either recycle directly back to the

cell surface or return indirectly through recycling endosomes, which could also deliver rafts to the Golgi (Puri et al., 1999).

Caveolae represent just one type of cholesterol-rich microdomains on the plasma membrane. Recently, additional proteins such as the Flotillins have been found to organise lipid rafts. Flotillins have been identified to be present in rafts by cell fractionation assay and electron microscopy (Bickel et al., 1997; Kokubo et al., 2003). Flotillins are palmitoylated scavenger proteins showing a subcellular localisation that is distinct or even complementary to that of Caveolins. Flotillin molecules cocluster with GPI-anchored adhesion molecules in non-caveolar domains (Lang et al., 1998). However, Flotillins can form a hetero-oligomeric 'caveolar' complex when coexpressed with caveolins (Volonte et al., 1999). These two types of proteins seem to be related but independent as the cellular localisation of Flotillin does not require caveolin expression (Fernow et al., 2007). These new results shed light on the complexity of raft domains.

Furthermore, raft-association might have an important role in the biogenesis of apical membrane domains during development (reviewed in Schuck and Simons, 2004). In polarised epithelia, two membrane domains are separated by tight junctions which prevent mixing of apical and basolateral components (reviewed in Tsukita et al., 2001). It has been shown that GPI-APs are enriched in raft domains (reviewed in Hooper, 1999). The presence of GPI-APs in lipid rafts is likely to have a physiological relevance, since the replacement of the GPI anchor by a transmembrane domain modulates signal transduction events (Incardona and Rosenberry, 1996). This is also true for Cripto (Watanabe et al., 2007). When, the GPI-anchor of Cripto was exchanged with a transmembrane (TM) domain, Nodal signalling was inhibited except upon ALK4 overexpression.

One way to consider rafts is that they form concentrating platforms for individual receptors, activated by ligand binding (reviewed in Hunter, 2000). Indeed, the most important role of rafts at the cell surface may be their function in signal transduction (reviewed in Simons and Toomre, 2000). Rafts also dictate the sorting of associated proteins and provide sites for assembling cell surface receptor such as T-cell antigen receptor (Janes et al., 2000) or receptor ligand such as GDNF (Tansey et al., 2000), and Hedgehog (Hh) (reviewed in Incardona and Eaton, 2000). Both cholesterol and the actin cytoskeleton are necessary in establishing a membrane environment that provides the suitable environment for raft-associated enzymes

(Chichili and Rodgers, 2007). Indeed, if receptors enter lipid rafts, the signalling complex is protected from non-raft enzymes, such as membrane phosphatases, that otherwise could affect the signalling process.

4.12 Specific markers define certain membrane vesicles during post-endocytic trafficking

Vesicle formation, motility and tethering to target compartments are regulated by specific effectors including small GTPases of the Rab family. Rab effectors are not randomly distributed on the organelle membrane but are clustered in distinct functional domains. In the early endocytic pathway, Rab5 regulates CCV transport from the plasma membrane to early endosomes (Bucci et al., 1992; Gorvel et al., 1991). Early endosome-associated antigen-1 (EEA1) is a key effector that mediates docking of early endosomes (Christoforidis et al., 1999). Three main populations of endosomes can be distinguished: one that contains primarily Rab5, a second that contains both Rab5 and Rab4, and a third one that carries Rab4 and Rab11 (reviewed in Zerial and McBride, 2001). The former two correspond to early/sorting endosomes and the latter to late/perinuclear recycling endosomes (**Fig. 11**).
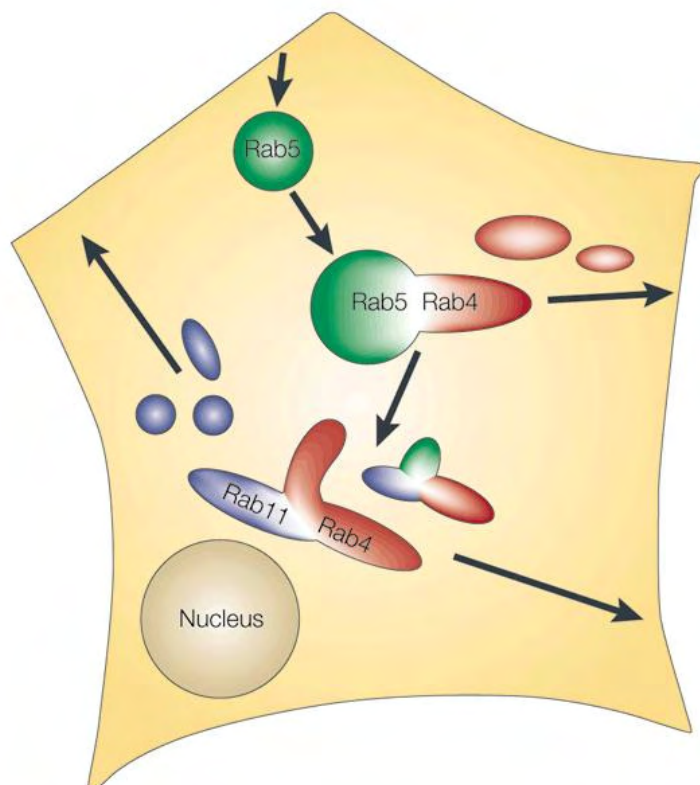

Figure 11. Rab-GTPases define specific vesicles along the endosomal pathway Rab5, Rab4 and Rab11 tagged with green fluorescent protein (GFP) mark distinct early endosomes. Cargo flows sequentially through these domains as indicated by the arrows. Source: Zerial and McBride, 2001.

In other words, while Rab5 provides a gateway into early endosomes, the Rab4 and Rab11 activate machineries that are necessary for protein sorting and recycling to the cell surface. Rab5, Rab4 and Rab11 can dynamically interact but keep a relatively stable distribution over time. After early endosome entry, proteins targeted for degradation are directed to late endosomes (marked by Rab7) after pH acidification. Late endosomes will then mature into lysosomes of the vesicular lumen for final protein degradation. Transport to lysosomes is preceded by the formation of intravesicluar vesicles present in compartments called multivesicular endosomes (MVEs) which further mature into multivesicular bodies (MVBs).

4.13 Multivesicular endosomes (MVEs) are specialised platforms required for sorting or further degradation

The early endosome is a mosaic and dynamic compartment (reviewed in Miaczynska and Zerial, 2002). It displays a highly complex and pleiomorphic organisation that consists of cisternal regions from which tubules and vesicles form protrusions. In addition, membrane invaginations which occur towards the centre of the vesicle can bud and lead to the formation of MVEs (reviewed in Gruenberg, 2001). Tubular elements resemble recycling endosomes, whereas multivesicular elements resemble the endosomal carrier vesicles/multivesicular bodies (ECV/MVBs) of the degradative pathway. In mammalian cells, MVBs are clearly distinct from both early and late endosomes. Recent ultrastructural studies point to the existence of distinct subpopulations of MVBs. Some MVBs are able to recycle vesicles, and thus proteins, to the plasma membrane, whereas others containing the lipid lysobisphosphatidic acid (LBPA) target proteins to lysosomal degradation (White et al., 2006). Proteins that are destined to be degraded accumulate on MVB internal membranes. Internalisation into MVB can be triggered by ubiquitination (**Fig. 12**). Ubiquitin (Ub) is a conserved protein of 76 amino acids that can be conjugated to other proteins. The predominant model proposes that internalised receptors are prevented from being recycled by becoming sequestered inside MVB, a compartment generated through inward budding of vesicles (reviewed in Di Fiore et al., 2003). Subsequently, MVBs fuse with lysosomes, resulting in degradation of their cargo by lysosomal acidic hydrolases (reviewed in Gruenberg, 2001). For example, the EGF receptor and its ligand are sorted into the lumen of MVB for degradation and ligand-induced receptor downregulation (reviewed in Katzmann et al., 2002; Sigismund et al., 2005)

Monoubiquitination can thus serve as a signal for both endocytosis and MVE sorting (reviewed in Raiborg and Stenmark, 2002). The Ub-binding protein Hrs/Vps27 is required in this sorting process (Bache et al., 2003). In addition, four conserved multisubunit complexes, endosomal sorting complex required for transport (ESCRT)-0, -I, -II, -III facilitate the trafficking of ubiquitinated proteins from endosomes to lysosomes via MVBs (reviewed in Williams and Urbe, 2007).
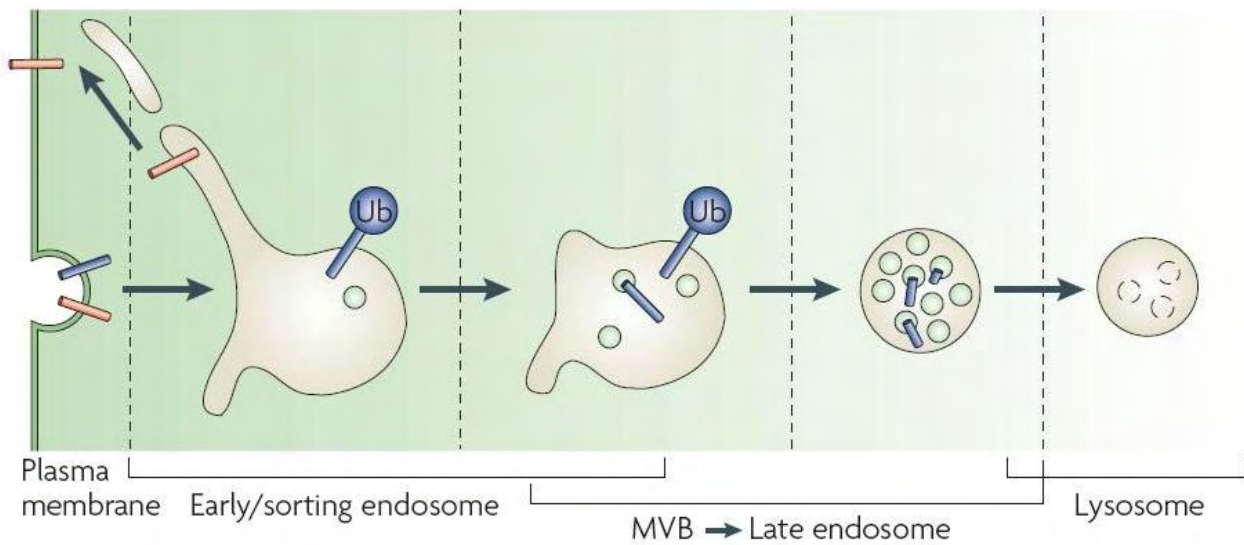
Figure 12. Transport from early endosomes to lysosomes via MVBs
Integral membrane proteins and their ligands can be removed from the plasma membrane by incorporation into endocytic vesicles that fuse with an early endosomal compartment (also known as a sorting vesicle). Both cargoes that are destined for degradation and for recycling pass through the sorting endosome. Tubular elements from this tubulovesicular compartment undergo fission to become incorporated into recycling endosomes from which the cargo is returned to the plasma membrane. Ub functions as the principal targeting signal to direct cargo incorporation into intralumenal vesicles to form MVBs that fuse with the late endosome. The progression from early to late endosomes is marked by replacement of Rab5 with Rab7. Source: Williams and Urbe, 2007.

The ESCRT complex is essential for both sorting and multivesicular endosome formation (reviewed in Raiborg et al., 2003). Hrs is part of the ESCRT-0 complex. Hrs is a FYVE-domain protein that is recruited to endosomes via PI(3) kinase binding (Raiborg et al., 2001). Hrs also mediates the recruitment of ESCRT-I to early endosome (Bache et al., 2003). In turn ESCRT-I binds ubiquitinated proteins. ESCRT-II then recruits ESCRT-III which orchestrates the deubiquitination of the cargo. Although the ubiquitin group is a sorting determinant for the selection of MVB cargo proteins, this group seems to be removed from these proteins before they are delivered into MVB vesicles. By contrast, polyubiquitin chains target proteins for degradation by the 26S proteasome (reviewed in Pickart, 2001).

50

Both cargoes that are destined for degradation and for recycling pass through the sorting endosome. It thus seems that certain platforms allow a communication between the established endocytic pathways.

4.14 Endocytic pathways communicate with each other

Recent data have shown that caveolin1-positive vesicles can interact with early endosomes in a Rab5-dependent process (Pelkmans et al., 2004). Caveolin1 was found on structures positive for endosomal makers as EEA1. These organelles were either small vesicles or larger structures with irregular shapes. It thus seems that caveolar vesicles can move from caveosomes to early endosomes. This communication involves a pathway regulated by Rab5. In addition, this study showed that release and uptake of caveolar cargo depends on how the cargo molecules interact with Caveolin1 or other caveolar proteins and with lipids. The enrichment of lipid rafts in caveolae would seem an ideal mechanism for sorting molecules such as lipids and lipid-associated proteins. Interestingly, it was first thought that lipid rafts were specific to caveolar domains. It has become clear that lipid rafts are not restricted to caveolae. Instead, these lipid-enriched domains are present in the plasma membrane, on endosomes, on the Golgi as well as on MVBs (reviewed in Rajendran and Simons, 2005).

Cells use various pathways to control cell-surface receptors and probably can adapt to different conditions such as serum deprivation. The understanding of these interdependent mechanisms is crucial to integrate all the possibilities that a protein has to do its job. Further discoveries on the regulation of cell signalling, receptor turnover, and the magnitude, duration and nature of signalling events is essential for defining the whole picture of endocytic itineraries.

5 Hypothesis of the present project

Given the characteristic trafficking of GPI-APs, and prompted by our observation that Cripto binds uncleaved Nodal, we hypothesised that Cripto may play an essential role in localising Nodal precursor processing to specific target membranes. In particular, it seemed possible that Nodal processing must be localised in order to shield the mature protein against preemptive degradation and/or to access endocytic compartments that are competent to activate Smad2/3 transcription factors in the cytoplasm.

To test this hypothesis, we characterised Nodal trafficking and its regulation by Cripto in cell transfection assays. In first place, we started to elucidate how Nodal is secreted to reach proprotein convertases. In particular, we investigated whether Nodal can bypass the TGN and thereby avoid proteolytic cleavage during exocytosis. We showed that Cripto captures Nodal already during secretion, partly via the propeptide, and assembles a processing complex with the proprotein convertases Furin at the cell surface. Subsequently, Cripto mediates uptake of mature Nodal via a nonclathrin, noncaveolar pathway to signalling endosomes. Our results suggest that Cripto is a receptor for proprotein convertases and couples Nodal processing and signalling in target cells.

6 RESULTS

6.1 Processing and secretion of Nodal and Cripto

As a basis to address how Cripto potentiates Nodal signalling, we determined how Nodal protein is modified during exocytosis in the absence of Cripto. Western blot analysis of transfected cells shows that incubation with endoglycosidase-H (EndoH) or N-glycosidase F (N-glycF) shifted the apparent molecular weight of intracellular Nodal from 42 kDa (N-42) to 39 kDa, the predicted size of unmodified precursor. In contrast, the 47 kDa (N-47) soluble Nodal precursor and propeptide (35 kDa) in conditioned medium were sensitive to N-glycF and neuraminidase (neuramin), but not to Endo-H, indicating that they have acquired complex carbohydrates in the Trans Golgi Network (TGN). (**Fig. 13A**). We also monitored processing of Cripto. Cripto is tethered to membranes via a GPI anchor (Kenney et al., 1996; Minchiotti et al., 2001). The predicted molecular weight of full-length Cripto is 18 kDa, but a prosegment is cleaved off after proline 52 (P52) during secretion by an unknown protease (Kenney et al., 1996; Minchiotti et al., 2001). Upon incubation with EndoH or N-glycF, the bulk of the 18 kDa form of Cripto in cell lysates was shifted to 13 kDa. Likewise, inhibition of N-glycoysyltransferases in the ER by tunicamycin (tunic) shifted Cripto to 13 kDa (**Fig. 13B**). This suggests that Cripto is cleaved and N-glycosylated before transport to the Golgi apparatus.
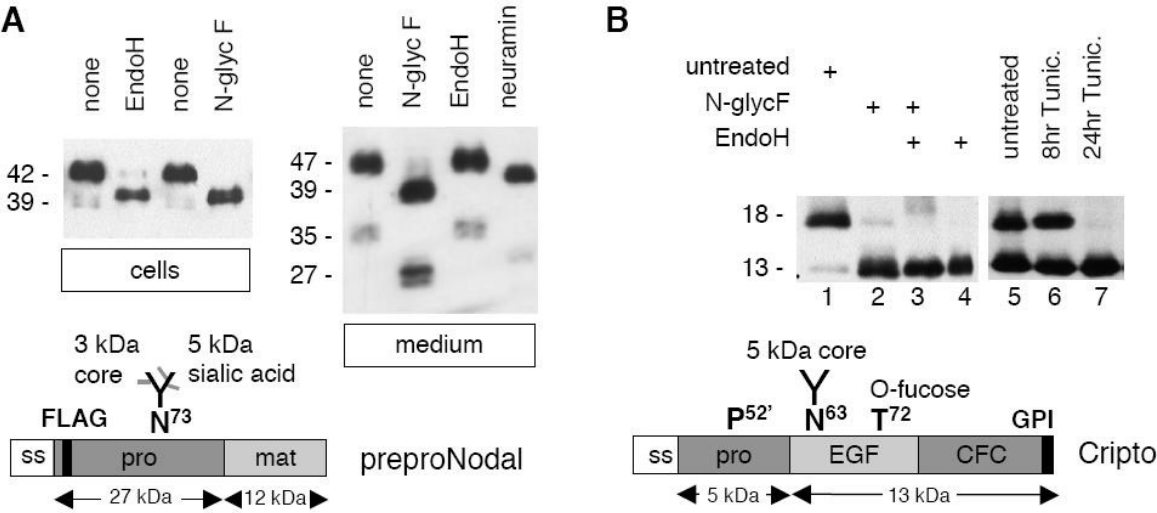

Figure 13. Post-translational modifications of Nodal and Cripto

(**A**) Western blot analysis of Nodal in lysates (left) and conditioned medium (right) of transfected COS1 cells. Upon treatment with either endoglycosidase-H or N-glycosidase F, intracellular Nodal (42 kDa) was shifted to an apparent molecular weight of 39 kDa, the predicted size of unmodified precursor. In contrast, soluble Nodal precursor and the propeptide in conditioned medium (47 kDa) were sensitive to N-glycosidase F and neuraminidase, but not to endoglycosidase H, indicating that they have acquired complex carbohydrates. The cartoon (bottom) summarizes the impact of processing on the size of Nodal. (This experiment was performed by J. Ann Le Good.)

(**B**) Western blot analysis of Cripto in COS1 cell lysates before and after treatment with N-glycosidase F (lane 2), endoglycosidase H (lane 3) or both (lane 4), or after incubation of cells with tunicamycin (lane 7). The bulk of Cripto corresponds to a processed 13 kDa form which lacks the N-terminal 52 amino acids (Minchiotti et al., 2001), but migrates at an apparent molecular weight of 18 kDa due to high mannose N-glycosylation. The threonine (T72) to which an O-fucose is linked in Cripto plays a key functional role. However, the sugar modification itself at the position 72 is not required for Cripto to function (Shi et al., 2007). (This experiment was performed by J. Ann Le Good.)

Immunofluorescence analysis of permeabilised transfected cells revealed that Cripto and Nodal colocalise in a reticular network which extends to the cell periphery and harbors the ER marker RFP-KDEL, indicating that both of these proteins reside in the ER (**Fig. 14**).
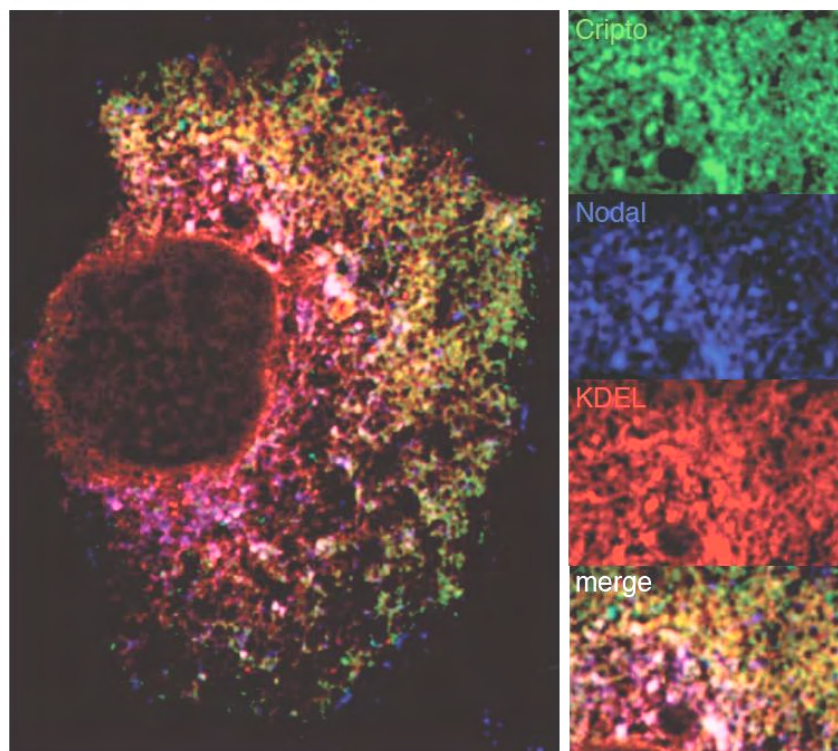
Figure14. Nodal and Cripto colocalise with ER marker KDEL
Immunofluorescence analysis of permeabilised COS1 cells expressing Cripto (green) together with Nodal (blue) reveals significant colocalisation (white) with RFP-KDEL (red), a marker of the endoplasmatic reticulum.

To assess how Cripto is secreted, we monitored the effect of brefeldin A (BFA), a compound which blocks ER to TGN transport. In control experiments, we analysed mutant Cripto

carrying a 6xHis tag instead of the GPI signal sequence (CriptoΔGPI). CriptoΔGPI is secreted and migrates with an apparent molecular weight of up to 29 kDa due to complex carbohydrate modifications (Kenney et al., 1996; Minchiotti et al., 2001). As expected, Western blot analysis and immunostaining of unpermeabilised cells revealed that treatment with BFA completely blocked the secretion and cell surface expression of CriptoΔGPI (**Fig. 15A, B**).
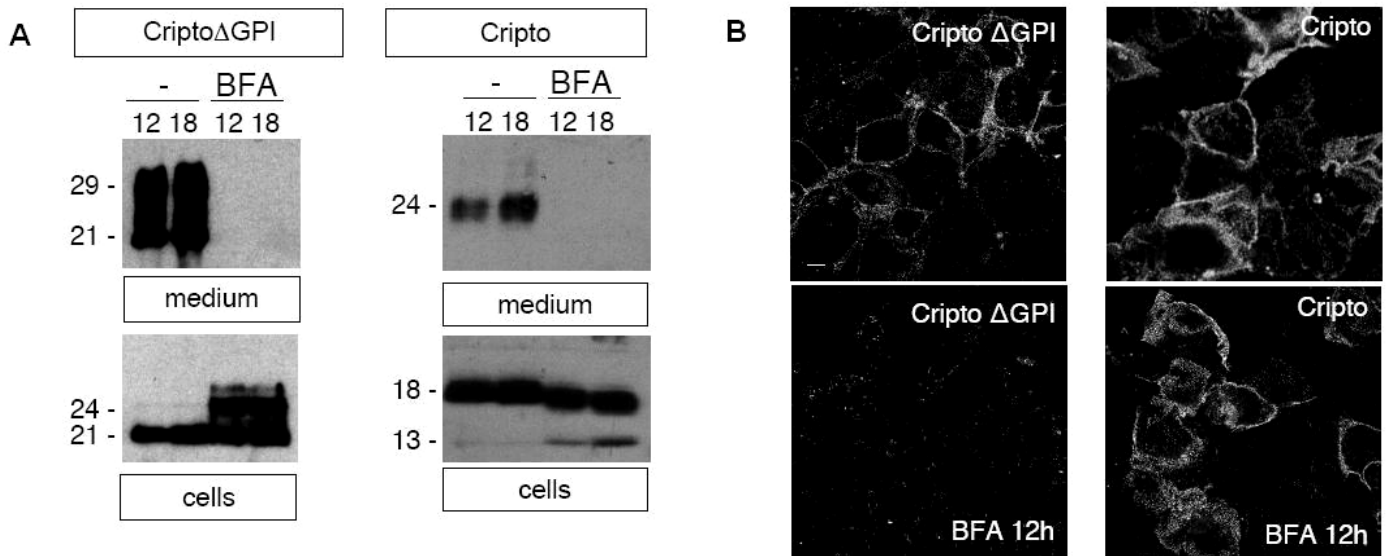
Figure15. BFA treatment inhibits Cripto secretion, but not its presentation at the plasma membrane
(**A**) Left: Truncated mutant Cripto lacking a GPI signal (CriptoΔGPI) is shifted in size to 29 kDa by complex carbohydrate modifications (Minchiotti et al., 2001), and its release into conditioned medium is blocked by BFA, indicating that it is secreted via the TGN. Right: Also shedding of wild-type Cripto into the medium is abolished in the presence of BFA.
(**B**) Immunostaining of unpermeabilised COS1 cells shows that BFA blocks expression of CriptoΔGPI at the cell surface, but not that of wild-type Cripto. Scale bar: 10 μm.

BFA also blocked shedding of the GPI anchor and secretion of wild-type Cripto into the medium (**Fig. 15A**). Unexpectedly, however, BFA completely failed to inhibit accumulation of GPI-anchored Cripto at the cell surface (**Fig. 15B**). This result suggests that GPI-anchored Cripto at the plasma membrane either fails to be cleared within the time frame analysed, or is maintained at the plasma membrane by TGN-independent exocytosis.

6.2 Cripto intercepts the Nodal precursor during exocytosis

To test whether Cripto regulates Nodal exocytosis or processing, wild-type Nodal or cleavage-resistant mutant precursor were cotransfected with increasing doses of Cripto. Cripto dose-dependently inhibited the release of the 47 kDa form of wild-type Nodal precursor into the medium. This effect was specific in that the SPC-resistant mutant Nodal (Nr) was barely affected by Cripto (**Fig. 16A**). Secondly, the secretion of Cripto is not diminished, but rather increases in cells coexpressing Nodal (data not shown), suggesting that non-specific trapping in the ER is unlikely. Thirdly, the release of the 47 kDa form of wild-type Nodal is rescued when Cripto lacks a GPI signal (**Fig. 16B**). These results suggest that membrane-bound Cripto directly or indirectly reduces the stability of the Nodal precursor by a mechanism that requires SPC-mediated processing.
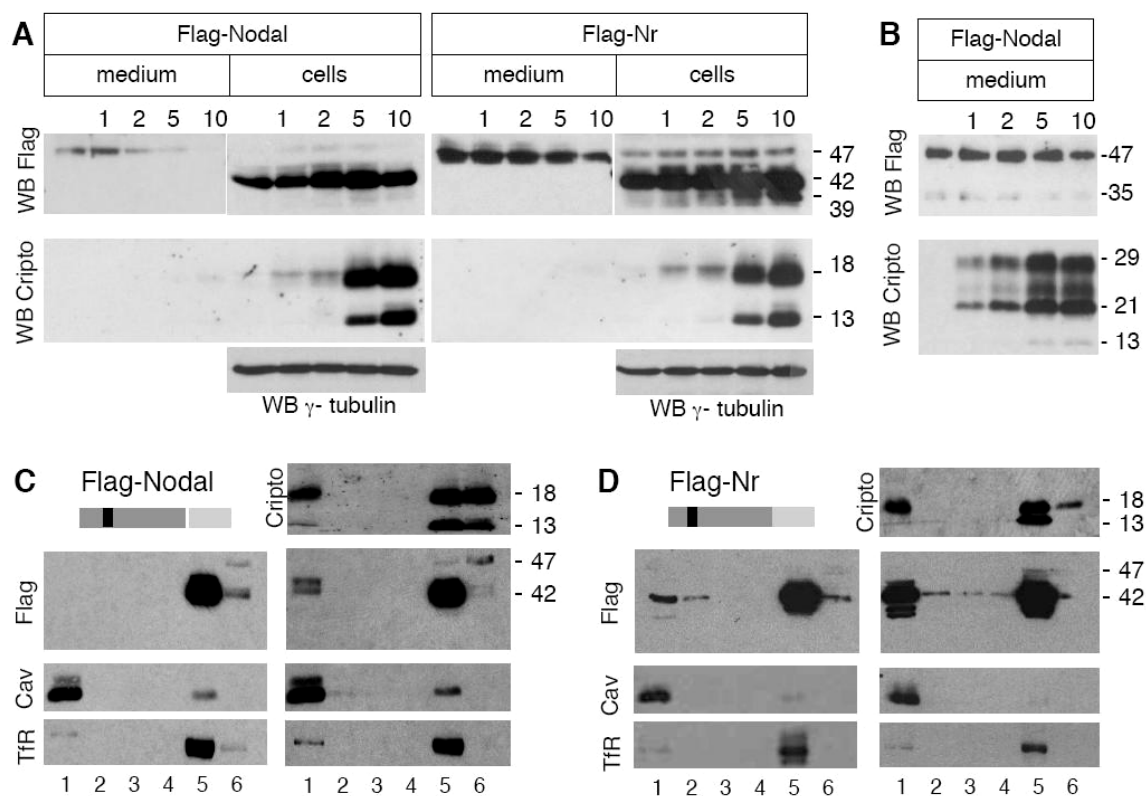
Figure 16. GPI-anchored Cripto intercepts the Nodal precursor in lipid rafts
(**A**) In cotransfection assays, Cripto dose-dependently reduces the amount of soluble Flag-tagged Nodal precursor (47 kDa) in conditioned medium (top left panels). Compared to wild-type Nodal, mutant precursor lacking the SPC cleavage site (Nr, right panels) is more resistant to Cripto-induced turnover. Bottom panels : GPI-anchored Cripto accumulated in cell lysates, but remained below detectable levels in conditioned medium, except at the maximal concentration examined (10 µg) or after prolonged exposure of the blot (not shown). The anti-Flag Western blot of cell lysates is overexposed to detect terminally modified Nodal precursor (47 kDa).

(**B**) Truncated Cripto lacking the GPI anchor is released without affecting Nodal secretion or turnover. The Nodal propeptide (35 kDa) can be detected in small amounts in conditioned medium, but is below detectable levels in cell lysates (Constam and Robertson, 1999).

All results are representative of more than three independent experiments. Cripto cDNAs (1 to 10 µg) were balanced with empty vector to ensure that the total amount of transfected Cripto DNA in all transfections was 10 µg. Western blot analysis of γ-tubulin served as a loading control.

(**C, D**) Unlike wild-type Nodal (C), cleavage–resistant precursor (Nr) is detected together with a breakdown product (38 kDa) in the density fraction 1 even in the absence of Cripto (D, left panels). Cripto increases the amount of wild-type precursor and Nr (42 kDa) in fraction 1 (C-D, right panels).

A common feature of GPI-anchored proteins is their localisation in lipid microdomains known as rafts. To assess whether Cripto recruits the Nodal precursor to lipid rafts, detergent lysates of transfected cells were fractionated by density gradient centrifugation. In the absence of Cripto, the Nodal precursor was only detected in high density fractions 5 and 6, together with transferrin receptor. By contrast, when cotransfected with Cripto, a significant amount of uncleaved Nodal localised to detergent resistant membrane fraction 1 containing the raft marker Caveolin-1 (**Fig. 16C**). Nodal protein in the raft fraction migrated with an apparent molecular weight of 42 kDa, suggesting that it corresponds to the EndoH-sensitive precursor pool that has not yet passed the TGN (**cf. Fig. 13A**). To exclude that the secreted 47 kDa form of Nodal simply escaped detection in rafts due to proteolytic processing, we also monitored the raft partitioning of the mutant precursor Nr, which is resistant to SPC-mediated processing. The 42 kDa form of Nr, but no Nr-47 was detected at low levels in fraction 1 even in the absence of Cripto (**Fig. 16D**). Furthermore, the levels of Nr-42 in the raft fraction dramatically increased upon cotransfection of Cripto, whereas Nr-47 was detected after overexposure in fractions 5 and 6 (**Fig. 16D**, and data not shown). Overall, these results indicate that Cripto intercepts a pre-TGN 42 kDa form of Nodal precursor in specific membrane microdomains leading to Nodal processing and turnover in an SPC-dependent manner.

6.3 The Nodal precursor reaches the cell surface via a TGN-independent route

Proteases of the SPC family rely on pH-dependent autocleavage of their propeptides in acidic endosomes as they cycle between the plasma membrane and TGN (Anderson et al., 2002; Chapman and Munro, 1994; Mallet and Maxfield, 1999; reviewed in Thomas, 2002). Endosomal recycling also appears to be crucial for secretion, since inhibitors of endosomal

acidification such as NH$_4$Cl block the release of Furin and PACE4 in medium (**Fig. 17A**, and data not shown).
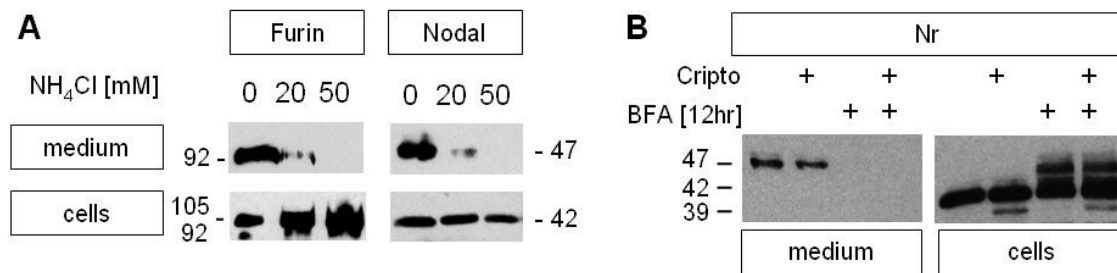
Figure 17. Transport through the TGN/endosomal system is essential for the secretion and processing of Nodal precursor
(**A**) Transfected COS1cells and conditioned medium analysed by immunoblotting for expression of Flag-tagged Furin and SPC-resistant Nodal precursor (Nr) after treatment for 20 hr with or without NH$_4$Cl. (This experiment was performed by J. Ann Le Good.)
(**B**) In cells treated with BFA (5 µg/ml), modification of Nodal by complex carbohydrates (47 kDa) is not inhibited even after prolonged treatment (18 hr, right panel), indicating that Nodal still reaches the BFA compartment (reviewed in Nebenfuhr et al., 2002). However, Nodal secretion into the medium is blocked by BFA irrespective of whether or not the cells were cotransfected with Cripto (left panel).

Prompted by these observations, we asked how N-42 can access an activated pool of SPCs already before entering the TGN. This paradox may be resolved if Nodal precursor first reaches the plasma membrane for cleavage by extracellular SPCs, before secretion via the TGN. In this scenario, both BFA and inhibitors of endosomal acidification should block Nodal secretion. In contrast, if Nodal reaches the TGN independently of endosomes, only BFA should have an effect. Western blot analysis of cells expressing Nr revealed that both BFA and NH$_4$Cl inhibit the release of Nodal precursor (**Fig. 17A, B**).

Figure 18. BFA treatment corresponds with an increase of intracellular Nodal precursor
(**A**) After treatment with BFA (5 µg/ml), the amount of resistant to cleavage Nodal (Nr) were increase in the cell lysate.
(**B**) After treatment with BFA (5 µg/ml), similar results were found with wild-type Nodal.

58

In BFA-treated cells, there was a corresponding increase in the intracellular levels of Nodal precursor carrying complex carbohydrates (Nr-47), indicating that Nr is retained in the so-termed BFA compartment together with sialyltransferases that are shunted from the TGN to endoso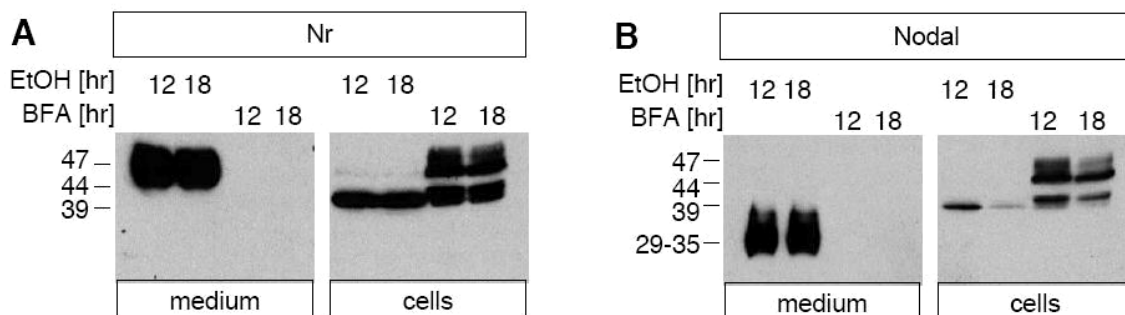mes (reviewed in Nebenfuhr et al., 2002). Similar results were obtained in 293T cells (**Fig. 18A**). Next, we analysed the effect of BFA on wild-type Nodal precursor and its proprotein convertases. As predicted, BFA also abolished the release of cleavable Nodal (**Fig. 18B**), as well as of Furin and PACE4 (data not shown). Overall, these results show that acidic compartments and the TGN are essential to release Nodal and its convertases into the medium.

To test whether BFA also blocks Nodal expression at the cell surface, unpermeabilised cells were stained by indirect immunofluorescence after addition of fresh medium. Expression of Nodal precursor at the cell surface was not inhibited even after 12 hr of incubation with BFA, although the signal became more patchy (**Fig. 19**).
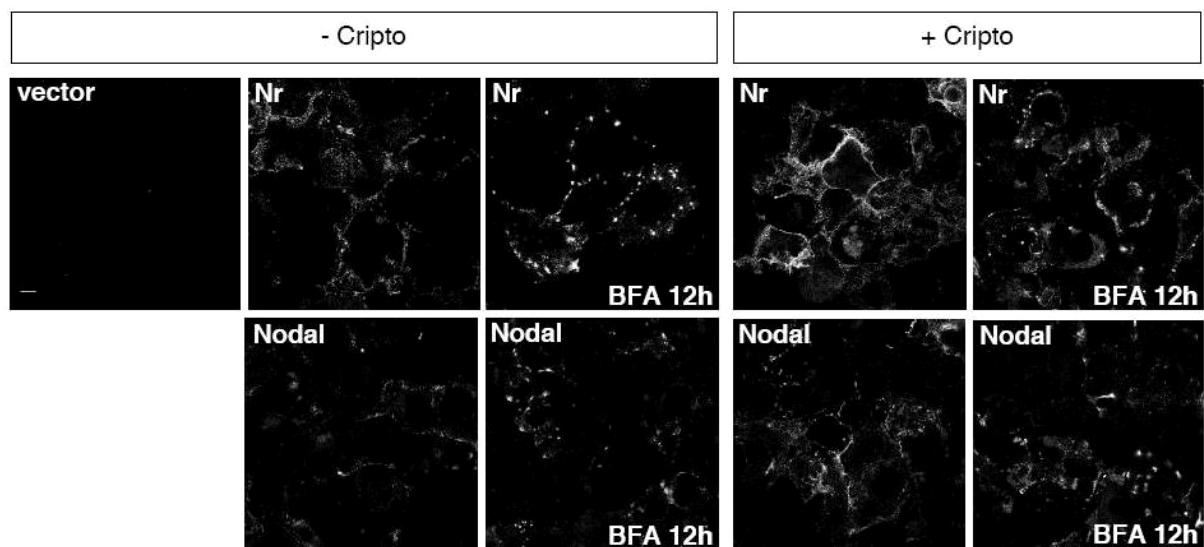
Figure 19. Transport through the TGN/endosomal system is not required for Nodal cell surface expression
Immunostaining of Flag-tagged Nr and wild-type Nodal precursor at the surface of unpermeabilised COS1 cells that had been treated with or without BFA. Note that BFA does not prevent the accumulation of uncleaved Nodal precursor at the cell surface. The fact that BFA fails to prevent the accumulation of uncleaved Nodal precursor and Cripto at the plasma membrane suggests that both proteins reach the cell surface by a TGN-independent route. However, release into the culture medium requires transport through the TGN, possibly via NH$_4$Cl-sensitive endocytic pathways implicated to supply the TGN also with Furin (Anderson et al., 2002; Chapman and Munro, 1994; Mallet and Maxfield, 1999). Scale bar: 10μm.

Similarly, in cells cotransfected with Cripto, treatment with BFA failed to block cell surface expression of either Nr or wild-type Nodal (**Fig. 19**). This is unlikely due to inefficient endocytosis and a prolonged half life of Nodal at the cell surface, because the Nodal precursor under these conditions enters the intracellular BFA compartment, and because Nodal in conditioned medium was cleared within less than 4 hr of BFA treatment (data not shown). More importantly, immunoprecipitation analysis of cell surface complexes after reversible chemical crosslinking by the membrane-impermeable reagent DTSSP clearly shows that Nodal and Cripto at the cell surface correspond in size exclusively to pre-TGN pools in the ER (Ben-Haim et al., 2006; Chen and Shen, 2004; Yan et al., 2002). Thus, we propose that Nodal and Cripto expression at the cell surface is sustained by a BFA-insensitive TGN-independent exocytic pathway, whereas transport through the TGN releases these proteins into conditioned medium.

6.4 Cripto independently interacts with processed Nodal and its propeptide

To assess whether Nodal binds Cripto before undergoing proteolytic maturation, a mixture of soluble Nodal propeptide, mature form and residual uncleaved precursor (**Fig. 20A**, top panels) was incubated with metal agarose beads soaked with (lanes 1, 2) or without (lanes 3, 4) CriptoΔGPI. Cripto mainly pulled down uncleaved Nodal (first two panels, lane 1), despite of a molar excess of processed Nodal and propeptide in the input (last two panels, lane 1). However, the mutant cleavage site Nodal-sc (Nodal super-cleaved) which is more efficiently processed (Constam and Robertson, 1999) facilitated pull-down of both mature Nodal and propeptide by Cripto (lane 2). These results indicate that Nodal can interact with Cripto before and after proteolytic maturation.

To validate this conclusion, and to determine how Cripto interacts with intracellular Nodal, the GPI-anchored form was solubilised and coimmunoprecipitated with various Flag-tagged mutant Nodal proteins. In cell extracts, both N-42 and Nr-42 precursor proteins precipitated the 18 and 13 kDa forms of Cripto (**Fig. 20B**, lanes 1, 2). Both forms of Cripto were also pulled down by constitutively mature Nodal (Nmat, lane 3) fused to a secretory signal sequence whitout the prodomain (Le Good et al., 2005). Likewise, the Nodal propeptide alone efficiently precipitated Cripto, although this complex was less soluble in detergent extracts

(Npro, lane 4, and data not shown). In control experiments, Cripto was not precipitated by the TGF-β family member Dorsalin (data not shown). These results demonstrate that membrane-anchored Cripto, similar to its soluble mutant derivative, specifically binds uncleaved Nodal both via the mature domain and the propeptide.
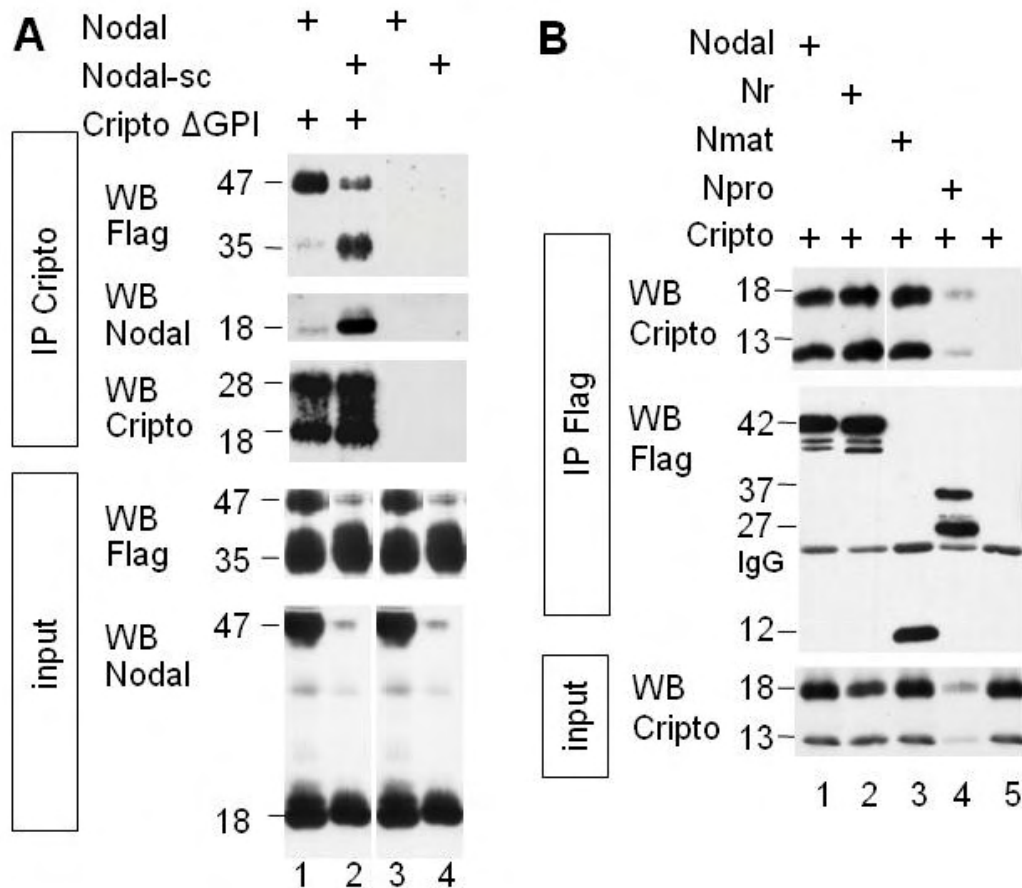
Figure 20. Cripto interacts with both mature Nodal and the prodomain to bind uncleaved precursor
 (**A**) Precipitation of Flag-tagged Nodal precursor and cleaved fragments (pro, mat) by truncated soluble Cripto devoid of a GPI anchor. Supernatant of 293T cell lines containing a mixture of Nodal prodomain, mature form and residual uncleaved precursor (bottom panels, input) was incubated with metal agarose beads soaked with (lanes 1, 2) or without (lanes 3, 4) histidine-tagged Cripto (CriptoΔGPI). Western blot (WB) analysis of precipitates revealed that soluble Cripto (18-25 kDa) precipitates uncleaved Nodal precursor (53 kDa), together with small amounts of prodomain (35 kDa) and mature form (18 kDa, lane 1). When the Nodal cleavage site RQRRHHL is mutated to RQRRH<u>LE</u> (Nodal supercleaved) to increase processing (Constam and Robertson, 1999), binding of Cripto to mature Nodal and cleaved prodomain fragment is increased (lane 2). The molecular weights of mature Nodal (12 kDa) and precursor (47 kDa) are shifted by 6 kDa due to an N-glycosylation site from *Xenopus* Nodal proteins, which was added to the C-terminal domain to improve protein stability (Le Good et al., 2005). Non-specific binding of Nodal to empty beads was below detectable levels (lanes 3, 4). (This experiment was performed by J. Ann Le Good.)
(**B**) Both wild-type Nodal and an SPC-resistant mutant precursor (Nr) carrying a Flag epitope in the prodomain pull down GPI-anchored Cripto from detergent-soluble COS1 cell extracts (lanes 1-2). GPI-anchored Cripto was also precipitated by mature Nodal (Nmat, lane 3) or propeptide (Npro, lane 4), but not in the absence of Nodal (lane 5). High levels of Npro reduce the detergent solubility of Cripto (lane 4). (This experiment was performed by J. Ann Le Good.)

6.5 Cripto and Nodal precursor associate before Nodal cleavage

Our finding that Cripto and Nodal in coimmunoprecipitates lack complex carbohydrates confirms that they already associate before reaching the dwellings of active Furin or PACE4. Therefore, we wished to identify a Cripto-interacting region in the Nodal propeptide and test whether it is necessary to activate Nodal. Alignment of prodomain sequences revealed that residues 215-226 upstream of the SPC cleavage motif are highly conserved among the Nodal proteins, but not in other TGF-βs (**Fig. 21**, and data not shown).

Figure 21. Position of a highly conserved motif among the Nodal proteins
Residues 211-240 of the murine Nodal prop peptide flanking the SPC cleavage motif (RXXR, not shown) and related sequences of Nodal homologs (top) and other TGFβ family members which interact with Cripto (murine Lefty1 and -2, Gdf1, Gdf3 and Xenopus Vg1). Conserved amino acids within the Cripto-interacting region 202-229 (CIR) are indicated in red. Mutated residues (216-223) are indicated in blue. Neither L216 nor Ser223 are conserved in TGFβ1-3, but present in BMPs and Activin βA,B chains, respectively.


```
Cyc      QDGASLLHTAGASKFLFSRNKKEVKRG
Sqt      AKTSTLIRTAEHSKYVALDRAGGGSEPVP
Spw      HSASSLMNTVAQSKYVTLNRPADGTQGR
Xnr1     IGFPSLIKTAESSKYVDIEKASRVPGIRRH
Xnr2     FGSPSLIHTVESSKYVMSENTVRVTDTR
Xnr3     PDPPSLGQTLFPSKYGIDDNANKVNGFR
Xnr4     SGTATLLQTAAHSKYLVVMPGIQTIAHTR
Parac.   VTDVTLVVFSRASTKPIILSDAYGSERT
hNodal   LGGSTLLWEAESSWRAQEGQLSWEWGK
mNodal   LGGATLLWEAESSWRAQEGQLSVERGGWGR
CIRmut   LGGATGLWEAGAHWRAQEGQLSVERGGWGR
                216   223

Lft1&2   VQREHLGPGTWSSHKLVRFAAQGTPDGKGQ

xVg1     DECKDIQTFLYTSLLTVTLNPLRCKRP
mGdf1    GATAACGRLAEASLLLVTLDPRLCPLP
mGDF3    QFNLQGALKDWSSNRLKNLDLHLEILVKED

mBmp2    RISRSLHQDEHSWSQIRPLLVTFGHDGKRHPLHK
mBmp4    RISRSLPQGSGDWAQLRPLLVTFGHDGRGHTLTRR
mBmp7    SINPKLAGLIGRHGPQNKQPFMVAFFKATEVHL

hActßA   EGGAGADEEKEQSHRPFLMLQARQSEDHPHR
hActßB   AVVPVFVDPGEESHRPFVVVQARLGDSRHR

hTß1     TGRRGDLATIHGMNRPFLLLMATPLERAQHLQSS
hTß2     GKTIKSTRKKNSGKTPHLLLMLLPSYRLESQQTNR
hTß3     NGDLGRLKKQKDHHNPHLILMMIPPHRLDNPGQGGQ
```

Deletion of this motif in the Npro-GFP fusion was not sufficient to abrogate binding to Cripto (data not shown). Therefore, to test whether the distal prosegment comprises a Cripto interacting region (CIR), it was fused to secreted CFP. Coimmunoproecipitation analysis showed that residues 203-229 of Nodal were sufficient to mediate binding of CFP to Cripto (**Fig. 22A**). This interaction was significantly diminished in three independent experiments upon mutation of the conserved residues L216 and S223 (**Fig. 22A**). These results suggest that the distal end of the Nodal prodomain significantly contributes to Cripto binding.

To assess whether the CIR controls Nodal activation, we monitored processing and signalling of mutant precursors lacking the CIR. Western blot analysis of transfected cells shows that deleting or mutating the CIR of the Nodal precursor barely affects Cripto-independent secretion or processing (**Fig. 22B** and data not shown). However, Cripto-mediated Nodal signalling was reduced more than 2.5-fold (**Fig. 22B**). Thus, the CIR is essential for Cripto-mediated activation of the Nodal precursor.
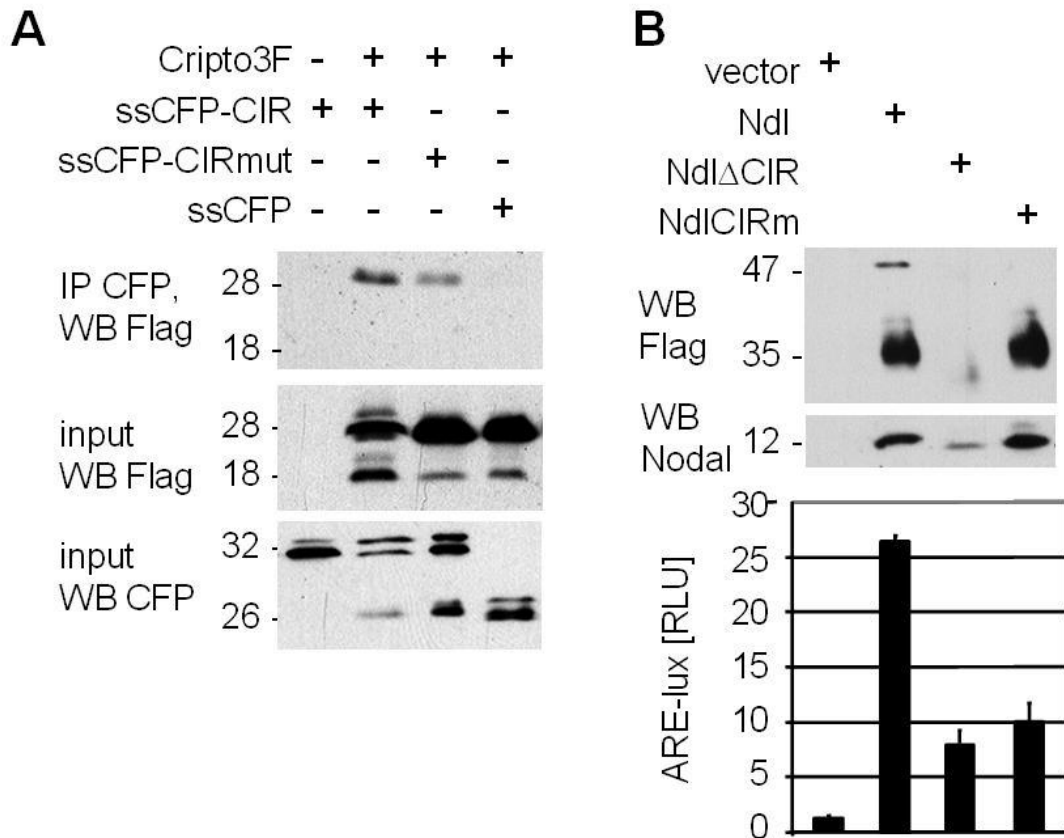
Figure 22. The Cripto interacting region (CIR) is required for efficient binding to Cripto and Smad2/3 activity
(**A**) Mutation of 4 conserved residues in the CIR (CIRmut, figure 21) reduces Cripto binding of a secreted CFP-CIR fusion protein to background levels.
(**B**) Western blot analyis of transfected 293T cells showing that both NdlΔCIR and NdlCIRmut can be processed independently of Cripto similar to the wild-type. Activation of wild-type and CIR-deficient Nodal precursors in 293T cells expressing Cripto together with the luciferase reporter ARE-lux. Data is representative of two separate experiments. Error bars indicate standard deviation of triplicate values.

6.6   Cripto binds the Nodal convertases Furin and PACE4

Since Cripto associates with uncleaved Nodal precursor, we asked whether it also recruits Nodal convertases. To test this hypothesis, cells were cotransfected with Cripto and Flag-tagged Furin or PACE4. Immunoprecipitation revealed that both Furin and PACE4 can pull down Cripto and vice versa (**Fig. 23A, B**).
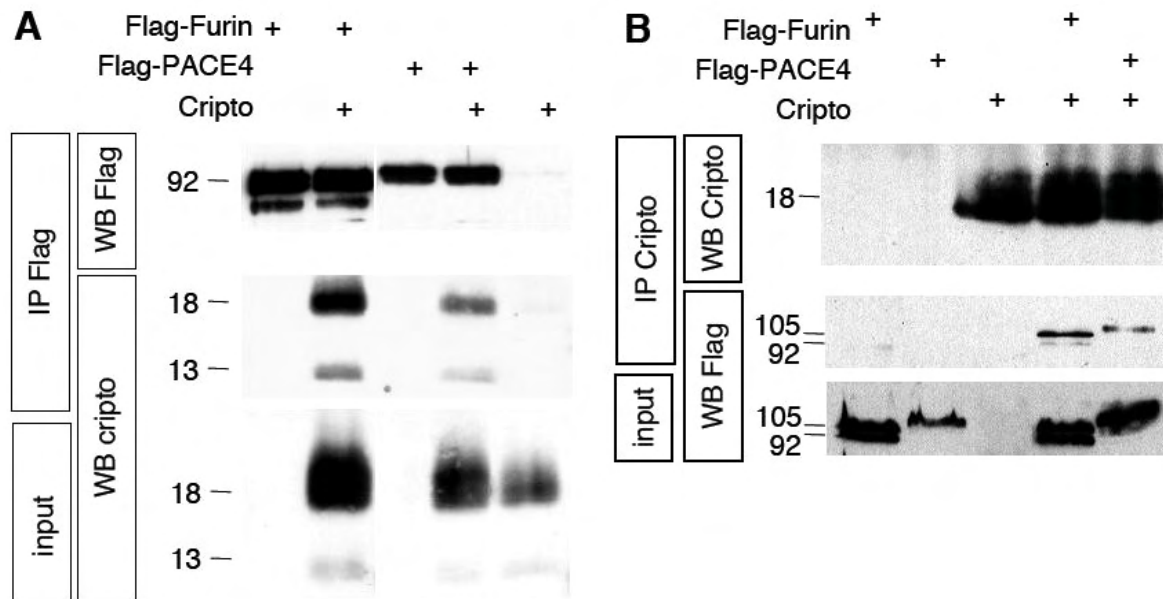
Figure 23. Binding of Cripto to Furin and PACE4
(**A**) Upon cotransfection in COS1 cells, Cripto can be coprecipitated with Flag-tagged Furin or PACE4, but not by control beads. (This experiment was performed by J. Ann Le Good.)
(**B**) Reverse pulldown of Furin and PACE4 by Cripto confirms the specificity of binding. (This experiment was performed by J. Ann Le Good.)

Deletion of the cysteine-rich domain (CRD) and the cytoplasmic tail of Furin did not abolish binding (data not shown), suggesting that Cripto interacts with upstream sequences such as the P-domain or the catalytic domain, or both. Deletion mutants of SPCs lacking the P-domain fail to undergo autocleavage and do no exit the ER (Gluschankof and Fuller, 1994; Takahashi et al., 1995). Therefore, to assess potential interactions with Cripto, the P-domain of Furin was separately expressed as a secreted CFP fusion protein, or only with a Flag tag inserted after an N-terminal hydrophobic leader. Cripto specifically immunoprecipitated the CFP fusion (**Fig. 24A**); conversely, Flag-tagged P-domain pulled down Cripto (**Fig. 24B**).

Together with data in **figure 20**, these results show that Cripto can independently bind the Nodal precursor and its convertases.
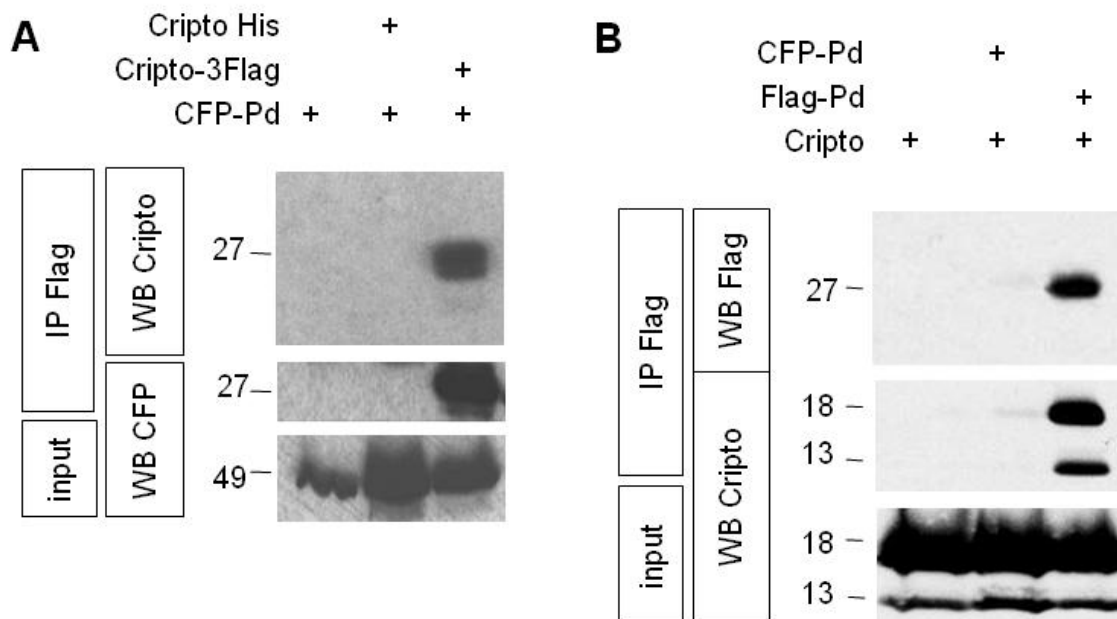
Figure 24. Cripto binds SPCs through their P-domain
(**A**) Coimmunoprecipitation of Cripto with the P-domain of Furin. The P-domain was fused to the C-terminus of secreted CFP (CFP-Pd).
(**B**) Coimmunoprecipitation of Cripto with Furin P-domain provided with an N-terminal hydrophobic signal sequence followed by a Flag epitope (Flag-Pd).

6.7 Activation of a preassembled complex of Cripto and uncleaved Nodal by convertases from neighbouring cells

During embryogenesis, Cripto and Nodal are coexpressed in the epiblast ((Brennan et al., 2001; Ding et al., 1998; Dono et al., 1993; Mesnard et al., 2006) and **Fig. 25A, B**), whereas Furin and PACE4 are produced in neighbouring extraembryonic cells (Beck et al., 2002; Mesnard et al., 2006). This spatial compartmentalisation requires that Furin and PACE4 activate Nodal cell non-autonomously in neighbouring cells. To mimic this situation in culture, 293T cells were transfected with Furin or PACE4 and cocultured with cells expressing Nodal, Cripto and the luciferase reporter ARE-lux (**Fig. 25C**). As a positive control, all components were transfected together in one cell population (**Fig. 25D**). Furin or

PACE4 increased Nodal activity 2-2.5-fold above endogenous levels, regardless of whether they were transfected separately or together with Nodal and Cripto. No luciferase activity was induced in the absence of Nodal. These results show that Furin and PACE4 can activate Nodal protein that is expressed together with Cripto by neighbouring cells.
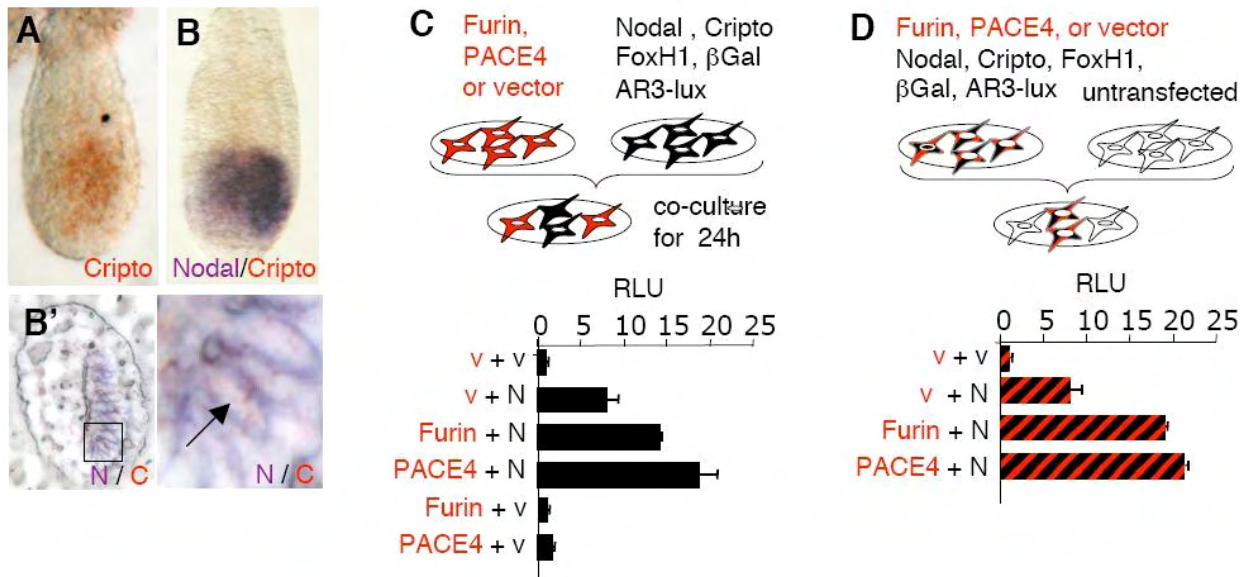
Figure 25. Furin and PACE4 activate a preassembled complex of Cripto and Nodal at the surface of signal-receiving cells

(**A, B**) Whole mount view (A, B) and frozen section (B') of mouse embryos stained 6.25 days after fertilization first for Cripto (B, red) and subsequently for Nodal mRNA (B', purple). Nodal and Cripto transcripts colocalise in the same cells (B'). Nodal transcripts are enriched near cell borders (stippled outline). (This experiment was performed by D. Mesnard.)

(**C**) Human embryonic kidney 293T cells expressing Cripto and a luciferase reporter with or without Nodal (N) were co-cultured with cells expressing elevated levels of Furin or PACE4 or empty vector (v). SPCs increase luciferase activity in neighbouring cells which express Nodal in a complex with Cripto, but not in cells lacking Nodal, confirming that they can activate Nodal signalling in a cell non-autonomous manner. (This experiment was performed by J. Ann Le Good.)

(**D**) As a positive control, SPCs, Nodal, Cripto and luciferase reporter were co-transfected into a single population of cells that were cultured together with an equal number of untransfected cells. (This experiment was performed by J. Ann Le Good.)

6.8   Cripto assembles Nodal processosomes at the cell surface

If Cripto presents the Nodal precursor for extracellular cleavage, the two proteins should colocalise at the plasma membrane. Immunostaining of unpermeabilised cells revealed an overlapping distribution of Cripto and cleavage-resistant Nr at the plasma membrane (**Fig. 26A, B**).

By comparison, the steady state concentrations of constitutively mature Nodal (Nmat, **Fig. 26C, D**) at the cell surface were undetectable or strongly reduced. However, in cells treated in parallel with the peptidic SPC inhibitor decanoyl-RVKR-CMK, expression of wild-type Nodal at the plasma membrane was significantly stabilized (**Fig. 27A, B**). These results together with our published data on the stability of mature Nodal (Le Good et al., 2005) support our model that Nodal matures in a complex with Cripto at the cell surface.
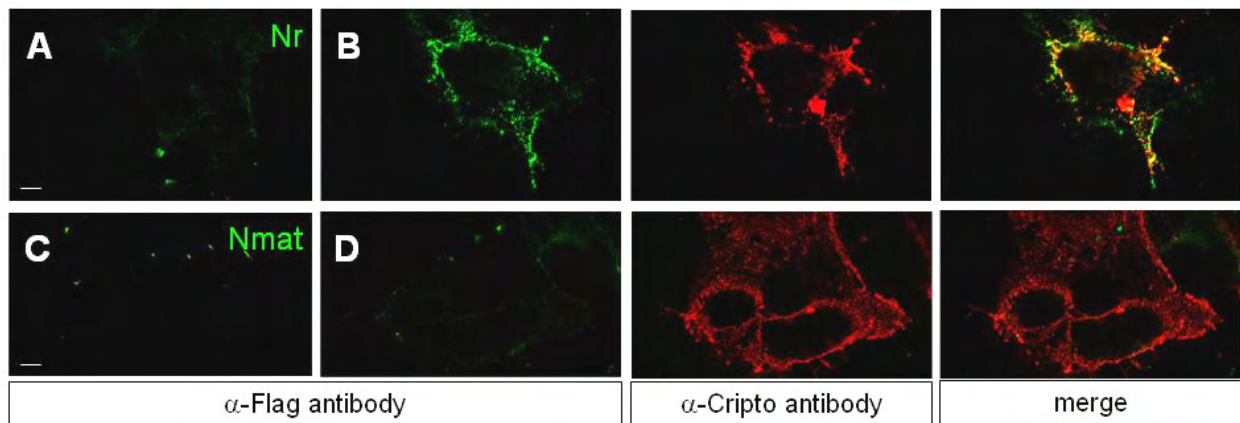
Figure 26. Cripto presents Nodal precursor at the cell surface
Immunofluorescence analysis of non-permeabilised COS1 cells expressing Flag-tagged cleavage-resistant Nodal (Nr) or constitutively mature form (Nmat) alone (A, C) or together with Cripto (B, D). Cell surface expression of Nodal (green) and Cripto (red) was visualised by indirect immunofluoresence using anti-Flag and anti-Cripto antibodies. Uncleaved Nodal is anchored by Cripto at the plasma membrane, but upon maturation is sequestred in intracellular compartments and rapidly metabolised (compare B and D)(Le Good et al., 2005, and Suppl. Fig. S3C). Scale bar: 10 μm. (This experiment was performed by J. Ann Le Good.)

To test whether Cripto recruits Nodal convertases at the plasma membrane, separately transfected cells expressing Furin were co-cultured with cells producing Cripto with or without Nodal cleavage resistant (Nr). Coimmunoprecipitation analysis of chemically crosslinked cell surface proteins revealed that Furin is pulled down by Cripto together with Nodal precursor (**Fig. 27C**). These data suggest that Cripto can assemble a Nodal processing complex at the plasma membrane.
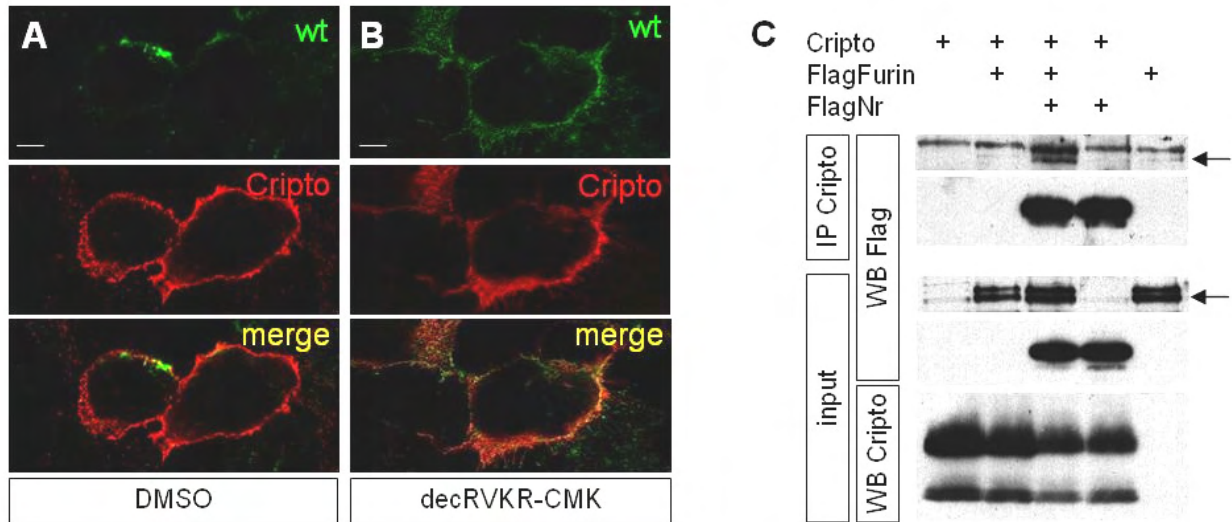
Figure 27. Inhibition of Nodal cleavage stabilises a Nodal/Furin/Cripto complex at the cell surface

(**A, B**) Colocalisation of wild-type Nodal precursor (green) and Cripto (red) at the surface of cells treated without (A) or with decanoyl-RVKR-chloromethylketone (B), an inhibitor of endogenous Nodal convertases (Le Good et al., 2005). Scale bar: 10 μm. (This experiment was performed by J. Ann Le Good.)

(**C**) Cos1 cells transfected with Flag-tagged Furin were co-cultured for 24 h with a separate cell population expressing Cripto with or without uncleaved Nodal precursor (Nr). The resulting complexes were chemically crosslinked with a membrane-impermeable crosslinker, and immunoprecipitated by anti-Cripto antibody. Anti-Flag immunoblotting showed that significant amounts of Furin (arrow, 92 kDa) are specifically pulled down by a complex of Cripto and uncleaved Nodal precursor. (This experiment was performed by J. Ann Le Good.)

6.9 Retrieval of Nodal from the cell surface involves multiple endocytic carriers

Previous studies suggest that proteolytic maturation stimulates Nodal endocytosis (Le Good et al., 2005). To determine how Nodal is internalised, cells were cotransfected with Flag-tagged Nodal with or without Cripto, followed by incubation with anti-Flag antibody to monitor Nodal-mediated antibody uptake. Already after 5 min, numerous small foci were present in Nodal-transfected cells, but not in control cells. Irrespective of the presence or absence of Cripto, no significant overlap was detected between Nodal-positive carriers and early endosomes marked by GFP-Rab5 (**Fig. 28A**). Since Cripto increased the levels of Nodal in detergent-resistant membranes (**Fig. 16**), we monitored Nodal uptake in vesicles which expressed GFP-Caveolin (**Fig. 28B**) or GFP-Flotillin (**Fig. 28C**) to monitor clathrin-independent endocytosis. Only a small amount (3.6 %) of internalised antibody colocalised with GFP-Caveolin, which moderately increased to 9.0 % in the presence of Cripto (**Fig. 28D**). After 10 min uptake, the colocalisation with GFP-Caveolin was comparable in the absence (7.2 %) and presence of Cripto (8.9 %).
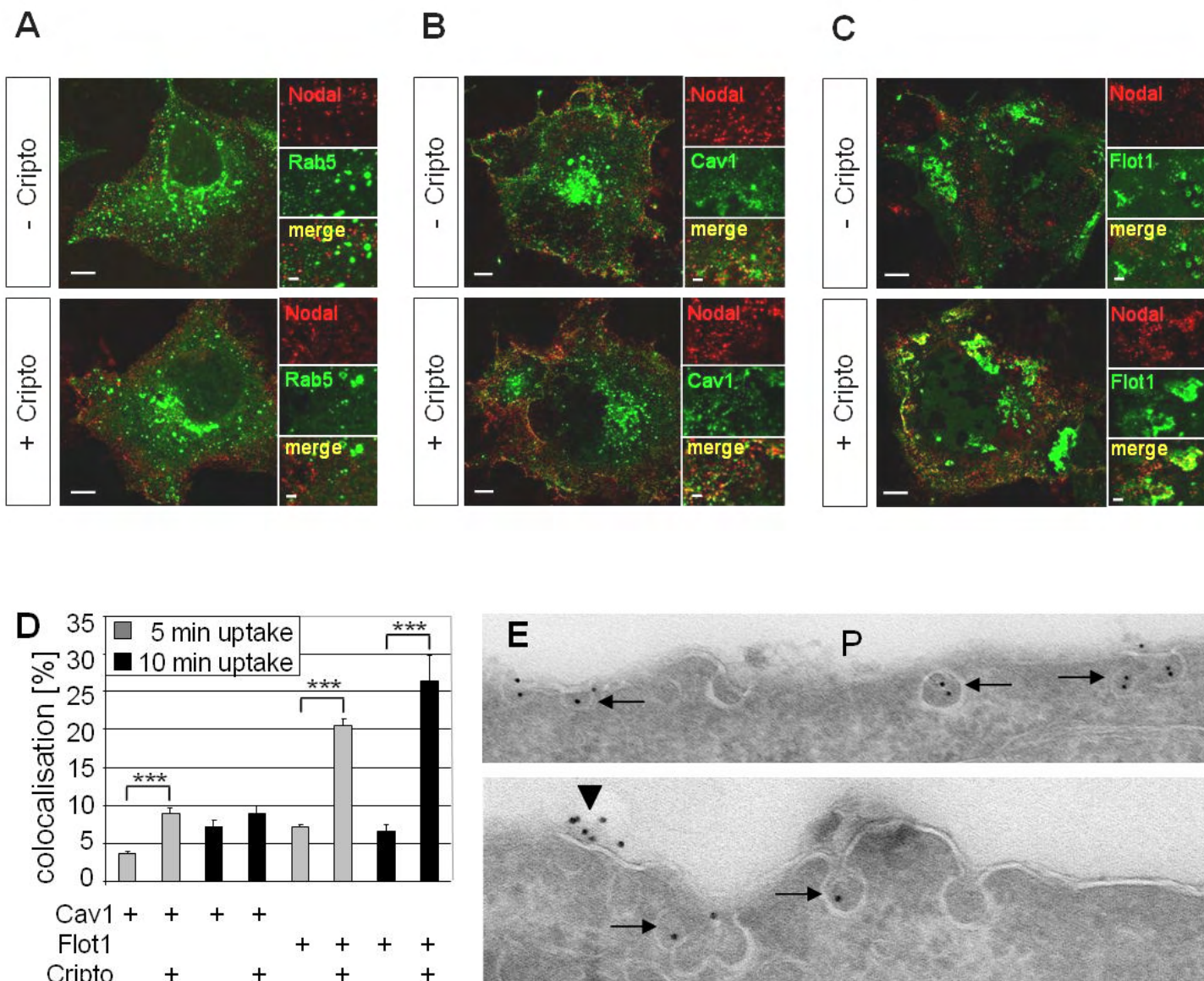
Figure 28. Cripto recruits Nodal to non-clathrin, non-caveolar endocytic compartments marked by Flotillin-1

(**A**) Antibody uptake by Flag-tagged Nodal (red) in early endosomes expressing Transferin receptor was undetectable after 5 minutes irrespective of the presence or absence of Cripto. Scale bars: 10μm on the image showing the whole cell, 2μm on the zoom.

(**B**) Antibody uptake by Flag-tagged Nodal (red) on GFP-caveolin-1 positive domains was undetectable after 5 minutes irrespective of the presence or absence of Cripto. Scale bars: 10μm on the image showing the whole cell, 2μm on the zoom.

(**C**) Antibody uptake by Flag-tagged Nodal (red) on GFP-Flotillin1 positive domains was undetectable after 5 minutes irrespective of the presence or absence of Cripto. Scale bars: 10μm on the image showing the whole cell, 2μm on the zoom.

(**D**) The histogram shows the percentage of Nodal (red) colocalising with either Caveolin1 or Flotillin1 (green). Colocalisation was performed with Metamorph software (Universal Imaging Corporation). Uptake experiments were performed with different timing: 5 min or 10 min in absence or presence of Cripto. We calculate Costes' approach and found that the random images were never showing better colocalisation that the original image. Manders' coefficient was calculated to relate the percentage of colocalisation. The histograms represent at least three independent experiments, and the variations around the mean values are indicated. Student's t test was performed to assess the significance of the results (*** $p < 0.001$).

69

(**E**) Electron microscopy in Cos1 cells of Nodal immunoglod labelled. Nodal is internalised from the extracellular space (E) into vesicles at the plasma membrane (P). These vesicles are typically non-clathrin coated vesicles. (This experiment was performed by Viola Oorschot, Klumperman laboratory, Cell Microscopy Center, Utrecht.)

In contrast, Cripto significantly increased the percentage of Nodal vesicles overlapping with GFP-Flotillin from 7.1 % to 20.5 % after 5 min, and from 6.6 % to 26.3 % after 10 min (**Fig. 28D**). Consistent with these results, electron microscopy analysis showed that Cripto stimulates Nodal uptake in uncoated, rather than in clathrin-coated plasma membrane invaginations (**Fig. 28E**). These findings suggest that while Nodal enters cells via several clathrin-independent pathways, Cripto preferentially stimulates uptake in Flotillin carriers.

Next, we wished to determine whether endocytosis via specific microdomains is necessary to activate Nodal. In order to associate with lipid rafts, Caveolin and Flotillin must be palmitoylated (Dietzen et al., 1995; Morrow et al., 2002). Thus, if Nodal relies on uptake in specific membrane microdomains for efficient proteolytic maturation, we predicted that activation should be sensitive to inhibitors of palmitoylation. Indeed, luciferase reporter assays and antibody uptake (10min) experiments revealed that 2-bromopalmitate (2BP) also inhibited Nodal endocytosis and signalling, while stimulating Nodal staining at the cell surface (**Fig. 29A**). Furthermore, treatment of transfected cells with 2BP drastically inhibited Nodal processing by endogenous convertases and by transfected Flag-tagged Furin and PACE4, even though the release of these proteases into conditioned medium was only marginally impaired (**Fig. 29B**). However in conditioned medium, the reduction in the levels of cleaved Nodal propeptide resulting from 2BP treatment was only partially matched by a corresponding increase in uncleaved precursor, suggesting a net decrease in Nodal secretion (**Fig. 29B**).

This inhibition of Nodal secretion into the medium is reminiscent of the effect of inhibitors of endosomal acidification such as NH_4Cl, even though the latter in addition also blocks the shedding of SPCs (**Fig. 17**). Overall, these results are consistent with a model that Nodal uptake in specific plasma membrane microdomains is necessary for proteolytic maturation and signalling and precedes the release of Nodal into culture medium.
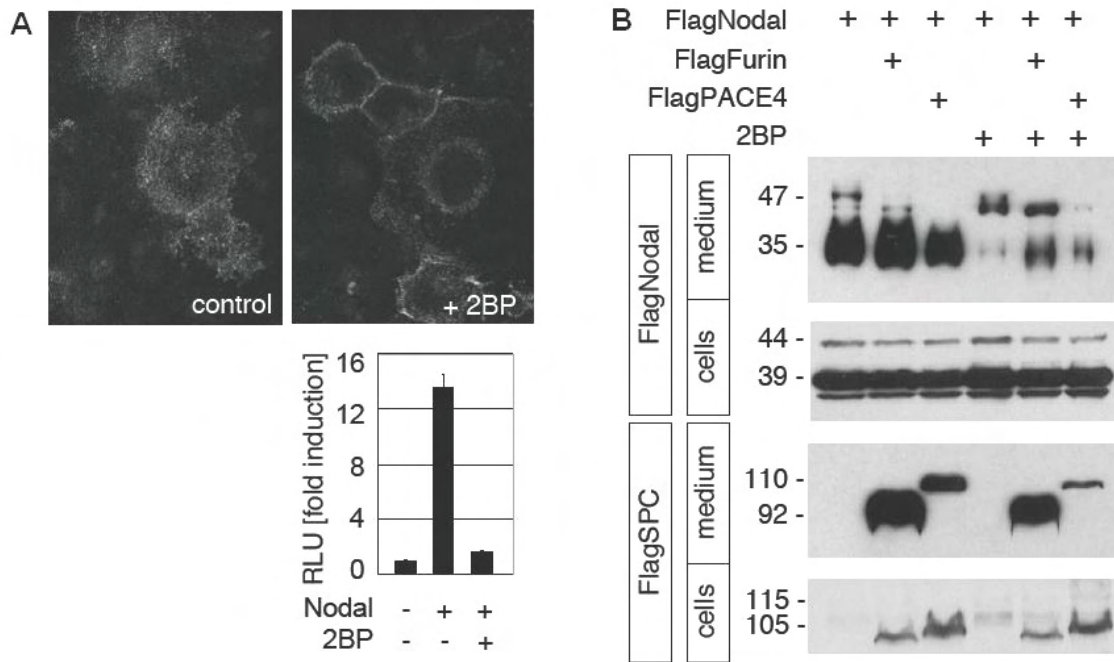
Figure 29. 2-bromo-palmitate (2BP) inhibits Nodal processing and signalling
(**A**) 2BP inhibits Nodal endocytosis and signalling. Control experiments show that 2BP does not block the secretion of Furin and PACE4.
(**B**) Effect of 2-bromo-palmitate (2BP) on Nodal processing in 293T cells. Cells were transfected with Nodal and Cripto. In addition, either Furin or Pace4 was cotransfected. Cells were then incubated with or without 2-BP [8 µg/ml] for 24 hours. Control experiments show that 2-BP does not block the secretion of Furin and PACE4.

6.10 Cripto localises Nodal at the limiting membrane of endosomes competent for signalling

To address how Cripto-mediated uptake might promote Smad2/3 signalling, we investigated its effects on the post-endocytic trafficking of Nodal. In order to activate Smad2/3 transcription factors, Nodal/Activin- and TGF-β receptors must be targeted to early endosomes by the FYVE domain protein SARA (Di Guglielmo et al., 2003; Panopoulou et al., 2002; Penheiter et al., 2002; Tsukazaki et al., 1998). To visualize this compartment, we transfected COS1 cells with GFP fused to the small GTPases Rab5 or Rab4, which decorate and, at elevated expression levels, enlarge early endosomes (Bucci et al., 1992; van der Sluijs et al., 1992). Indirect immunofluorescence analysis revealed that early endosomes marked by GFP-Rab4 also harboured ALK4, Cripto, as well as endogenous Rab5 and SARA (**Fig. 30A-O**).
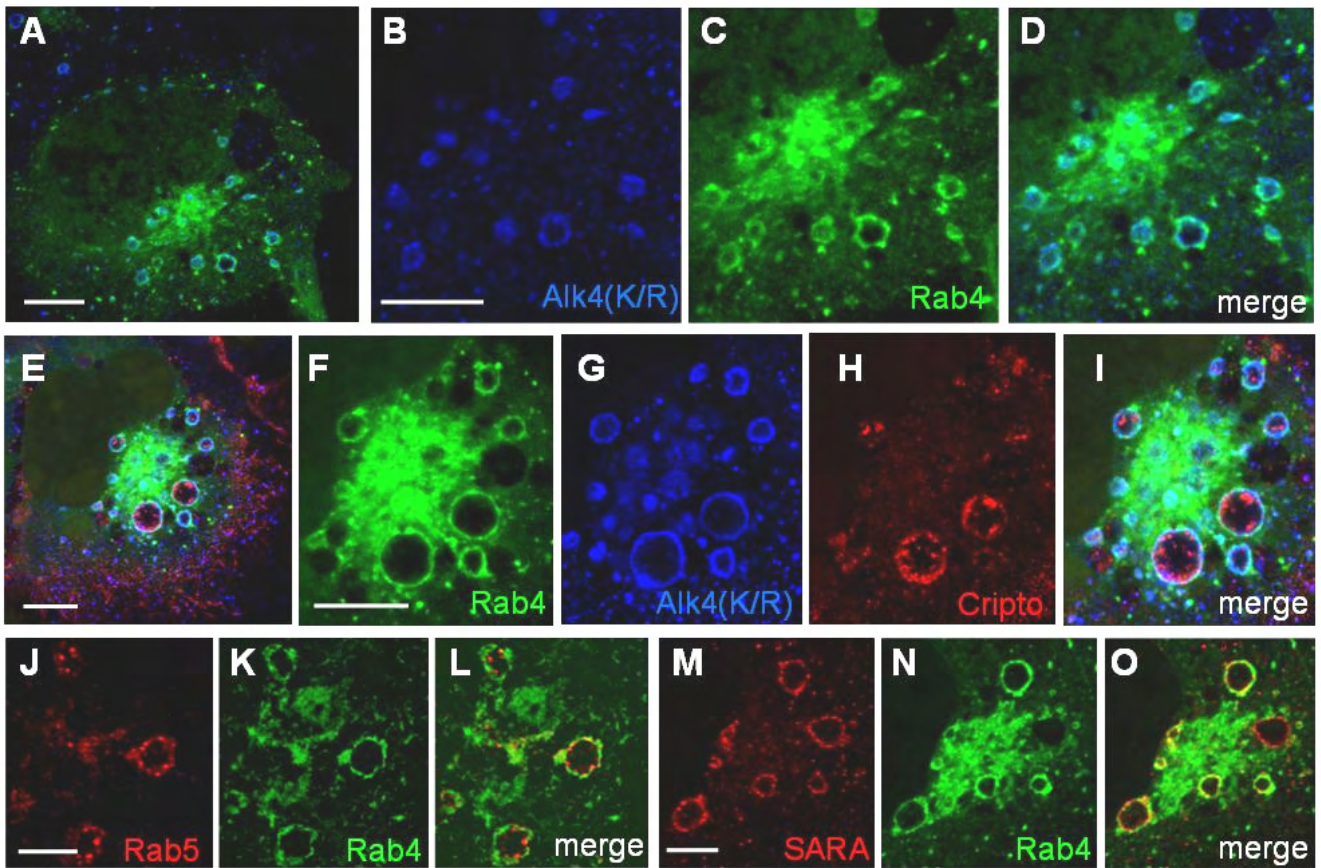
Figure 30. GFP-Rab4 endosome harbour Alk4 and SARA

(**A-I**) Immunostaining of human HA-tagged ALK4 (blue) without (A-D) or with Cripto (red, E-I) at the limiting membrane of GFP-Rab4-expressing endosomes (green). A kinase-inactive mutant version (K/R) of ALK4 was used to reduce toxicity. Panels B-D and F-I show magnifications of panels A and E, respectively, for individual and merged colour channels). Scale bar: 10 µm.

(**J-O**) GFP-Rab4-expressing vesicles are decorated on the cytoplasmic side by endogenous Rab5 (J-L) and SARA (M-O). Scale bar: 5 µm.

To assess whether COS1 cells endogenously express Nodal signalling receptors, they were transfected with CAGA::GFP, a reporter of active Smad3 (Neptune et al., 2003). Incubation of COS1 cells with TGF-β (control) or recombinant Activin A significantly increased the expression of transfected CAGA::GFP above basal levels, whereas the compound SB-431542 which blocks ALK4, 5, 7 signalling was inhibitory (**Fig. 31**). These results suggest that COS1 cells endogenously express Nodal/Activin receptors.
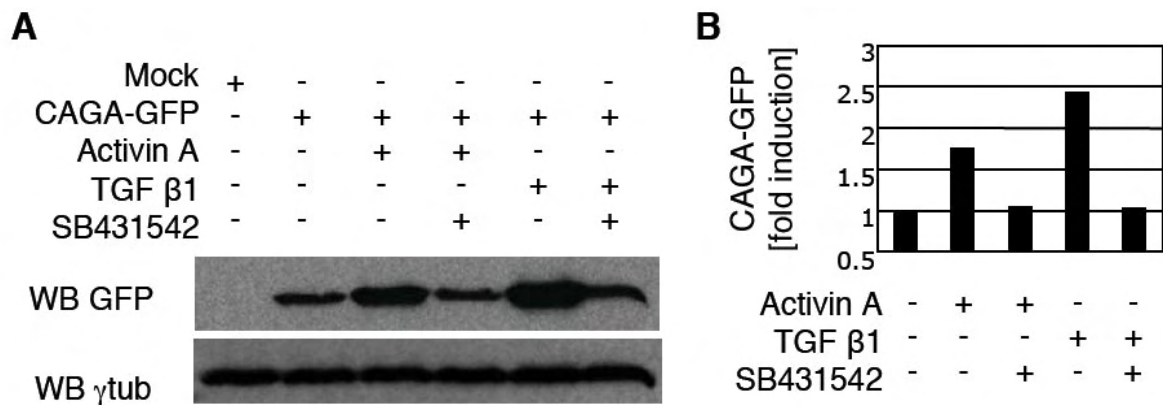
Figure 31. Activin and TGF-β receptor signalling in COS1 cells
(**A**) Western blot analysis of CAGA-GFP expression, a reporter of Nodal/Activin/TGF-β receptor signalling in COS1 cells stimulated for 24 hrs by recombinant Activin A or TGF-β (50 ng/ml) in the presence or absence of the ALK4, 5, 7 inhibitor SB431542 (10 µM). Western blot analysis of γ-tubulin served as a loading control. (**B**) Densitometric quantification of CAGA-GFP induction.

To determine whether Nodal is internalised in early endosomes, we conducted indirect immunofluorescence and antibody uptake experiments. During the first 10 min of uptake, internalised antibody was detected in cells expressing Nodal, but not in control cells. However, at these early time points, irrespective of whether Nodal was transfected with or without Cripto, there was no significant overlap with early endosomes marked by GFP-Rab5, GFP-Rab4 or by Transferrin receptor (TfR) (**Fig. 28,** and data not shown). In cells cotransfected with Cripto and Nodal, antibody to detect Nodal was internalised after 40 min at the limiting membrane of early endosomes (**Fig. 32A**).
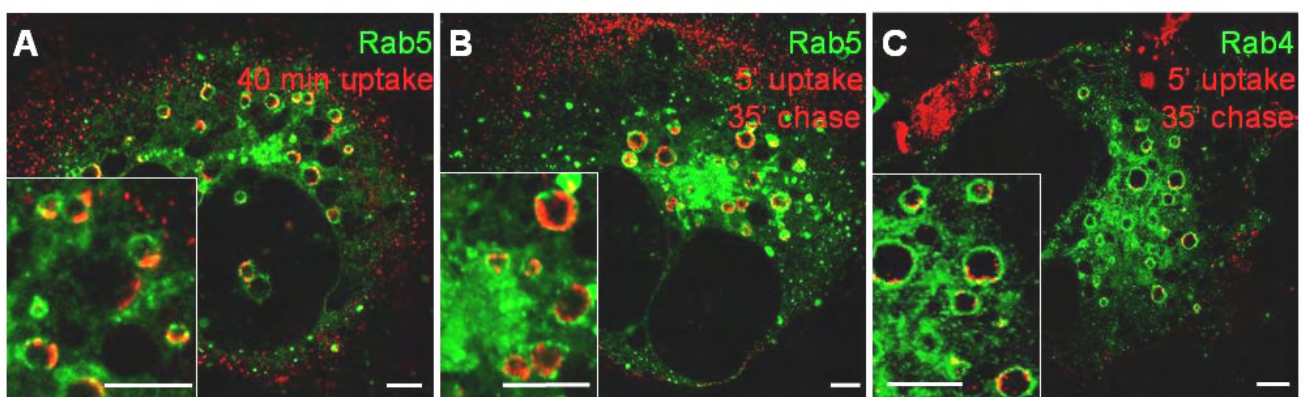
Figure 32. In presence of Cripto, Prolonged antibody uptake, localises Nodal at the limiting membrane of GFP-Rab5 and GFP-Rab4 endosomes
(**A**) Prolonged antibody uptake (40 min) in cells transfected with Cripto reveals the presence of Nodal (red) in early endosomes. Scale bar: 10 µm (inset, scale bar 5 µm).

(**B, C**) After 5 min uptake, followed by a 35 min chase, antibody detecting Nodal localizes in early endosomes marked by GFP-Rab5 (B) and GFP-Rab4 (C). Non-specific background staining was below detection levels (not shown). Scale bar: 10 µm (inset, scale bar 5 µm).

Likewise after 5 min uptake followed by a 35 min chase, internalised antibody was efficiently delivered to GFP-Rab5 and GFP-Rab4 endosomes (**Fig. 32B, C**). Staining of Cripto confirmed its colocalisation with internalised Nodal at the limiting membrane (**Fig. 33A, B**). We conclude that Nodal is delivered to early endosomes following initial uptake in smaller vesicles.
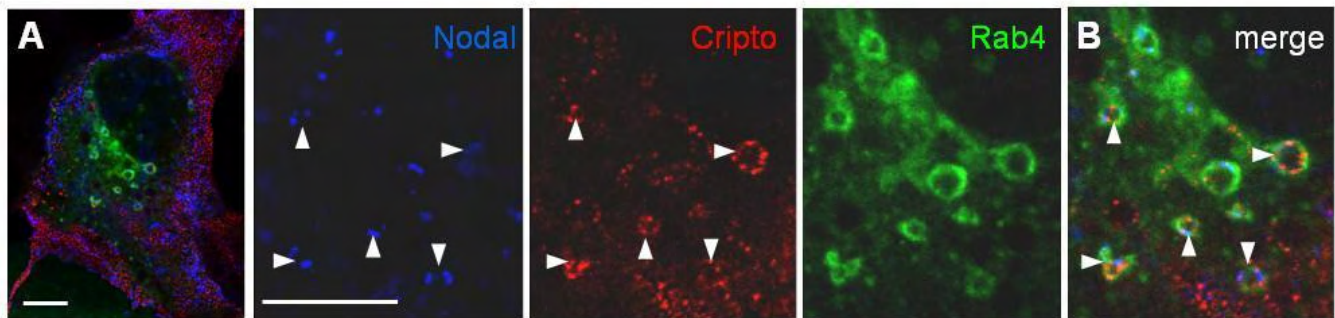
Figure 33. Both Nodal and Cripto can be colocalised on GFP-Rab4 endosomes
(**A, B**) Immunostaining of Cripto (red) showing colocalisation with internalised Nodal (blue) at the limiting membrane of early endosomes. Magnifications of panel A are shown in B. Scale bar: 10 µm.

6.11 Nodal is target to the lumen of multivesicular endosomes in absence of Cripto

To test whether Nodal transport to early endosomes is regulated, Nodal-mediated antibody uptake after 40 min was monitored in cells transfected in parallel with or without Cripto. There was no obvious difference between these two cell populations in the amounts of internalised antibody associated with early endosomes. However, Nodal only accumulated at the endosome-limiting membrane when cotransfected with Cripto, whereas the staining in cells transfected with Nodal alone was in the endosome lumen (**Fig. 34A, B**). Moreover, compared with control cells, the diameter of early endosomes in cells transfected with Cripto was increased. Potential artefacts of antibody uptake were excluded since identical results were obtained using immunofluorescence to directly stain internalised Nodal protein (**Fig. 34C, D**).

74
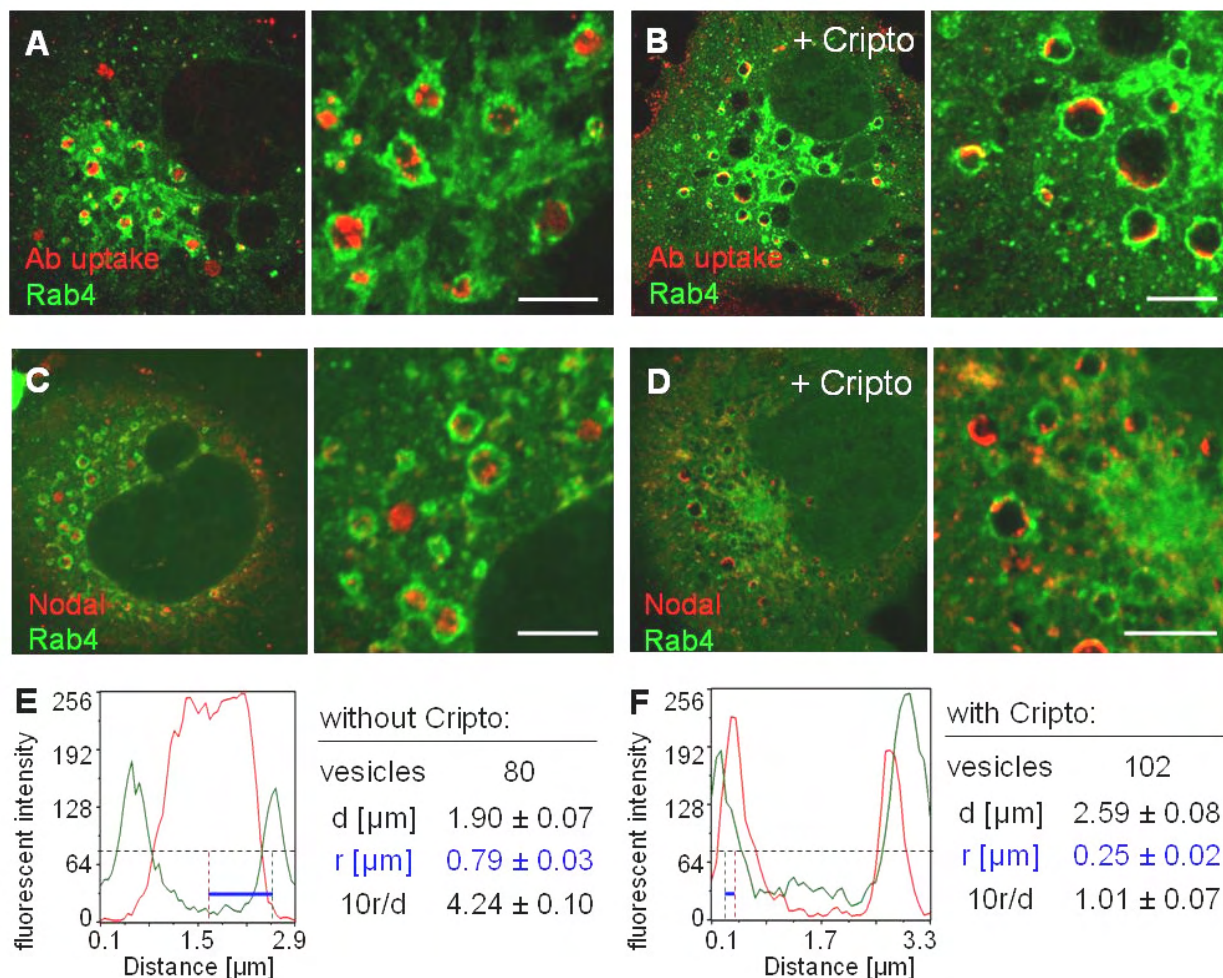
Figure 34. Cripto is necessary to retain Nodal at the limiting membrane of early endosomes
(**A-D**) Antibody uptake experiments (A, B) and immunostaining (C, D) show that early endosomes expressing GFP-Rab4 sequester Nodal (red) in the lumen (A, C). By contrast, in cells cotransfected with Cripto, early endosomes retain Nodal at the limiting membrane (B, D). Scale bars: 5 µm.
(**E, F**) Quantification of Nodal in the lumen of early endosomes of cells transfected with (F) or without Cripto (E). The average vesicle diameter (d) and distance (r, blue lines) of the centre of Nodal staining (red) from the limiting membrane (green) were measured at a fluorescent intensity of 80 pixels (stippled line). To normalise for endosomal size and its increase by Cripto, distance was multiplied by 10/diameter.

To quantify the effect of Cripto on Nodal localisation, the average distribution of internalised antibody was calculated by measuring the shortest possible distance from the centre of the lumenal staining to the nearest limiting membrane. On average, Cripto reduced the distance of Nodal from the limiting membrane 3.2-fold or, after normalising with respect to endosome size, by a factor of 4.2 (**Fig. 34E, F**).

Sorting into intralumenal vesicles is a powerful strategy to sequester signalling molecules from cytoplasmic effectors (reviewed in van der Goot and Gruenberg, 2006). To determine whether Cripto binding simply prevents diffusion of Nodal into the endosome lumen, or

whether it inhibits sorting into intralumenal vesicles, we employed electron microscopy. Immunogold labelling of internalised antibodies revealed that Nodal is trapped on intralumenal vesicles (**Fig. 35A, B**). However, upon cotransfection with Cripto, Nodal remained at the limiting endosomal membrane, and intralumenal vesicle formation was diminished (**Fig. 35B**). Similar results were obtained in cells that did not overexpress GFP-Rab4 (data not shown). To our knowledge, Nodal thus is the first TGF-β family member shown to partition to intraendosomal vesicles. Furthermore, these data reveal a novel function for Cripto in attenuating intraendosomal budding and sorting of associated cargo.
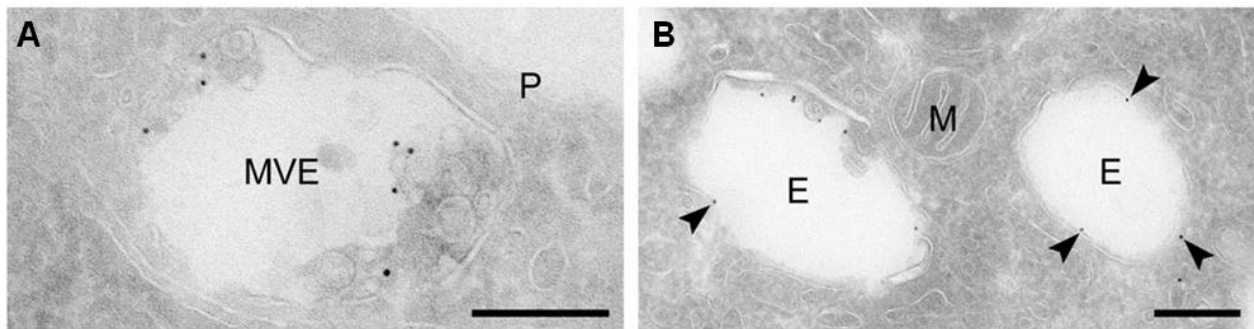
Figure 35. Cripto in attenuating intraendosomal budding of endosomes
(**A, B**) Electron microscopy analysis of immunogold labelled antibodies detecting Nodal-mediated anti-Flag antibody uptake in multivesicular endosomes (MVE) in cells cotransfected without (A) or with Cripto (B). When cotransfected with Cripto, Nodal localised at the limiting membrane of endosomes (E) devoid of intralumenal vesicles (arrowheads), whereas the signal in multivesicular endosomes was diminished (not shown). M: mitochondrium; P: plasma membrane. Scale bars: 200 nm. (This experiment was performed by Viola Oorschot, Klumperman laboratory, Cell Microscopy Center, Utrecht.)

6.12 Cripto localisation at the limiting membrane of endosome is specific to Nodal activity

The experiments described above were conducted using Flag-tagged Nodal precursor. Since the Flag epitope was in the propeptide, we asked whether the mature form is similarly localised. Similar to full-length wild-type Nodal, a constitutively mature mutant form (Nmat) lacking the propeptide strictly depended on Cripto to accumulate at the limiting membrane (**Fig. 36A, B**).

In contrast, immunofluorescent staining of Activin A, which does not rely on Cripto for signalling, was detected at the limiting membrane independently of Cripto (**Fig. 37)**. These results suggest that Nodal, but not Activin, critically depends on Cripto to escape trapping in the lumen of early endosomes.
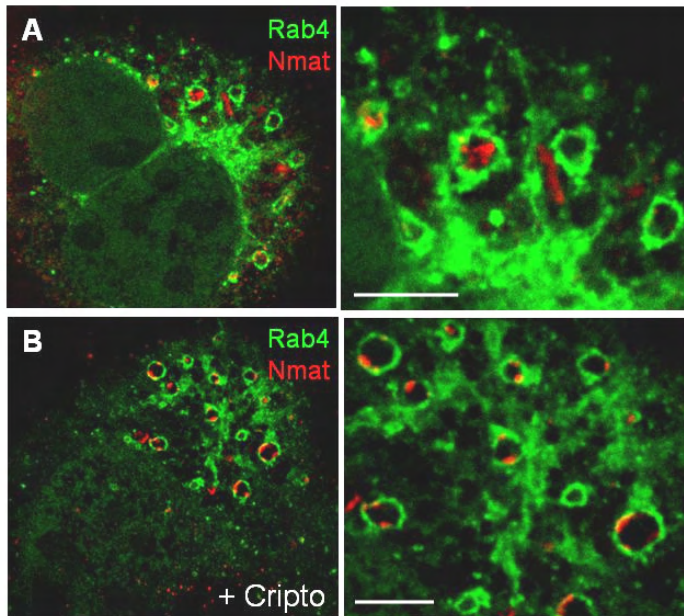
Figure 36. Mature Nodal also depends on Cripto to accumulate at the limiting membrane of early endosomes (**A, B**) Antibody uptake into GFP-Rab4 endosomes (green) by Flag-tagged constitutively mature Nodal (Nmat, red) transfected without (A) or with Cripto (B). Scale bars: 5 µm

Figure 37. Activin does not depend on Cripto for signalling
Immunostaining of Myc-tagged Activin A (red) showed that Activin A could localise even without Cripto at the limiting membrane of early endosomes (green). Scale bars: 5 µm.
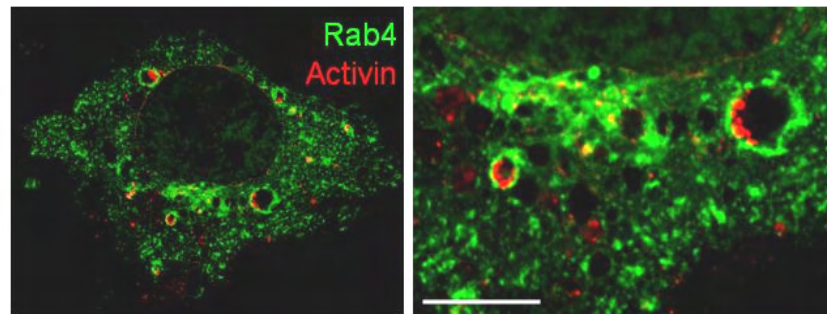
6.13 The EGF domain of Cripto, although dispensable for Nodal binding, is essential for Smad-dependent Nodal signalling

To further evaluate whether Cripto-mediated localisation of Nodal is functionally relevant, we tested whether it is blocked by specific loss-of-function mutations in the EGF or CFC domains. Upon deletion of the EGF motif or mutation of its conserved residues G71 or F78, Cripto is unable to stimulate Nodal signalling (**Fig. 38A**), apparently due to loss of Nodal binding at the cell surface (Yan et al., 2002; Yeo and Whitman, 2001b). However, cell surface

staining and coimmunoprecipitation analysis revealed that deletion of the EGF domain only reduced cell surface expression levels while leaving specific interactions with Alk4 and intracellular Nodal intact (**Fig. 38B and Fig. 40H**).
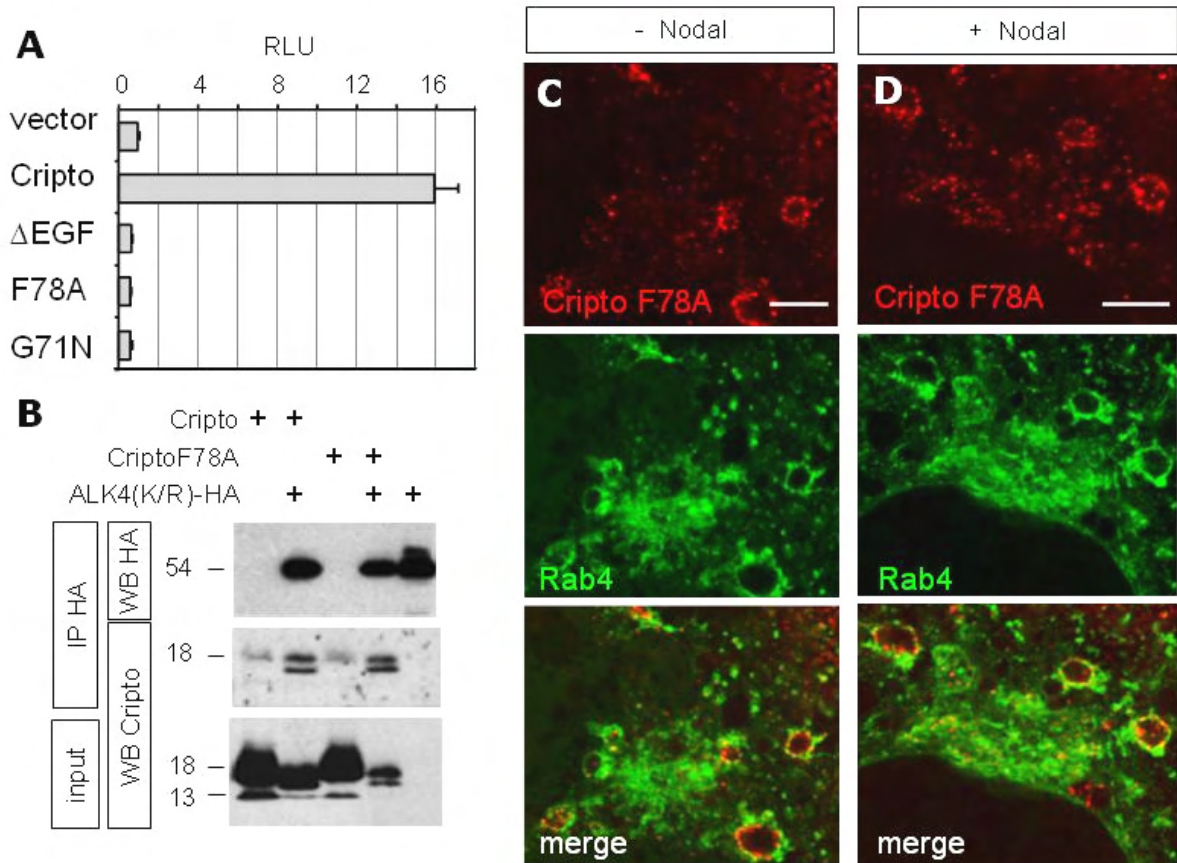
Figure 38. The EGF domain of Cripto is essential for Smad-dependent Nodal signalling
(**A**) Deletion of the entire EGF motif (CriptoΔEGF) and specific point mutations (F78A, G71N) in this domain block induction of the Smad-dependent luciferase reporter ARE-lux by Nodal (A). This is not due to loss of Nodal binding, since GPI-anchored Cripto does not depend on the EGF domain to efficiently bind full length Nodal, its propeptide and the mature form (data not shown).
(**B**) In coimmunoprecipitation assays, CriptoF78A also interacts normally with ALK4. (This experiment was performed by J. Ann Le Good.)
(**C, D**) Localisation of CriptoF78A (red) to early endosomes marked by GFP-Rab4 (green) is not inhibited in cells transfected without (C) or with Nodal (D). Scale bars: 5 µm

Similar to wild-type Cripto, the EGF domain mutant F78A also coimmunoprecipitated both Nodal and ALK4 (**Fig. 38B**) and reached early endosomes irrespective of the presence or absence of Nodal (**Fig. 38C, D**). Therefore, we performed antibody uptake experiments to test whether the EGF domain regulates Nodal trafficking. Mutant Cripto lacking residue F78 or the entire EGF domain failed to retain Nodal at the limiting membrane of early endosomes

(**Fig. 39A , B, C**). Similarly, mutating G71 in the EGF domain abolished Nodal localisation and signalling (**Fig. 39D**). Finally, also the inactivating mutations H104G and W107G in the CFC domain, which prevent docking of ALK4 (Yeo and Whitman, 2001b), inhibited as well accumulation of Nodal at the limiting endosomal membrane (**Fig. 39E**).
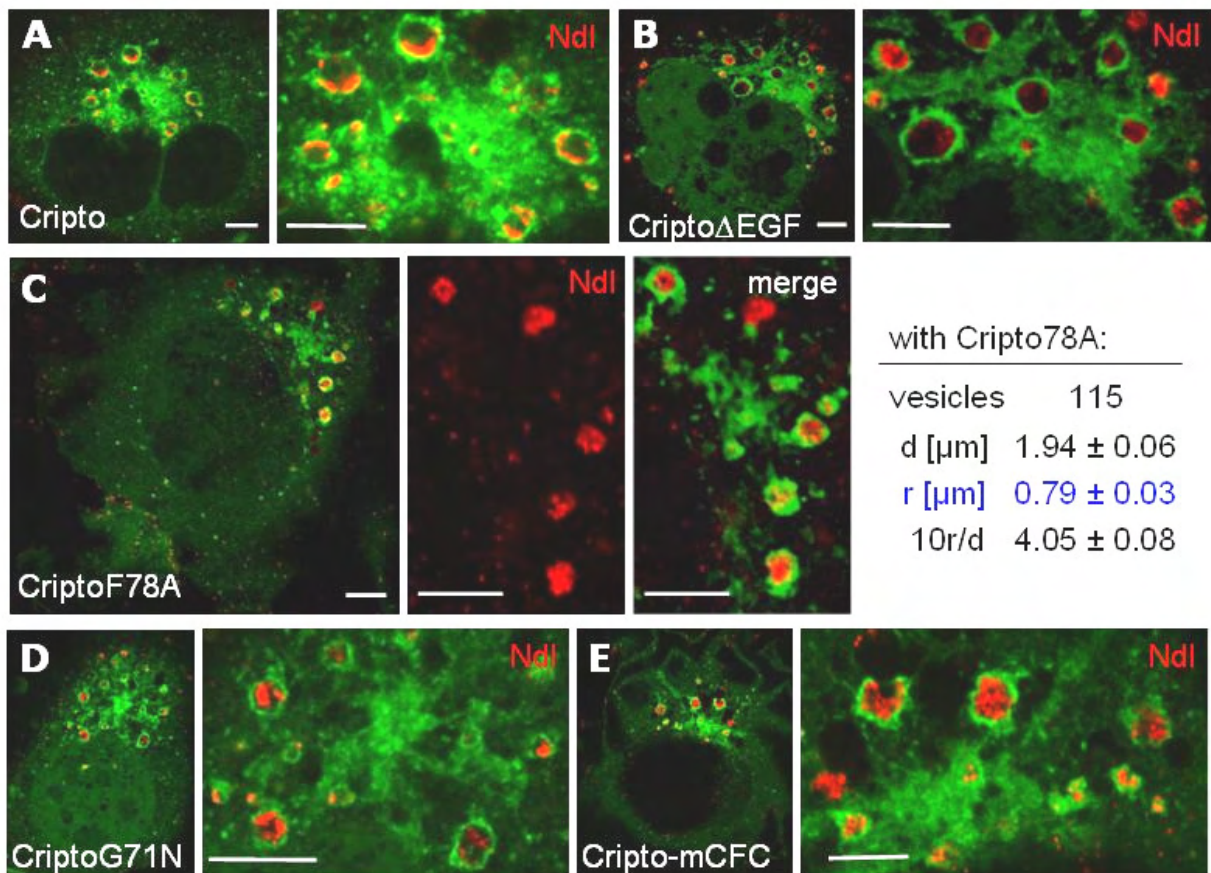
Figure 39. The EGF domain of Cripto is required for Nodal localisation at the limiting membrane of to endosomes
(**A-E**) EGF domain mutants (B-E) fail to localise Nodal at the limiting membrane of early endosomes. In A-E, selected areas are shown at higher magnification (right panels). In (C), analysis of the red channel alone (second panel from the left) clearly shows that Nodal localises to the early endosome lumen. Scale bars: 5 µm.

To validate that wild-type and Cripto mutants reach the cell surface, unpermeabilised COS1 cells were analysed by indirect immunofluorescent staining. Consistent with results obained in 293T cells (Minchiotti et al., 2000), wild-type Cripto was detected at the plasma membrane (**Fig. 26 and 40A**). Cell surface expression was not reduced, but rather increased upon cotransfection of Nodal, or if the ALK4 docking site in the CFC domain was mutated (**Fig. 40B, F**) (Yeo and Whitman, 2001b).
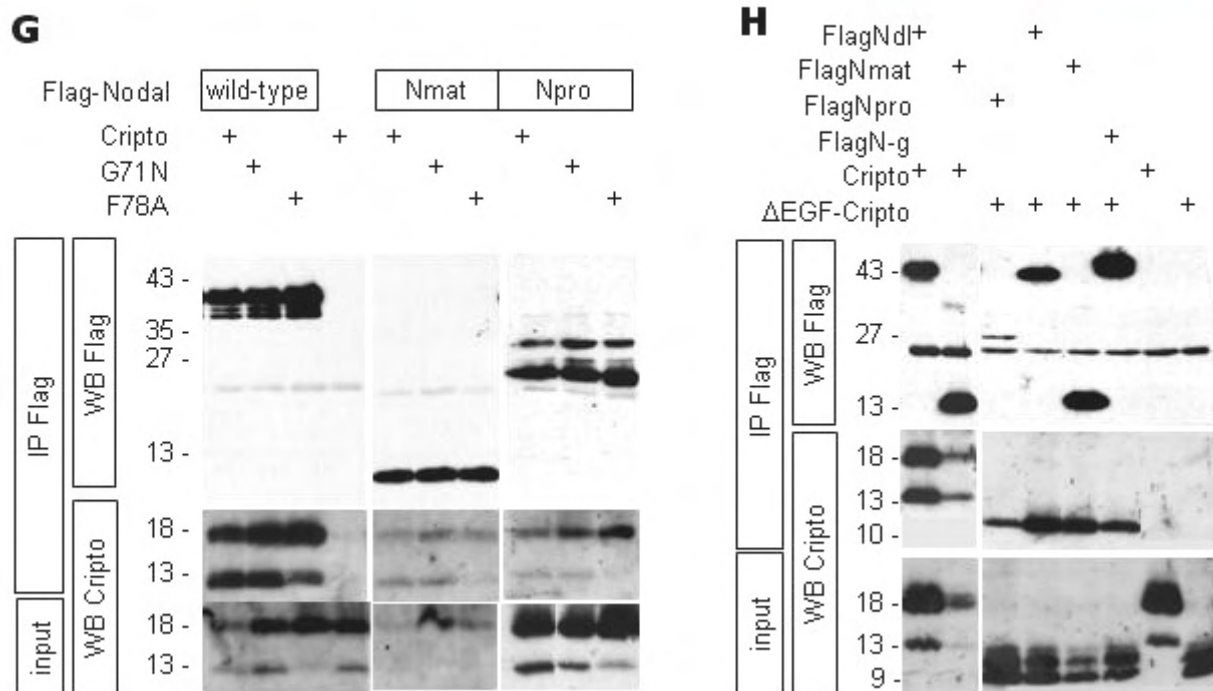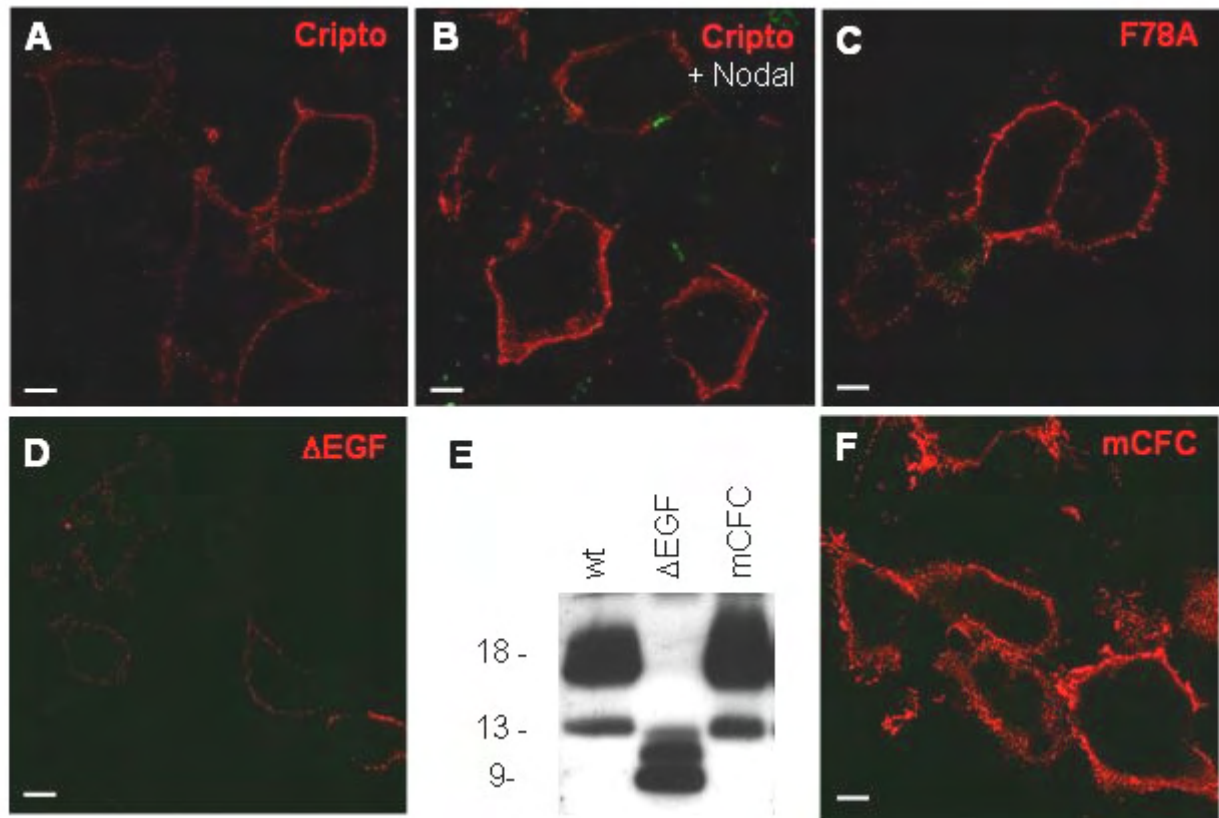
Figure 40. The EGF domain is essential for Cripto cell surface expression
(**A-C**) Immunostaining of Cripto (red) at the surface of unpermeabilised Cos1 cells (A). Cotransfection of Nodal does not inhibit transport of Cripto to the cell surface (B). Scale bars: 10 µm. (These experiments were performed by J. Ann Le Good.)

(**D-F**) Compared to the wild-type (A), mutant Cripto which cannot dock to ALK4 due to the amino acid substitutions H104G and W107G in the CFC domain (mCFC) (Yeo and Whitman, 2001a) was expressed at elevated levels at the cell surface in three independent experiments (F). (This experiment was performed by J. Ann Le Good.)

(**G**) Compared to wild-type, the F78A and G71N mutations do not impair Cripto binding to full length Nodal precursor, its pro peptide (Npro) or constitutively mature form (Nmat) in coimmunoprecipitation assays. Nmat significantly reduced the levels of detergent-soluble Cripto in the input fraction.

(**H**) Binding of Cripto ΔEGF to Nodal (lanes 3-8) is comparable to that of wild-type (lanes 1-2).

Conversely, although the mutant with the deletion of the EGF-like domain was expressed in these cells, this mutation greatly diminished cell surface expression of Cripto (**Fig. 40D, E**). However, the point mutation F78A in the EGF domain had no detectable effect on cell surface expression levels (**Fig. 40C**). Besides confirming that Cripto is secreted, these results indicate that cell surface expression relies on the presence of the EGF domain.

Previous analysis of chemically crosslinked cell surface complexes by co-immunoprecipitation suggested that Cripto directly binds processed Nodal, and that this interaction relies on the EGF domain. However in a separate study, we observed that Cripto also specifically coprecipitates uncleaved Nodal precursor and its propeptide, and vice versa (J.A.L., unpublished observation). Moreover, neither the point mutations F78A or G71N, nor deletion of the entire EGF domain inhibited binding of Cripto to full length Nodal, its pro peptide or the mature form (**Fig. 40G, H**). In part, this discrepancy may reflect the fact that Cripto was not Flag-tagged at the C-terminus in our experiments, because we wished to preserve a functional GPI-signal. Furthermore, since deletion of the EGF domain reduces Cripto cell surface expression (**Fig. 40D**), complexes of Nodal with CriptoΔEGF may have escaped detection by chemical crosslinking under the conditions examined. In any case, our results do not support the view that the EGF domain is essential for Nodal binding. They are consistent, though, with a model that the EGF domain regulates trafficking of Cripto and associated cargo.

These results strongly support the model that Cripto stimulates the Smad pathway by localising a complex of Nodal and signalling receptors at the limiting membrane of early endosomes. This observation is consistent with an essential role for Cripto in recruiting cargo to signalling-competent membrane domains.

7 DISCUSSION

Nodal is a protein essential in early embryogenesis. The role of Nodal specifying the A/P axis and the L/R axis, as well as the induction of endoderm and mesoderm is well established. However, the properties of the protein and how its activity is potentiated by Cripto have still remained unclear. Here, I have characterised the exocytic and endocytic trafficking of Nodal and its regulation by Cripto. Previously, Cripto was proposed to increase Nodal binding to the receptors (Yeo and Whitman, 2001b). However, it has been shown that both Nodal precursor and the mature form can bind Nodal receptors even without Cripto (Ben-Haim et al., 2006; Chen and Shen, 2004). Therefore, the function of Cripto in Nodal signalling along the Smad2/3 pathways remained obscure. Our results suggest a new model whereby Cripto serves to assemble a Nodal processing complex and subsequently localises mature Nodal at the limiting membrane of early endosomes.

7.1 Nodal and Cripto are secreted through an unconventional pathway

Furin is an endoprotease (reviewed in Thomas, 2002) which cycles between the plasma membrane, endosomes and the TGN (Schapiro et al., 2004). The compartment-specific regulation of Furin determines its activation, and its access to specific substrates. Furin is a proprotein that is cut twice in order to be fully active (Anderson et al., 2002). Furin undergoes two autoproteolytic cleavages in its prodomain. The first one occurs already in the ER, whereas the second cleavage happens in the TGN/endosomal compartment. The first cleavage occurs during exocytosis and induces a conformational change of the protease. The second cleavage allows Furin activation by releasing the propeptide (Vey et al., 1994). Furin is internalised into endosomes from the plasma membrane. Its activation occurs in the acidified TGN/endosomal compartment and is calcium dependent. Processing compartments might be formed by the fusion of endocytic furin-containing compartments with vesicles that contain the substrate proteins (Band et al., 2001). Furin has a broad set of protein processing and a broad enzymatic activity (between pH 5 to 8). In addition, Furin can be shed into the extracellular space which suggests a possible activity at a distance of the producing cells. Consistent with published data (Molloy et al., 1994), we confirmed that Furin secretion was blocked by the fungal drug, BFA and by inhibitors of endosomal acidification, as expected if

shedding relies on prior transport through the TGN/endosomal system. As Furin cleavage is required for Nodal activation along the Smad2/3 pathway, we have investigated the possible exocytic itinerary that Nodal could take in order to meet Furin and to be active.

Nodal is a glycoprotein. The conventional pathway for glycoprotein secretion is the following: translation of the protein in the endoplasmic reticulum (ER), addition of carbohydrate cores to the side chain of an asparagine (NXT/S consensus sequence), modifications of these sugar units in the Golgi, and protein secretion in the extracellular space via vesicles. In the Cis and Medial Golgi, carbohydrates are mannosylated and finally acquire their terminal glycosylation in the TGN. To analyse Nodal processing, Ann Le Good (former postdoc in the lab) monitored the maturation of the carbohydrate modifications during exocytosis. When Nodal protein in whole cell lysates was treated with Endoglycosidase-H, Nodal size was shifted. This was not the case for the Nodal proteins present in the conditioned medium. These results show that the bulk of intracellular Nodal has not yet acquired terminal modifications characteristic of the TGN before secretion.

To further characterise the exocytic route of Nodal, I assessed the effects of BFA. This drug inhibits the retrograde transport from the Golgi to the ER by breaking down the physical separation of the ER and the Cis Golgi. In addition, BFA treatment breaks the continuity between the Cis and the Trans Golgi. After treatment with BFA, Nodal could still be detected on the plasma membrane of cells. Similar results were observed for Cripto. We speculated that Cripto might TGN-independent transport of Nodal to the cell surface. However, Cripto was not essential for Nodal to reach the cell surface. This result suggests that both Nodal and Cripto are likely to access the plasma membrane via a TGN-independent route, but they can do so independently of each other. However, Nodal and Cripto secretion in the medium were blocked in presence of BFA. Thus while Nodal and Cripto do not require the Trans Golgi compartment for their location at the cell surface, the TGN is necessary for their shedding into the medium. As a control, we used His-tagged Cripto, lacking its GPI anchor, which passes through the TGN prior to secretion. This mutant form of Cripto was neither detected on the plasma membrane nor secreted in the medium after BFA treatment.

Exactly how Nodal reaches the cell surface remains unknown. Nodal is secreted as a precursor comprising a prodomain of 27 kDa, whereas the mature part only accounts for 12 kDa. Could Nodal prodomain deviate the precursor from the conventional ER-Golgi-plasma

membrane pathway? It seems unlikely that the prodomain plays such a role since on its own, it passes the TGN far more efficiently than the precursor. Thus, the unconventional exocytosis of Nodal is most likely to be determined by the mature domain.

So far, the ER compartment was thought to be the first step for protein translation, protein modification and protein quality control before secretion. It has become more and more evident that the roles of the ER are more complex than what was previously thought (reviewed in Desjardins, 2003). The discovery by Desjardins and coworkers that phagocytosis by mouse macrophage cell line involves the donation of ER membrane to nascent phagosomes suggests a potential mechanism by which intracellular proteins could be secreted in the extracellular space (Desjardins et al., 1994; Gagnon et al., 2002). This peripheral compartment in macrophages and dentritic cells serves as an organelle for major histocompatibility complex (MHC) class-I-restricted cross-presentation of exogenous antigens (reviewed in Ackerman and Cresswell, 2004). The role of ER in protein exocytosis has also been studied for CD45, a receptor protein-tyrosine phosphatase essential for T cell development and lymphocyte activation. CD45 is able to reach the plasma membrane via two distinct routes (Baldwin and Ostergaard, 2001). The first involves a slow Golgi-dependent pathway that allows fully processed CD45 to be expressed. The second is independent of the TGN, and allows more rapid delivery of CD45 with immature carbohydrate to the cell surface.

TGN-independent secretion is not restricted to cells of the immune system. In the central nervous system, the paranodes separate Ranvier node from the internode which constitute myelinated axon between nodes (Marcus and Popko, 2002). The edges of these myelinated segments form the paranode structure. It has been shown that the paranodal complex contains GPI-linked F3/Contactin and Caspr/Paranodin (Bonnon et al., 2003). This complex is involved in cell adhesion and has a crucial role in the generation of functional junctions at paranodes. When associated, the paranodal complex of F3/Contactin and Caspr/Paranodin was recruited in lipid rafts and insensitive to BFA. This suggests that this complex reaches the cell surface via a TGN-independent pathway.

7.2 Cripto allows the formation of a Nodal 'processosome' located on specific domains competent for signalling

The mature form of Nodal is hardly detected in conditioned medium or cell lysate. In order to have sufficient amount of Nodal protein, wild-type Nodal or a supercleaved mutant form of Nodal were expressed in cells expressing high levels of SPCs (Le Good et al., 2005). The switch of HHL to HLE after the SPC recognition motif (RQRR) renders Nodal super-sensitive to processing (Constam and Robertson, 1999). Using the conditioned medium, we analysed which domain of Nodal could bind to Cripto. It turned out that the precursor, the prodomain and the mature domain could assemble with Cripto. Further experiments showed that each domain can separately bind to Cripto.

We further analysed the role of Cripto in the regulation of Nodal processing. Nodal is a relatively unstable protein (Le Good et al., 2005). Our laboratory recently demonstrated that after maturation, Nodal is rapidly internalised and degraded. This observation suggests a tight regulation of Nodal processing and activity. Using immuno-fluoresence staining on non-permeabilised cells, both Nodal resistant to cleavage (Nr) and a constitutively mature mutant form (Nmat), could barely be detected on the plasma membrane. The addition of Cripto only marginally increased the amount of these Nodal forms at the cell surface. However, accumulation of a cleavage-resistant Nodal precursor was greatly increased by Cripto at the cell surface. These findings suggest that processing drastically reduces the residence time of Nodal at the cell surface.

In addition, Cripto can bind to the SPCs. Pull-down assay allowed us to detect an interaction between Cripto and Nodal convertases. This interaction involves the P-domain which is highly conserved in Furin and Pace4. Furthermore, we tested whether the SPCs were able to activate the Nodal and Cripto complex after secretion. This experiment mimics what should happen in the embryo where Nodal and its convertases are not coexpressed in the same cells. Nodal and Cripto are expressed in the epiblast, whereas the proteases are provided by the extraembryonic ectoderm. Activity assays showed that a similar level of Nodal activation was induced if the convertases were present or not in the same cells. As SPCs are able to activate Nodal at a distance, this experiment suggests that the convertases may reach Nodal precursor after having moved to the epiblast. Whether the SPCs traffic through the epithelium or diffuse

in the cavity is currently under investigation. We propose that Cripto serves as a SPC receptor to assemble a Nodal processing complex in signal receiving cells.

In order to produce a signal along the Smad2/3 pathway, Nodal upon cleavage by SPCs must activate the type receptor I Alk4. However, direct binding between Nodal, Cripto and SPC had never been conclusively demonstrated (Chen and Shen, 2004; Reissmann et al., 2001; Yeo and Whitman, 2001b). After crosslinking, Ann Le Good was able to detect a complex between Nodal, Cripto and Furin at the cell surface. Cripto might thus allow the formation and stabilisation of a complex between the substrate and the proteases. We propose the term 'processosome' for this type of complex. It is important to mention that the formation of the complex might not directly imply Nodal activation. Indeed, as previously described, Furin is active under a certain pH depending on the substrate that it has to cleave. Whether, Furin cleave Nodal at the plasma membrane or in specific vesicles is still not known. Indeed, until now, Nodal intracellular localisation was not known.

I next tested if Cripto could bring Nodal to a specific compartment competent in Nodal processing. To this end, I used several endocytic markers. It turned out that Nodal was enriched in Flotillin-1 rafts in presence of Cripto. Moreover, after treatment with 2BP, a drug that inhibits protein palmitoylation, the amount of processed Nodal was drastically reduced even if Furin or Pace4 were overexpressed. It thus seems that the environment in these domains is essential to produce or stabilise processed Nodal. Activity assays showed that also Nodal signalling was dramatically reduced in the presence of 2BP. These results provide the first indication that uptake via lipid rafts is essential for the production and/or survival of processed Nodal.

It has been demonstrated that the localisation of EGFR is essential for signal induction. EGFR follows different internalisation routes, depending whether the concentration of the ligand is high or low (both doses were physiologically relevant) (Sigismund et al., 2005). When EGF was present at low concentration, the receptor was internalised through the clathrin pathway. In this condition, the receptor was phosphorylated and fully competent for Erk signal transduction. However, if EGF was more abundant, the receptors were endocytosed partly through the caveolar pathway for degradation. In addition, non-clathrin endocytosis correlates with the appearance of detectable ubiquitinated EGFR. Surprisingly, monoubiquitination of the receptor seems to be required for the CCV internalisation. Recently, diverse functions

have been attributed to monoubiquitination. Stability, protein–protein recognition, activity and intracellular localisation are regulated by monoubiquitination (at one or multiple lysine residues) of transmembrane proteins (reviewed in d'Azzo et al., 2005).

7.3 Cripto prolongs Nodal signalling by localising Nodal at the limiting membrane of endosomes

To address how Cripto-mediated uptake might promote Smad2/3 signalling, I investigated its effects on the post-endocytic trafficking of Nodal. Nodal could be detected after prolonged antibody uptake in the lumen of Rab5 and Rab4 sorting endosomes (**Fig. 41**). However, in presence of Cripto, Nodal was localised at the limiting membrane of endosomes. A pulse of antibody uptake followed by a chase gave the same result. In order, to understand the purpose of this localisation, we characterised in further details the nature of the sorting endosome. Alk4 and SARA were detected on the periphery of these endosomes. We further analysed Rab4 endosomes using electron microscopy. After antibody uptake and gold-labelling, we could see Nodal on intralumenal vesicles. But in presence of Cripto, Nodal accumulated at the periphery of the endosome. This localisation was independent of the Nodal propeptide since constitutively mature Nodal showed an identical distribution.

Moreover, we tested the effect of several mutants of Cripto on Nodal localisation. All of these mutants were unable to induce Nodal activity in luciferase assay. Specifically, we examined a complete deletion of the EGF domain and the mutants G71N and F78A, two point mutations known to abolish Cripto activity in zebrafish injection assays (Minchiotti et al., 2001). None of these mutants were able to localise Nodal on the periphery of endosomes even though they bind Nodal similar to wild-type Cripto. We further focused our attention on the mutant F78A because a collaborator, G. Minchiotti, introduced this mutation in the mouse using a knock-in strategy. Similar to wild-type Cripto, the point mutation F78A also coimmunoprecipitated both Nodal and ALK4 and reached the plasma membrane and early endosomes irrespective of the presence or absence of Nodal. Thus, we conclude that Cripto potentiates Nodal activity by localising a signalling platform in proximity to the cytoplasmic Smad2/3.
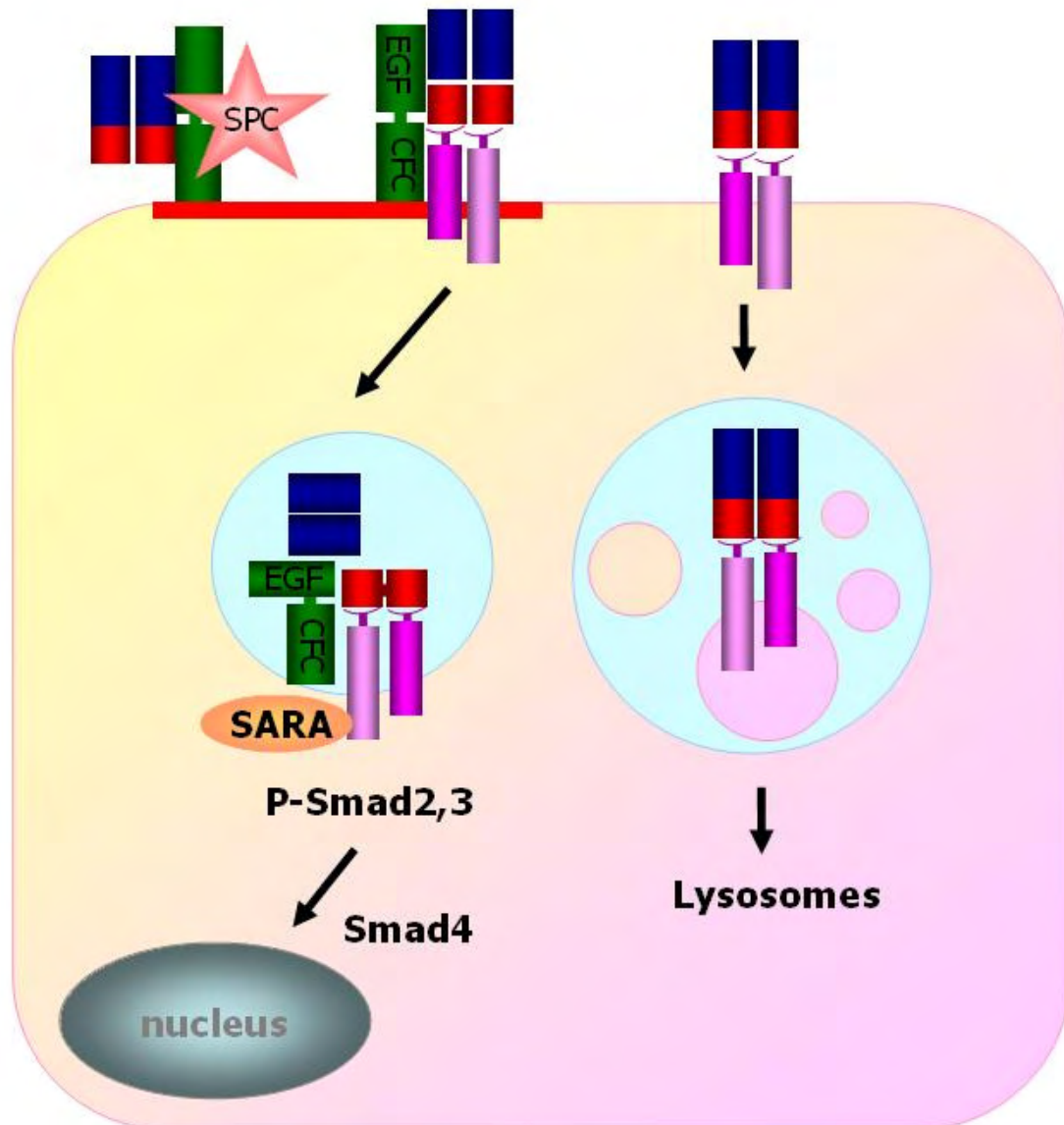
Figure 41. Cripto couples Nodal processing and endosomal signalling
Left: Proteolytic processing of the Nodal precursor (red: mature domain; blue: propeptide) in a complex with SPC (pink) and GPI-anchored Cripto (green) facilitates access to ALK4 (light purple), type II Activin receptors (dark purple) and SARA (orange) at the limiting membrane of early endosomes, apparently via uptake in Flotillin-rafts (red bar). Residue F78 in the EGF domain of Cripto, which promotes detergent solubility of a truncated 13 kDa form of Cripto, and residues H104 and W107 in the CFC domain which mediate binding to ALK4 are essential for correct Nodal localisation.
Right: In the absence of Cripto, Nodal is sequestered by default on intraendosmal vesicles *en route* to lysosomes, possibly because the receptors are internalised via caveosomes and ubiquitinated similar to TGF-β receptors (Di Guglielmo et al. 2003).

The strict requirement for Cripto to localise cargo seems to be specific for Nodal. Indeed, the scenario was different for ActivinA, a ligand of Alk4, that can signal without Cripto. Activin was able to localise on the limiting membrane even in the absence of Cripto. Cripto-mediated

trafficking thus may serve to specifically prolong the duration of Nodal signalling, a key determinant of cell fate (Ben-Haim et al., 2006; Hagos and Dougan, 2007).

7.3.1 Cripto can inhibit intralumenal vesicle formation in multivesicular endosomes

In the presence of Cripto, Nodal is located at the limiting membrane of endosomes, whereas in the absence of Cripto, it is trapped in intralumenal vesicles of multivesicular endosomes (MVE). Our results suggest that lumenal sequestration in early endosomes also inhibits Nodal signalling, and that this sorting step can be blocked by the pathway agonist Cripto. In correlation with this hypothesis, Cripto seems to enlarge the size of early endosomes. In addition, no intralumenal vesicles were detected when Nodal was retained at the limiting membrane. It thus seems that Cripto has an effect on shaping the endosomal membrane.

How could Cripto inhibit vesicle formation of multivesicular endosome? Intraendosomal sorting is best known for its role in the EGF pathway to mediate signal termination and ligand-induced receptor downregulation (reviewed in van der Goot and Gruenberg, 2006). Ubiquitination of EGFR recruits Hrs and the ESCRT complex, thereby forcing the limiting membrane to bud into the endosomal lumen, where associated cargo is sequestered from cytoplasmic signal transduction molecules and delivered to lysosomes (reviewed in Raiborg et al., 2003; reviewed in van der Goot and Gruenberg, 2006). Also, TGF-β receptor II enters lysosomes via multivesicular endosomes (Shim et al., 2006). TGF-β receptor I and BMP receptor II are targeted for degradation after polyubiquitination in caveolae (Di Guglielmo et al., 2003; Satow et al., 2006). Receptor degradation can be blocked by proteasome inhibitors. Since proteasome inhibitors also interfere with intraendosomal vesicle formation, they may stabilize TGF-β receptors indirectly by blocking transport to lysosomes (reviewed in Raiborg et al., 2003). Thus, it is tempting to speculate that Cripto-mediated Nodal uptake helps to evade ubiquitin ligases and ligand-induced receptor degradation. It will be interesting to characterise in future studies how the trafficking of Nodal receptors is regulated, and whether Cripto-mediated Nodal uptake serves to evade ubiquitin ligases and ligand-induced receptor degradation.

Cripto may also alter membrane properties such as rigidity to directly inhibit membrane curvature. Some molecules are able to act on the membrane property allowing vesicles formation. Membrane coats define specific membrane domains required for

compartmentalisation. The best known coat is composed of clathrin (reviewed in Kirchhausen, 2000). Clathrin has a 3-fold symmetric structure called triskelion. These triskelons are able to assemble together. Their organisation results in the formation of a cage-shaped vesicle that pinches off and becomes a CCV in the cytosol (reviewed in Pearse et al., 2000). However, other types of molecules are able to define certain domains and are also taking part in the formation of vesicles. These scaffold proteins have a hairpin-like hydrophobic topology that gets integrated into the cytosolic leaflet of the membrane. Three proteins of this type have been identified so far: Caveolin, Reticulon and Reggie/Flotillin (Bauer and Pelkmans, 2006). The mechanism of organisation is less clear than the one for Clathrin. However, it seems that an assembly in polymeric coat stabilised by the presence of cholesterol is the most plausible model. Indeed, caveolar coat appears to have a higher affinity for cholesterol than the oligomeric and monomeric Caveolin. This assembly involves proteins and lipids suggesting that caveolin coat formation relies on a cooperative effect. How Reticulon and Flotillin induce membrane curvature is even less clear. Could Cripto increase the rigidity of membrane domains by inhibiting the function of Flotillin? Whether the GPI-anchor Cripto and the hairpin-like protein Flotillin can directly interact remains to be determined.

7.3.2   Implications for Nodal signalling in gradient models

Cripto is required to potentiate Nodal signalling along the Smad2/3 pathway. My work suggests a new mechanism, namely that Cripto is required to stabilise Nodal at the limiting membrane of early endosomes. Cripto could thus be involved in maintaining Nodal signal over a certain time. This result is in accordance with the finding that internalised Nodal receptors remain active for several hours (Dyson and Gurdon, 1998). This recent study proposes a new view for cellular determination after receptor activation (reviewed in Gurdon and Bourillot, 2001). According to this model, a cell recognises the number of activated receptors that are internalised over time, and their lasting activity in the cell. Cells sense a ligand concentration by the absolute number of occupied receptor per cell. The amount of receptors activated thus generates a cellular memory which translates into the choice of target gene expression based on the total signal duration. In other words, a memory of the ligand concentration may be linked to a relatively long-lasting pool of activated receptors. The

memory ensures that the cell will make a specific response to a given concentration to achieve one particular outcome.

In addition, it was shown that SARA endosomes store signalling molecules including the Dpp receptor Thickvein (Tkv). During the cell division, SARA-positive endosomes congregate at the cleavage plane and are equally distributed in daughter cells during mitosis (Bokel et al., 2006). These endosomes contain transmembrane receptor Thickvein (Tkv). When SARA was mutated, Tkv failed to localise to the central spindle. SARA is thus involved in targeting signalling cargo to endosomes associated with the spindle machinery. This ensures the maintenance of the Dpp readout within a gradient across mitosis. Indeed, the presence of SARA is required for the recruitment of Smad2/3 to the receptor complex for phosphorylation and thus further signal transduction (Tsukazaki et al., 1998).

Consistent with a role for SARA in regulating the duration of Smad2/3 signalling, Dougan and coworkers were able to show by conditionally inactivating Nodal receptors that cell fate specification in zebrafish embryo at gastrulation stage depends on Nodal signal duration (Hagos and Dougan, 2007). Nodal signals were able to specify mesodermal tissues at any time within a three-hour period. In other words, cells do not respond to Nodal signals at a particular time but instead generate a response corresponding to the highest total dose to which they are exposed over time. This spatio-temporal gradient model proposes that the cellular response is determined by both the length of time a cell is exposed to the Nodal signal and the distance a cell is from the Nodal source.

How do moving cells remember their position in a gradient? In the mid nineties, a model termed the 'ratchet-like process' was proposed (Gurdon et al., 1995). That study showed that cells start to respond to Activin continuously over a certain period. Moreover, cells expressed genes characteristic of the highest concentration of morphogen to which they have been exposed during their period of competence. Therefore, it seems that cells are able to identify their position in a gradient and can directly respond to the morphogen induction. Our data is in accordance with this model. Nodal signalling would depend on the amount of Nodal activated and maintained over a certain period at the limiting membrane of endosome allowing the expression of particular genes. However, it remains to be determined how long Nodal/Cripto complex can persist on endosomes, and how that time frame correlates with cellular decision taking in the mammalian embryo.

7.3.3 The GPI-AP Dally and Dally-like are involved in morphogen trafficking

In addition to the EGF-CFC family, heparin sulphate proteoglycans (HSPGs) may also influence Nodal signalling (Oki et al., 2007). Due to their strong charge, glypicans can bind secreted growth factors and ECM components (reviewed in Bernfield et al., 1999). HSPGs are implicated in many cellular aspects such as adhesion, proliferation, differentiation, morphogenesis, and protein motility. More precisely, biochemical studies and cell culture assays have implicated HSPGs as coreceptors for specific extracellular ligands and their signal-transducing receptors (reviewed in Lin, 2004). Indeed, studies have shown that sugar-modified HSPGs can sequester cargo proteins within secretory vesicles (Tooze and Huttner, 1990). HSPGs have shown to have a role in other growth factor signalling such as Wingless (Wg) and Decapentaplegic (Dpp) in *Drosophila Melanogaster* (reviewed in Lin and Perrimon, 2002; reviewed in Nybakken and Perrimon, 2002).

Direct evidence linking proteoglycans to pattern formation and growth factor signalling came first from the studies of two glypicans: Division abnormally delayed (Dally) and Dally-like (Dly) in *Drosophila* (Nakato et al., 1995). Like vertebrate glypicans, Dally is linked to GPI and modified by heparin sulphate (Tsuda et al., 1999). Dally might serve as a co-receptor for Dpp. Compromising Dally reduces the expression of genes activated by Dpp, without appreciably affecting the levels of dpp expression (Jackson et al., 1997). Conversely, ectopic expression of Dally results in enhanced Dpp signalling in the fly wing disc (Fujise et al., 2003). So far, Dally has been found to act on Dpp signalling only in imaginal discs. However, it is not clear how Dally increases signalling.

The trafficking of one of several Nodal homologs has recently been studied in *Xenopus* (Williams et al., 2004). These studies suggest that Xnr2 may establish a gradient by diffusion through the extracellular space. However, Xenopus has many Nodal homologs. Like other morphogens, mouse Nodal could require the presence of HSPGs to traffic from one cell to the other (Han et al., 2004; Tsuda et al., 1999). Indeed, recently it has been shown that sulphated glycosaminoglycans (GAG) are necessary for Nodal signalling during L/R axis formation (Oki et al., 2007). Inhibition of GAG biosynthesis prevents Nodal expression in the lateral plate mesoderm (LMP). Sulfated GAGs seem thus required for Nodal transmission from the node to the left lateral plate in the mouse embryo. This model does not exclude the possibility that Nodal trafficking is regulated in a tissue-specific manner.

7.3.4   Different mechanisms allow a gradient formation patterning

Lander and coworkers have proposed on theoretical grounds that Dpp diffusive mechanisms are more likely than non-diffusive mechanisms (Lander et al., 2002). However, an alternative model proposes that a Dpp gradient is established through repeated cycles of secretion and cellular internalisation (reviewed in Gonzalez-Gaitan, 2003). Accordingly, a signalling gradient is formed via intracellular trafficking of ligand, and is mediated by receptor-dependent endocytosis in receiving cells (reviewed in Entchev and Gonzalez-Gaitan, 2002; Entchev et al., 2000). This 'planar transcytosis' model proposes that recycling endosomes can release Dpp, thereby propagating its spreading from cell to cell. Signal propagation in this model is restricted by its endosomal degradation. The gradient slope is controlled by Dpp fate after endocytosis: recycling versus degradation. Using a GFP-Dpp fusion, Dpp trafficking was monitored throughout the target tissue (Entchev et al., 2000). Evidence showed that long-range Dpp movement involves Dpp receptor, Thickveins and Dynamin functions (Kruse et al., 2004).

Dynamin-dependent endocytosis is required for Dpp movement. Gonzalez-Gaitan and coworkers further defined four key parameters that characterise a morphogen gradient: the production rate, the effective diffusion coefficient, the degradation rate and the immobile fraction (Kicheva et al., 2007). The way signalling molecules shape their gradient differs from one morphogen to another. Their results showed that Dpp forms a long-range gradient whereas Wg makes a shorter one. In addition, Wg transport was independent of Dynamin endocytosis. By contrast, Dynamin-mediated endocytosis is required for Dpp signalling (Belenkaya et al., 2004). However, whether or not Dynamin is also required for Dpp movement from cell to cell is controversial (Belenkaya et al., 2004; Entchev et al., 2000). According to the Lin laboratory, Dpp moves from cell to cell along the wing epithelium through restricted extracellular diffusion involving Dally and Dly. However, it is possible that Dynamin was not completely eliminated in their heat shock experiments.

A major difference between Dpp and Wg is that Wg is itself modified by lipid (Micchelli et al., 2002; Willert et al., 2003). Thus, similar to the lipid-linked morphogen Hedgehog (Hh), Wg seems to be secreted and to establish a signalling gradient through lipoprotein particles (Panakova et al., 2005) termed argosomes (Greco et al., 2001). Dally and Dlp are also involved in Wg and Hh signalling (Baeg et al., 2001; Khare and Baumgartner, 2000; Tsuda et al., 1999). HSPGs must be present in the producing cells in order for Wg to accumulate

normally in vesicular structures. HSPGs might thus be required for the incorporation of Wg in argosomes. Moreover, after heparinase treatment, Wg level in punctuate structures was strongly reduced in the surrounding tissue. HSPGs are also required in receiving tissues for the Wg gradient establishment. The amount of HSPG seems to be tightly regulated by Wg itself. Wg contributes to shaping its own gradient by regulating the expression of Notum, a member of the α/β-hydrolase superfamily. Notum downregulates Wg signalling by modifying Dally and Dlp cleavage (Giraldez et al., 2002; Han et al., 2005). Since Dally and Dlp are GPI-APs, an interesting question for future studies is whether Cripto might also play a role in Nodal transport from cell to cell.

It has been postulated that the zebrafish Nodal homolog, Squint, is a morphogen (Chen and Schier, 2001). In order to avoid a relay mechanism created by a Nodal autoinduction, the Schier laboratory monitored Squint signalling across a field of cell deficient in Oep, the Cripto homolog. Indeed, when squint RNA was injected in a single cell of MZoep mutants, Squint could induce the expression of notail in grafted wild-type cells at a distance. However, in our model, Cripto traps Nodal in the producing cells to potentiate autocrine signalling whenever Nodal is cleaved. Furthermore, the presence of Cripto in cell mixing assay seems to correlate with a marked inhibition of paracrine signalling (unpublished observation, Constam lab). However, we do not exclude the possibility that Cripto assists in the transport of uncleaved Nodal, if the amount of SPCs are rate-limiting for cleavage. Unfortunately, technical issues related to the monitoring of intracellular trafficking in the mouse embryo are still making analyses difficult.

8 SIGNIFICANCE

Ectopic activation of embryonic signalling networks contributes to tumorigenesis.

The activities of TGF-β family members are very pleiotropic (reviewed in Derynck et al., 2001; reviewed in Massague et al., 2000). In normal cellular conditions, TGF-βs are tightly linked to the control of cell cycle and the maintenance of genetic information. Indeed, TGF-β ligands have tumor suppressor activities when they are well regulated. The secretion of a latent complex may represent an important safeguard against inadvertent activation of the TGF-β complex (Constam et al., 1992), because excessive activation of TGF-βs during tumor progression elicits pro-oncogenic effects. Possibly, TGF-β has a dual role as tumor suppressor and oncogene because it can induce distinct cellular responses depending on its concentration (reviewed in Wakefield and Roberts, 2002). At low levels, TGF-β may act in an autocrine fashion to inhibit cell proliferation. However, when overexpressed, TGF-β may act on different target cells in stromal compartments and/or induce distinct target genes to promote uncontrolled cell divisions and invasive behaviors. The fact that TGF-β production and maturation is highly upregulated in a majority of malignant tumors is consistent with such a model. Paradoxically, however, a decrease in TβRII expression levels leads to selective loss of growth inhibitory responses while oncogenic effects are retained (Chen et al., 1993). At first glance, this would suggest that tumor suppressor activity is mediated by peak levels of TGF-β signalling. Alternatively, and perhaps more likely, downregulation of TGF-β RII may causally contribute to excess accumulation and hence spreading of ligand to the stromal environment

My work has focused on the function of Cripto in Nodal signalling. Elevated levels of Cripto expression have been detected in more than 80% of human breast cancers, and in many other epithelial tumors e.g. in the ovary, cervix, pancreas or lung (reviewed in Persico et al., 2001). Recently it has been shown that ectopic induction of *NODAL* correlates with increased aggressiveness of human melanoma (Topczewska et al., 2006). The same study also has shown that endogenous Nodal is responsible for inducing an undifferentiated and invasive phenotype in cultured human melanoma cell lines. It will be important, therefore, to determine how Nodal trafficking is regulated in human metastatic melanoma, and whether the new role for Cripto in the trafficking of specific cargo proteins may offer a therapeutic opportunity to block oncogenic effects.

9 Materials and methods

Expression Vectors

Full length murine Cripto (Genbank NM 007685) and C-terminally Flag-tagged mutant forms carrying the H104G and W107G point mutations in the CFC domain (mCFC-Cripto-3F) or lacking the EGF domain (ΔEGF-Cripto-3F), HA-tagged kinase inactive ALK4 receptor and myc-tagged murine FoxH1 have been described (Minchiotti et al., 2000; Yeo and Whitman, 2001a). To remove the Flag epitopes and restore the function of the GPI signal sequence, HindIII-Nhe1 cDNA fragments of mCFC- and ΔEGF-Cripto-3F were used to replace the corresponding region of wild-type Cripto. Furthermore, to delete the GPI signal sequence and generate a soluble form of wild-type Cripto, coding sequence was amplified using the primers GTGAATTCCACCATGGGGTACTTCTCATCCAGT and AGTGCGGCCGCCGTCACAGACGGCGTTTGAC and fused to six C-terminal His residues followed by a myc epitope. Expression vectors for full-length murine Nodal, its pro (Npro) and mature domain (Nmat) were as previously described (Constam and Robertson, 1999 ; Le Good et al., 2005). Likewise, mutations of the Nodal precursor to generate either an SPC-resistant Nodal (Nr) or a form which is more susceptible to cleavage have been described (Constam and Robertson, 1999).

To generate the Npro-GFP fusion protein, an EcoR I – PshA I cDNA fragment encoding M1-Q230 of the Nodal propeptide was ligated into EcoR I – Sma I of pEGFP-N2 (Invitrogen). The NdlΔCIR precursor lacking the CIR was constructed from two PCR fragments. The 5' fragment encoding residues M1-S202 of the Flag-tagged Nodal propeptide (Constam and Robertson, 1999; Le Good et al., 2005) was amplified using primers R1fug1 GGAATTCCACCATGAGTGCCCACAG and DelDistPro CCTACGCGTATCGCCTCCTCGTTCGACAGAGAGTTGACTGTACAACATGAGCACA TTGGTGCTG. The 3' fragment encompassing R240 to L354 was amplified using primers MluNmatFw AAGTGGCTTAAGCCCACGCGTAGGCAACGCCGACATCATTT and Nmat3Xho TTGTCGAGTCAGAGGCA CCCACACTCC. The resulting fragments were ligated to each other via Mlu1 into the EcoR1-Xba1 sites of CS2+. To derive Flag-NproΔCIR-GFP, an EcoR I – BsrG I fragment of NdlΔCIR comprising M1 to Y201 of the prodomain was ligated into EcoR I and Asp718 sites of pEGFP-N2.

The expression vector Ndl-CIRmut was cloned in CS2+ by amplifying two mutant PCR fragments of Nodal cDNA that were fused by overlap extension PCR: Primers R1fug1 and CIRmut1Rev (GGCCCCAGCTTCCCAAAGCCCAGTGGCG) were used to amplify the 5' fragment, whereas the 3' fragment was obtained using primers CIRmut1Fw GCTTTGGGAAGCTGGGGCCCATTGGCGG and Nmat3Xho. ssCFP was generated in pcDNA3.1 (Invitrogen) by ligating the lactase phlorizin hydrolase signal sequence to CFP via a PCR-derived BamH1 site.

To generate ssCFP-Pbox and ssCFP-CIR, the P-domain (Q394-T573) of mouse Furin and the CIR of Nodal were amplified using the primer pairs GGAATTCCTGCAGCACCTGGTAGTGCAGA and CGTCTAGATTATGTGCCATACAGAACGAGAG, or AGAATTCCAGCCCTACACCCCACC and CGTTCTAGATTATACAGAC AGCTGTCCCTCC, respectively, and the resulting fragments were ligated to the 3'end of ssCFP cDNA via EcoR1 in pcDNA3.1. To generate Flag-Pd expression vector, a PCR fragment amplified by primers GGAATTCCTGCAGCACCTGGTAGTGCAGA and CGTCTAGATTATGTGCCATACAGAACGAGAG was ligated at the 5' end via Pst I to a Flag epitope fused to the signal sequence of influenza hemagglutinin in the pCR3 vector (Invitrogen).

To express Myc-tagged human Activin A (kind gift of T. Jessell), a cDNA fragment comprising nucleotides 224-1609 of refseq NM_002192.2 carrying the insertion CAGAAGCTGATATCCGAGGAGGACCTG between the codons for E313 and C314 was cloned between the EcoRI and XhoI sites of pMT21 (Basler et al., 1993). Expression vectors for Flag-tagged full-length mouse Nodal precursor, its propeptide (Npro), and constitutively mature Nodal (Nmat) have been described (Constam and Robertson, 1999 ; Le Good et al., 2005).

Enzymatic removal of carbohydrates

Immunoprecipitated Cripto was incubated with N-glycosidase F or Endoglycosidase-H (Roche) for 1 h at 37 ^{0}C in 50 mM sodium phosphate buffer pH 5.5. Deglycosylated proteins were dissolved in SDS sample buffer and analysed by immunoblotting.

Immunofluorescent staining of permeabilised and non-permeabilised cells

To visualise the localisation of Nodal and Cripto, cells transfected on coverslips were fixed in 4% paraformaldehyde for 15 min. Where indicated, cells were permeabilised with 0.02% Triton X-100 followed by indirect immunofluorescence analysis using fluorescein- or Cy3-coupled secondary anti-mouse or anti-rabbit antibodies at the recommended concentrations (Molecular Probes). Cell surface expression of Nodal and Cripto on non-permeabilised cells was detected using anti-Flag M2 (Sigma) or anti-Cripto C-terminus antibody (dilution 1 : 400) (Minchiotti et al., 2001). For antibody uptake, transfected cells were incubated at 37 ^{o}C for the indicated time in culture medium containing 9 µg/ml anti-Flag M2 antibody. After washing with PBS, cells were fixed, permeabilised and stained as described above using Cy3-anti-mouse antibody. Stained coverslips were mounted in DABCO mounting medium and analysed by confocal microscopy (Zeiss LSM 510).

Tunicamycin treatment

Tunicamycin inhibits N-glycosylation. The day after transfection, Tunicamycin (2.5 µl/ml, Sigma) was added for 8 or 24 hours

NH$_4$Cl treatment

The day after transfection, cells were incubated for 20h in Optimem containing ammonium chloride (20 or 50mM) to inhibit endosomal acidification.

Brefeldin A treatment

BFA fuses the ER with the Cis Golgi and inhibit retrograde transport in the Golgi. The day after transfection, BFA (5 µg/ml, Sigma) was added for 12 or 18 hours to culture medium (Optimem).

Decanoyl-Arg-Val-Lys-Arg-chloromethylketone (CMK) treatment

To inhibit Furin activity, CMK (75 µM, Biomol) was added for 20 hours on cells a day after transfection.

Density fractionation gradients

All of the following steps were performed in the cold room. 48 hours after transfecting 6×10^5 COS1 cells, cells were incubated for 30 min on ice in 200 µl TNE buffer (25mM Tris HCl pH7.4, 150mM NaCl, 5mM EDTA) containing protease inhibitors (Complete Mini, Roche)

and 1% TritonX-100. The resulting cell suspensions were passed 10 times through a 26G needle, and protein concentrations were mesured (Bradford assay, Biorad) and adjusted to 1.2 µg/ml. Of the resulting homogenates, 90 µl was thoroughly mixed with 120 µl of 60% Optiprep (stock solution, Axon Lab) and then overlaid without mixing by 2 ml of 30% Optiprep (diluted in TNE) and 190 µl of TNE buffer. After centrifugation for 2 h (55000 rpm, 259000 x g at 4°C), six 400 µl fractions were precipitated by adding sodium deoxycholate (125 µg/ml) and trichloroacetic acid (4.8 mg/µl). After resuspension in SDS sample buffer, proteins of interest were visualized in each fraction by Western blot analysis.

Nodal and Cripto expression and immunoprecipitation in transiently transfected cells

All constructs were transiently transfected into COS1 or 293T cells in the presence of 0.4 mg/ml DEAE dextran (Constam and Robertson, 1999). After 48 h, cells were either directly lysed in SDS sample buffer for Western blot analysis, or extracted in RIPA buffer containing 1% v/v Triton X-100 and protease inhibitors (Roche Diagnostics GmBH), followed by immunprecipitation. Briefly, cells were homogenized in lysis buffer at 4$^\text{o}$C for 30 min, followed by incubation at 4$^\text{o}$C for 1-2 h with antibodies bound to protein G sepharose. Upon centrifugation, precipitated proteins were washed with lysis buffer and dissolved in SDS sample buffer for Western blot analysis. Proteins were visualized by Western blot analysis using rabbit anti-Nodal peptide (Constam and Robertson, 1999), anti-FLAG M2 (Sigma) or monoclonal anti-HA (Sigma) antibodies. Anti-Cripto antibodies have been described previously (Minchiotti et al., 2000).

In vitro immunoprecipitation assay

Soluble Cripto was coprecipitated in cell-free assays with a stabilized mutant form of Nodal (N-g) containing an engineered N-glycosylation site at position 292 (Le Good et al., 2005). Briefly, 20-fold concentrated conditioned medium from HEK 293T cell lines stably expressing stabilized Nodal was incubated with 6xHis-tagged soluble Cripto which was pre-bound to metal agarose Talon beads (BD Biosciences) in the presence of 150 mM imidazole. After 2 hours incubation at room temperature, complexes were precipitated, washed three times in RIPA buffer containing 150 mM imidazole, and eluted into SDS sample buffer for Western blot analysis.

Detection of Nodal signalling

Nodal acitivity was monitored using a luciferase assay in 293T cells (Yan et al., 2002). Briefly, 48 h after cotransfection with Nodal, Cripto and FoxH1, induction of the luciferase reporter ARE-lux was measured and normalised relative to the expression of transfected β-galactosidase. To mimic the situation in the embryo where Nodal and its convertases are expressed in separate cell populations, cells expressing Furin, PACE4 or empty vector were mixed 24 h after transfection with separate cells expressing Cripto, FoxH1 and the ARE-lux reporter with or without Nodal. Co-cultures were lysed after 24 h to measure the induction of luciferase activity.

Double whole mount in situ hybridisation

Embryos were dissected 6.5 days post coitum and fixed overnight at 4 ^{0}C in PBS containing 4% paraformaldehyde and 0.1% v/v Tween-20. DIG-labelled Nodal and fluorescein-labelled Cripto antisense mRNA probes were hybridized to whole mount embryos and sequentially revealed using BM purple and INT/BCIP to detect alkaline phosphatase conjugated to anti-DIG and anti-FLUO antibodies (Roche), respectively. Frozen sections (8 µm) were obtained after embedding stained embryos in glycerol containing 30 % (w/v) sucrose.

2 Bromo-palmitate (2BP) treatment

The day after transfection, cells were incubated for 24h in Optimem containing 8 µg/ml 2BP (ACROSCOM) was added for 24 hours on cells. Stock solution of 2BP was prepared in methanol.

Detection of ALK4, 5, 7 signalling

Effects of wild-type and mutant Cripto on Nodal activity were analysed using a luciferase assay in 293T cells (Yan et al., 2002). Briefly, 48 h after cotransfection with Nodal, Cripto and FoxH1, induction of the luciferase reporter ARE-lux was measured and normalised relative to the expression of transfected β-galactosidase. To monitor ALK4, 5, 7 signalling in COS1 cells, CAGA-GFP (Neptune et al., 2003) was transfected using Lipofectamine 2000 (Invitrogen). After 24 h, transfected cells were stimulated for 24 h by recombinant Activin A or TGF-β (50 ng/ml, R&D Systems) in the presence or absence of the ALK4, 5, 7 inhibitor SB431542 (10 µM, Sigma). After taking pictures on a Leica DC200 microscope, cells were lysed in 100 µl of SDS sample buffer and analysed by Western blotting using polyclonal

rabbit anti-GFP antibody (1:2000 dilution) and anti γ-tubulin, 1:5000 (Sigma). Signals were quantified using ImageJ software.

Colocalisation

Images were taken using a confocal microscope from Zeiss LSM510 Axiovert laser-scanning microscope (Carl Zeiss Inc using a 63x/NA 1.4 oil objective. Colocalisation analyses and statistics after FlagM2 labelling were generated using the Metamorph Offline software (version 7.1; Universal Imaging Corporation, West Chester, Pa.). The colocalisation of the amount red (Nodal) overlapping the amount of green (marker) was assessed after distance calibration. Colocalisation events were calculated based on the integrated density defined in the Metamorph software. Costes' approach and Manders' coefficient were used to assess the results given by Metamorph (Costes et al., 2004; Manders et al., 1992). Both methods were calculated with ImageJ. For Costes approach, a randomised image was created by shuffling pixel blocks with the dimension defined by the point spread function (PSF) for the image of the green channel. This process is done 200 times for a single image and the Pearson's coefficient is calculated each time between the random images of the green channel and the original image of the red channel. Manders' coefficient calculated using the JACoP tool (Bolte and Crodelières, 2006). Manders' coefficient varies from 0 to 1, corresponding to non-overlapping images and 100% colocalisation between the two images respectively. Statistical probabilities were determined by Student's t test. Relevance is shown by asterix (*** p<0.001).

Transmission electron microscopy

For electron microscopy, subconfluent COS1 cells were fixed by adding 4% freshly prepared formaldehyde and 0.4% glutaraldehyde in 0.1 M phosphate buffer pH 7.4 to an equal volume of culture medium for 10 min, followed by post-fixation in 2% formaldehyde and 0.2% glutaraldehyde in 0.1 M phosphate buffer pH 7.4 without medium overnight at 4°C. Cells were stored until further processing in 1% formaldehyde at 4ºC. Processing of cells for ultrathin cryosectioning and immuno-labeling according to the protein A-gold method was done as described (Slot and Geuze, 2007). In brief, fixed cells were washed with 0.05 M glycine in PBS, scraped gently from the dish in PBS containing 1% gelatin, resuspended and pelleted in 12% gelatin in PBS, 37°C. The cell pellet was solidified on ice and cut into small blocks. For cryoprotection, blocks were infiltrated overnight with 2.3 M sucrose at 4°C and afterwards mounted on aluminum pins and frozen in liquid nitrogen. To pick up ultrathin

cryosections (60 nm), a 1:1 mixture of 2.3 M sucrose and 1.8% methylcellulose was used. Thin cryosections were labeled with rabbit anti-mouse Ig (Dako Z0412) antibodies and protein-A-gold 10 nm (CMC–UMC, Utrecht).

10 BIBLIOGRAPHY

Ackerman, A. L., and Cresswell, P. (2004). Cellular mechanisms governing cross-presentation of exogenous antigens. Nat Immunol *5*, 678-684.

Ackland, M. L., Newgreen, D. F., Fridman, M., Waltham, M. C., Arvanitis, A., Minichiello, J., Price, J. T., and Thompson, E. W. (2003). Epidermal growth factor-induced epithelio-mesenchymal transition in human breast carcinoma cells. Lab Invest *83*, 435-448.

Aderem, A., and Underhill, D. M. (1999). Mechanisms of phagocytosis in macrophages. Annu Rev Immunol *17*, 593-623.

Amyere, M., Mettlen, M., Van Der Smissen, P., Platek, A., Payrastre, B., Veithen, A., and Courtoy, P. J. (2002). Origin, originality, functions, subversions and molecular signalling of macropinocytosis. Int J Med Microbiol *291*, 487-494.

Anderson, E. D., Molloy, S. S., Jean, F., Fei, H., Shimamura, S., and Thomas, G. (2002). The ordered and compartment-specfific autoproteolytic removal of the furin intramolecular chaperone is required for enzyme activation. J Biol Chem *277*, 12879-12890.

Anderson, R. G. (1998). The caveolae membrane system. Annu Rev Biochem *67*, 199-225.

Bache, K. G., Brech, A., Mehlum, A., and Stenmark, H. (2003). Hrs regulates multivesicular body formation via ESCRT recruitment to endosomes. J Cell Biol *162*, 435-442.

Baeg, G. H., Lin, X., Khare, N., Baumgartner, S., and Perrimon, N. (2001). Heparan sulfate proteoglycans are critical for the organization of the extracellular distribution of Wingless. Development *128*, 87-94.

Baldwin, T. A., and Ostergaard, H. L. (2001). Developmentally regulated changes in glucosidase II association with, and carbohydrate content of, the protein tyrosine phosphatase CD45. J Immunol *167*, 3829-3835.

Band, A. M., Maatta, J., Kaariainen, L., and Kuismanen, E. (2001). Inhibition of the membrane fusion machinery prevents exit from the TGN and proteolytic processing by furin. FEBS Lett *505*, 118-124.

Basler, K., Edlund, T., Jessell, T. M., and Yamada, T. (1993). Control of cell pattern in the neural tube: regulation of cell differentiation by dorsalin-1, a novel TGF beta family member. Cell *73*, 687-702.

Bauer, M., and Pelkmans, L. (2006). A new paradigm for membrane-organizing and -shaping scaffolds. FEBS Lett *580*, 5559-5564.

Beck, S., Le Good, J. A., Guzman, M., Ben Haim, N., Roy, K., Beermann, F., and Constam, D. B. (2002). Extraembryonic proteases regulate Nodal signalling during gastrulation. Nat Cell Biol *4*, 981-985.

Beddington, R. S. (1994). Induction of a second neural axis by the mouse node. Development *120*, 613-620.

Beddington, R. S., and Robertson, E. J. (1998). Anterior patterning in mouse. Trends Genet *14*, 277-284.

Belenkaya, T. Y., Han, C., Yan, D., Opoka, R. J., Khodoun, M., Liu, H., and Lin, X. (2004). Drosophila Dpp morphogen movement is independent of dynamin-mediated endocytosis but regulated by the glypican members of heparan sulfate proteoglycans. Cell *119*, 231-244.

Bellairs, R. (1986). The primitive streak. Anat Embryol (Berl) *174*, 1-14.

Ben-Haim, N., Lu, C., Guzman-Ayala, M., Pescatore, L., Mesnard, D., Bischofberger, M., Naef, F., Robertson, E. J., and Constam, D. B. (2006). The nodal precursor acting via activin receptors induces mesoderm by maintaining a source of its convertases and BMP4. Dev Cell *11*, 313-323.

Bernfield, M., Gotte, M., Park, P. W., Reizes, O., Fitzgerald, M. L., Lincecum, J., and Zako, M. (1999). Functions of cell surface heparan sulfate proteoglycans. Annu Rev Biochem *68*, 729-777.

Bianco, C., Adkins, H. B., Wechselberger, C., Seno, M., Normanno, N., De Luca, A., Sun, Y., Khan, N., Kenney, N., Ebert, A.*, et al.* (2002). Cripto-1 activates nodal- and ALK4-dependent and -independent signalling pathways in mammary epithelial Cells. Mol Cell Biol *22*, 2586-2597.

Bianco, C., Normanno, N., Salomon, D. S., and Ciardiello, F. (2004). Role of the cripto (EGF-CFC) family in embryogenesis and cancer. Growth Factors *22*, 133-139.

Bianco, C., Strizzi, L., Rehman, A., Normanno, N., Wechselberger, C., Sun, Y., Khan, N., Hirota, M., Adkins, H., Williams, K.*, et al.* (2003). A Nodal- and ALK4-independent signalling pathway activated by Cripto-1 through Glypican-1 and c-Src. Cancer Res *63*, 1192-1197.

Bickel, P. E., Scherer, P. E., Schnitzer, J. E., Oh, P., Lisanti, M. P., and Lodish, H. F. (1997). Flotillin and epidermal surface antigen define a new family of caveolae-associated integral membrane proteins. J Biol Chem *272*, 13793-13802.

Boivin, G. P., O'Toole, B. A., Orsmby, I. E., Diebold, R. J., Eis, M. J., Doetschman, T., and Kier, A. B. (1995). Onset and progression of pathological lesions in transforming growth factor-beta 1-deficient mice. Am J Pathol *146*, 276-288.

Bokel, C., Schwabedissen, A., Entchev, E., Renaud, O., and Gonzalez-Gaitan, M. (2006). Sara endosomes and the maintenance of Dpp signalling levels across mitosis. Science *314*, 1135-1139.

Bonnon, C., Goutebroze, L., Denisenko-Nehrbass, N., Girault, J. A., and Faivre-Sarrailh, C. (2003). The paranodal complex of F3/contactin and caspr/paranodin traffics to the cell surface via a non-conventional pathway. J Biol Chem *278*, 48339-48347.

Boyer, B., Valles, A. M., and Edme, N. (2000). Induction and regulation of epithelial-mesenchymal transitions. Biochem Pharmacol *60*, 1091-1099.

Brennan, J., Lu, C. C., Norris, D. P., Rodriguez, T. A., Beddington, R. S., and Robertson, E. J. (2001). Nodal signalling in the epiblast patterns the early mouse embryo. Nature *411*, 965-969.

Brodsky, F. M., Chen, C. Y., Knuehl, C., Towler, M. C., and Wakeham, D. E. (2001). Biological basket weaving: formation and function of clathrin-coated vesicles. Annu Rev Cell Dev Biol *17*, 517-568.

Brown, D. (1994). GPI-anchored proteins and detergent-resistant membrane domains. Braz J Med Biol Res *27*, 309-315.

Brown, D. A., and London, E. (1998). Functions of lipid rafts in biological membranes. Annu Rev Cell Dev Biol *14*, 111-136.

Bucci, C., Parton, R. G., Mather, I. H., Stunnenberg, H., Simons, K., Hoflack, B., and Zerial, M. (1992). The small GTPase rab5 functions as a regulatory factor in the early endocytic pathway. Cell *70*, 715-728.

Butikofer, P., Malherbe, T., Boschung, M., and Roditi, I. (2001). GPI-anchored proteins: now you see 'em, now you don't. Faseb J *15*, 545-548.

Camus, A., Perea-Gomez, A., Moreau, A., and Collignon, J. (2006). Absence of Nodal signalling promotes precocious neural differentiation in the mouse embryo. Dev Biol *295*, 743-755.

Casaroli-Marano, R. P., Pagan, R., and Vilaro, S. (1999). Epithelial-mesenchymal transition in proliferative vitreoretinopathy: intermediate filament protein expression in retinal pigment epithelial cells. Invest Ophthalmol Vis Sci *40*, 2062-2072.

Chapman, R. E., and Munro, S. (1994). Retrieval of TGN proteins from the cell surface requires endosomal acidification. Embo J *13*, 2305-2312.

Chatterjee, S., and Mayor, S. (2001). The GPI-anchor and protein sorting. Cell Mol Life Sci *58*, 1969-1987.

Chea, H. K., Wright, C. V., and Swalla, B. J. (2005). Nodal signalling and the evolution of deuterostome gastrulation. Dev Dyn *234*, 269-278.

Cheifetz, S., Bassols, A., Stanley, K., Ohta, M., Greenberger, J., and Massague, J. (1988). Heterodimeric transforming growth factor beta. Biological properties and interaction with three types of cell surface receptors. J Biol Chem *263*, 10783-10789.

Cheifetz, S., Weatherbee, J. A., Tsang, M. L., Anderson, J. K., Mole, J. E., Lucas, R., and Massague, J. (1987). The transforming growth factor-beta system, a complex pattern of cross-reactive ligands and receptors. Cell *48*, 409-415.

Chen, C., and Shen, M. M. (2004). Two modes by which Lefty proteins inhibit nodal signalling. Curr Biol *14*, 618-624.

Chen, R. H., Ebner, R., and Derynck, R. (1993). Inactivation of the type II receptor reveals two receptor pathways for the diverse TGF-beta activities. Science *260*, 1335-1338.

Chen, Y., and Schier, A. F. (2001). The zebrafish Nodal signal Squint functions as a morphogen. Nature *411*, 607-610.

Chen, Y. G., Hata, A., Lo, R. S., Wotton, D., Shi, Y., Pavletich, N., and Massague, J. (1998). Determinants of specificity in TGF-beta signal transduction. Genes Dev *12*, 2144-2152.

Cheng, S. K., Olale, F., Brivanlou, A. H., and Schier, A. F. (2004). Lefty blocks a subset of TGFbeta signals by antagonizing EGF-CFC coreceptors. PLoS Biol *2*, E30.

Chichili, G. R., and Rodgers, W. (2007). Clustering of membrane raft proteins by the actin cytoskeleton. J Biol Chem.

Christoforidis, S., McBride, H. M., Burgoyne, R. D., and Zerial, M. (1999). The Rab5 effector EEA1 is a core component of endosome docking. Nature *397*, 621-625.

Chu, J., Ding, J., Jeays-Ward, K., Price, S. M., Placzek, M., and Shen, M. M. (2005). Non-cell-autonomous role for Cripto in axial midline formation during vertebrate embryogenesis. Development *132*, 5539-5551.

Colas, J. F., and Schoenwolf, G. C. (2000). Subtractive hybridization identifies chick-cripto, a novel EGF-CFC ortholog expressed during gastrulation, neurulation and early cardiogenesis. Gene *255*, 205-217.

Conlon, F. L., Barth, K. S., and Robertson, E. J. (1991). A novel retrovirally induced embryonic lethal mutation in the mouse: assessment of the developmental fate of embryonic stem cells homozygous for the 413.d proviral integration. Development *111*, 969-981.

Conlon, F. L., Lyons, K. M., Takaesu, N., Barth, K. S., Kispert, A., Herrmann, B., and Robertson, E. J. (1994). A primary requirement for nodal in the formation and maintenance of the primitive streak in the mouse. Development *120*, 1919-1928.

Conner, S. D., and Schmid, S. L. (2003). Regulated portals of entry into the cell. Nature *422*, 37-44.

Constam, D. B., Philipp, J., Malipiero, U. V., ten Dijke, P., Schachner, M., and Fontana, A. (1992). Differential expression of transforming growth factor-beta 1, -beta 2, and -beta 3 by glioblastoma cells, astrocytes, and microglia. J Immunol *148*, 1404-1410.

Constam, D. B., and Robertson, E. J. (1999). Regulation of bone morphogenetic protein activities by pro domains and proprotein convertases. J Cell Biol *144*, 139-149.

Costes, S. V., Daelemans, D., Cho, E. H., Dobbin, Z., Pavlakis, G., and Lockett, S. (2004). Automatic and quantitative measurement of protein-protein colocalisation in live cells. Biophys J *86*, 3993-4003.

d'Azzo, A., Bongiovanni, A., and Nastasi, T. (2005). E3 ubiquitin ligases as regulators of membrane protein trafficking and degradation. Traffic *6*, 429-441.

D'Souza-Schorey, C., and Chavrier, P. (2006). ARF proteins: roles in membrane traffic and beyond. Nat Rev Mol Cell Biol *7*, 347-358.

Dandachi, N., Hauser-Kronberger, C., More, E., Wiesener, B., Hacker, G. W., Dietze, O., and Wirl, G. (2001). Co-expression of tenascin-C and vimentin in human breast cancer cells indicates phenotypic transdifferentiation during tumour progression: correlation with histopathological parameters, hormone receptors, and oncoproteins. J Pathol *193*, 181-189.

De Santis, M. L., Kannan, S., Smith, G. H., Seno, M., Bianco, C., Kim, N., Martinez-Lacaci, I., Wallace-Jones, B., and Salomon, D. S. (1997). Cripto-1 inhibits beta-casein expression in mammary epithelial cells through a p21ras-and phosphatidylinositol 3'-kinase-dependent pathway. Cell Growth Differ *8*, 1257-1266.

Derynck, R., Akhurst, R. J., and Balmain, A. (2001). TGF-beta signalling in tumor suppression and cancer progression. Nat Genet *29*, 117-129.

Derynck, R., Zhang, Y., and Feng, X. H. (1998). Smads: transcriptional activators of TGF-beta responses. Cell *95*, 737-740.

Desjardins, M. (2003). ER-mediated phagocytosis: a new membrane for new functions. Nat Rev Immunol *3*, 280-291.

Desjardins, M., Huber, L. A., Parton, R. G., and Griffiths, G. (1994). Biogenesis of phagolysosomes proceeds through a sequential series of interactions with the endocytic apparatus. J Cell Biol *124*, 677-688.

Di Fiore, P. P., Polo, S., and Hofmann, K. (2003). When ubiquitin meets ubiquitin receptors: a signalling connection. Nat Rev Mol Cell Biol *4*, 491-497.

Di Guglielmo, G. M., Le Roy, C., Goodfellow, A. F., and Wrana, J. L. (2003). Distinct endocytic pathways regulate TGF-beta receptor signalling and turnover. Nat Cell Biol *5*, 410-421.

Dietzen, D. J., Hastings, W. R., and Lublin, D. M. (1995). Caveolin is palmitoylated on multiple cysteine residues. Palmitoylation is not necessary for localization of caveolin to caveolae. J Biol Chem *270*, 6838-6842.

Ding, J., Yang, L., Yan, Y. T., Chen, A., Desai, N., Wynshaw-Boris, A., and Shen, M. M. (1998). Cripto is required for correct orientation of the anterior-posterior axis in the mouse embryo. Nature *395*, 702-707.

Dono, R., Scalera, L., Pacifico, F., Acampora, D., Persico, M. G., and Simeone, A. (1993). The murine cripto gene: expression during mesoderm induction and early heart morphogenesis. Development *118*, 1157-1168.

Drab, M., Verkade, P., Elger, M., Kasper, M., Lohn, M., Lauterbach, B., Menne, J., Lindschau, C., Mende, F., Luft, F. C.*, et al.* (2001). Loss of caveolae, vascular dysfunction, and pulmonary defects in caveolin-1 gene-disrupted mice. Science *293*, 2449-2452.

Dunn, N. R., Vincent, S. D., Oxburgh, L., Robertson, E. J., and Bikoff, E. K. (2004). Combinatorial activities of Smad2 and Smad3 regulate mesoderm formation and patterning in the mouse embryo. Development *131*, 1717-1728.

Dyson, S., and Gurdon, J. B. (1998). The interpretation of position in a morphogen gradient as revealed by occupancy of activin receptors. Cell *93*, 557-568.

Ebert, A. D., Wechselberger, C., Frank, S., Wallace-Jones, B., Seno, M., Martinez-Lacaci, I., Bianco, C., De Santis, M., Weitzel, H. K., and Salomon, D. S. (1999). Cripto-1 induces phosphatidylinositol 3'-kinase-dependent phosphorylation of AKT and glycogen synthase kinase 3beta in human cervical carcinoma cells. Cancer Res *59*, 4502-4505.

Ebisawa, T., Fukuchi, M., Murakami, G., Chiba, T., Tanaka, K., Imamura, T., and Miyazono, K. (2001). Smurf1 interacts with transforming growth factor-beta type I receptor through Smad7 and induces receptor degradation. J Biol Chem *276*, 12477-12480.

Entchev, E. V., and Gonzalez-Gaitan, M. A. (2002). Morphogen gradient formation and vesicular trafficking. Traffic *3*, 98-109.

Entchev, E. V., Schwabedissen, A., and Gonzalez-Gaitan, M. (2000). Gradient formation of the TGF-beta homolog Dpp. Cell *103*, 981-991.

Falcone, S., Cocucci, E., Podini, P., Kirchhausen, T., Clementi, E., and Meldolesi, J. (2006). Macropinocytosis: regulated coordination of endocytic and exocytic membrane traffic events. J Cell Sci *119*, 4758-4769.

Felberbaum-Corti, M., Van Der Goot, F. G., and Gruenberg, J. (2003). Sliding doors: clathrin-coated pits or caveolae? Nat Cell Biol *5*, 382-384.

Ferguson, M. A. (1999). The structure, biosynthesis and functions of glycosylphosphatidylinositol anchors, and the contributions of trypanosome research. J Cell Sci *112 (Pt 17)*, 2799-2809.

Fernow, I., Icking, A., and Tikkanen, R. (2007). Reggie-1 and reggie-2 localize in non-caveolar rafts in epithelial cells: cellular localization is not dependent on the expression of caveolin proteins. Eur J Cell Biol *86*, 345-352.

Fivaz, M., Vilbois, F., Thurnheer, S., Pasquali, C., Abrami, L., Bickel, P. E., Parton, R. G., and van der Goot, F. G. (2002). Differential sorting and fate of endocytosed GPI-anchored proteins. Embo J *21*, 3989-4000.

Fleming, T. P., and Pickering, S. J. (1985). Maturation and polarization of the endocytotic system in outside blastomeres during mouse preimplantation development. J Embryol Exp Morphol *89*, 175-208.

Fujise, M., Takeo, S., Kamimura, K., Matsuo, T., Aigaki, T., Izumi, S., and Nakato, H. (2003). Dally regulates Dpp morphogen gradient formation in the Drosophila wing. Development *130*, 1515-1522.

Gagnon, E., Duclos, S., Rondeau, C., Chevet, E., Cameron, P. H., Steele-Mortimer, O., Paiement, J., Bergeron, J. J., and Desjardins, M. (2002). Endoplasmic reticulum-mediated phagocytosis is a mechanism of entry into macrophages. Cell *110*, 119-131.

Giraldez, A. J., Copley, R. R., and Cohen, S. M. (2002). HSPG modification by the secreted enzyme Notum shapes the Wingless morphogen gradient. Dev Cell *2*, 667-676.

Glebov, O. O., Bright, N. A., and Nichols, B. J. (2006). Flotillin-1 defines a clathrin-independent endocytic pathway in mammalian cells. Nat Cell Biol *8*, 46-54.

Gluschankof, P., and Fuller, R. S. (1994). A C-terminal domain conserved in precursor processing proteases is required for intramolecular N-terminal maturation of pro-Kex2 protease. Embo J *13*, 2280-2288.

Gonzalez-Gaitan, M. (2003). Signal dispersal and transduction through the endocytic pathway. Nat Rev Mol Cell Biol *4*, 213-224.

Gorvel, J. P., Chavrier, P., Zerial, M., and Gruenberg, J. (1991). rab5 controls early endosome fusion in vitro. Cell *64*, 915-925.

Greco, V., Hannus, M., and Eaton, S. (2001). Argosomes: a potential vehicle for the spread of morphogens through epithelia. Cell *106*, 633-645.

Gritsman, K., Talbot, W. S., and Schier, A. F. (2000). Nodal signalling patterns the organizer. Development *127*, 921-932.

Gritsman, K., Zhang, J., Cheng, S., Heckscher, E., Talbot, W. S., and Schier, A. F. (1999). The EGF-CFC protein one-eyed pinhead is essential for nodal signalling. Cell *97*, 121-132.

Gruenberg, J. (2001). The endocytic pathway: a mosaic of domains. Nat Rev Mol Cell Biol *2*, 721-730.

Gurdon, J. B., and Bourillot, P. Y. (2001). Morphogen gradient interpretation. Nature *413*, 797-803.

Gurdon, J. B., Mitchell, A., and Mahony, D. (1995). Direct and continuous assessment by cells of their position in a morphogen gradient. Nature *376*, 520-521.

Guzman-Ayala, M., Ben-Haim, N., Beck, S., and Constam, D. B. (2004). Nodal protein processing and fibroblast growth factor 4 synergize to maintain a trophoblast stem cell microenvironment. Proc Natl Acad Sci U S A *101*, 15656-15660.

Hagos, E. G., and Dougan, S. T. (2007). Time-dependent patterning of the mesoderm and endoderm by Nodal signals in zebrafish. BMC Dev Biol *7*, 22.

Han, C., Belenkaya, T. Y., Wang, B., and Lin, X. (2004). Drosophila glypicans control the cell-to-cell movement of Hedgehog by a dynamin-independent process. Development *131*, 601-611.

108

Han, C., Yan, D., Belenkaya, T. Y., and Lin, X. (2005). Drosophila glypicans Dally and Dally-like shape the extracellular Wingless morphogen gradient in the wing disc. Development *132*, 667-679.

Heldin, C. H., Miyazono, K., and ten Dijke, P. (1997). TGF-beta signalling from cell membrane to nucleus through SMAD proteins. Nature *390*, 465-471.

Herpin, A., Lelong, C., and Favrel, P. (2004). Transforming growth factor-beta-related proteins: an ancestral and widespread superfamily of cytokines in metazoans. Dev Comp Immunol *28*, 461-485.

Hogan, B. L. (1996). Bone morphogenetic proteins in development. Curr Opin Genet Dev *6*, 432-438.

Hooper, N. M. (1999). Detergent-insoluble glycosphingolipid/cholesterol-rich membrane domains, lipid rafts and caveolae (review). Mol Membr Biol *16*, 145-156.

Hunter, T. (2000). Signalling--2000 and beyond. Cell *100*, 113-127.

Ikezawa, H. (2002). Glycosylphosphatidylinositol (GPI)-anchored proteins. Biol Pharm Bull *25*, 409-417.

Ikonen, E. (1997). Molecular mechanisms of intracellular cholesterol transport. Curr Opin Lipidol *8*, 60-64.

Ikonen, E. (2008). Cellular cholesterol trafficking and compartmentalization. Nat Rev Mol Cell Biol *9*, 125-138.

Incardona, J. P., and Eaton, S. (2000). Cholesterol in signal transduction. Curr Opin Cell Biol *12*, 193-203.

Incardona, J. P., and Rosenberry, T. L. (1996). Replacement of the glycoinositol phospholipid anchor of Drosophila acetylcholinesterase with a transmembrane domain does not alter sorting in neurons and epithelia but results in behavioral defects. Mol Biol Cell *7*, 613-630.

Itoh, F., Divecha, N., Brocks, L., Oomen, L., Janssen, H., Calafat, J., Itoh, S., and Dijke Pt, P. (2002). The FYVE domain in Smad anchor for receptor activation (SARA) is sufficient for localization of SARA in early endosomes and regulates TGF-beta/Smad signalling. Genes Cells *7*, 321-331.

Jackson, S. M., Nakato, H., Sugiura, M., Jannuzi, A., Oakes, R., Kaluza, V., Golden, C., and Selleck, S. B. (1997). dally, a Drosophila glypican, controls cellular responses to the TGF-beta-related morphogen, Dpp. Development *124*, 4113-4120.

Janes, P. W., Ley, S. C., Magee, A. I., and Kabouridis, P. S. (2000). The role of lipid rafts in T cell antigen receptor (TCR) signalling. Semin Immunol *12*, 23-34.

Johnson, M. H., and Ziomek, C. A. (1981). The foundation of two distinct cell lineages within the mouse morula. Cell *24*, 71-80.

Jullien, J., Guili, V., Derrington, E. A., Darlix, J. L., Reichardt, L. F., and Rudkin, B. B. (2003). Trafficking of TrkA-green fluorescent protein chimerae during nerve growth factor-induced differentiation. J Biol Chem *278*, 8706-8716.

Kalia, M., Kumari, S., Chadda, R., Hill, M. M., Parton, R. G., and Mayor, S. (2006). Arf6-independent GPI-anchored protein-enriched early endosomal compartments fuse with sorting endosomes via a Rab5/phosphatidylinositol-3'-kinase-dependent machinery. Mol Biol Cell *17*, 3689-3704.

Kannan, S., De Santis, M., Lohmeyer, M., Riese, D. J., 2nd, Smith, G. H., Hynes, N., Seno, M., Brandt, R., Bianco, C., Persico, G., *et al.* (1997). Cripto enhances the tyrosine phosphorylation of Shc and activates mitogen-activated protein kinase (MAPK) in mammary epithelial cells. J Biol Chem *272*, 3330-3335.

Katzmann, D. J., Odorizzi, G., and Emr, S. D. (2002). Receptor downregulation and multivesicular-body sorting. Nat Rev Mol Cell Biol *3*, 893-905.

Kawagoe, K., Kitamura, D., Okabe, M., Taniuchi, I., Ikawa, M., Watanabe, T., Kinoshita, T., and Takeda, J. (1996). Glycosylphosphatidylinositol-anchor-deficient mice: implications for clonal dominance of mutant cells in paroxysmal nocturnal hemoglobinuria. Blood *87*, 3600-3606.

Keah, H. H., and Hearn, M. T. (2005). A molecular recognition paradigm: promiscuity associated with the ligand-receptor interactions of the activin members of the TGF-beta superfamily. J Mol Recognit *18*, 385-403.

Kenney, N. J., Smith, G. H., Maroulakou, I. G., Green, J. H., Muller, W. J., Callahan, R., Salomon, D. S., and Dickson, R. B. (1996). Detection of amphiregulin and Cripto-1 in mammary tumors from transgenic mice. Mol Carcinog *15*, 44-56.

Khare, N., and Baumgartner, S. (2000). Dally-like protein, a new Drosophila glypican with expression overlapping with wingless. Mech Dev *99*, 199-202.

Kicheva, A., Pantazis, P., Bollenbach, T., Kalaidzidis, Y., Bittig, T., Julicher, F., and Gonzalez-Gaitan, M. (2007). Kinetics of morphogen gradient formation. Science *315*, 521-525.

Kimura, C., Shen, M. M., Takeda, N., Aizawa, S., and Matsuo, I. (2001). Complementary functions of Otx2 and Cripto in initial patterning of mouse epiblast. Dev Biol *235*, 12-32.

Kinder, S. J., Tsang, T. E., Wakamiya, M., Sasaki, H., Behringer, R. R., Nagy, A., and Tam, P. P. (2001). The organizer of the mouse gastrula is composed of a dynamic population of progenitor cells for the axial mesoderm. Development *128*, 3623-3634.

Kinoshita, N., Minshull, J., and Kirschner, M. W. (1995). The identification of two novel ligands of the FGF receptor by a yeast screening method and their activity in Xenopus development. Cell *83*, 621-630.

Kirchhausen, T. (2000). Clathrin. Annu Rev Biochem *69*, 699-727.

Kokubo, H., Helms, J. B., Ohno-Iwashita, Y., Shimada, Y., Horikoshi, Y., and Yamaguchi, H. (2003). Ultrastructural localization of flotillin-1 to cholesterol-rich membrane microdomains, rafts, in rat brain tissue. Brain Res *965*, 83-90.

Kruse, K., Pantazis, P., Bollenbach, T., Julicher, F., and Gonzalez-Gaitan, M. (2004). Dpp gradient formation by dynamin-dependent endocytosis: receptor trafficking and the diffusion model. Development *131*, 4843-4856.

Kunwar, P. S., Zimmerman, S., Bennett, J. T., Chen, Y., Whitman, M., and Schier, A. F. (2003). Mixer/Bon and FoxH1/Sur have overlapping and divergent roles in Nodal signalling and mesendoderm induction. Development *130*, 5589-5599.

Kurzchalia, T. V., and Parton, R. G. (1999). Membrane microdomains and caveolae. Curr Opin Cell Biol *11*, 424-431.

Lander, A. D., Nie, Q., and Wan, F. Y. (2002). Do morphogen gradients arise by diffusion? Dev Cell *2*, 785-796.

Lang, D. M., Lommel, S., Jung, M., Ankerhold, R., Petrausch, B., Laessing, U., Wiechers, M. F., Plattner, H., and Stuermer, C. A. (1998). Identification of reggie-1 and reggie-2 as plasmamembrane-associated proteins which cocluster with activated GPI-anchored cell adhesion molecules in non-caveolar micropatches in neurons. J Neurobiol *37*, 502-523.

Lawson, K. A., Meneses, J. J., and Pedersen, R. A. (1991). Clonal analysis of epiblast fate during germ layer formation in the mouse embryo. Development *113*, 891-911.

Le Good, J. A., Joubin, K., Giraldez, A. J., Ben-Haim, N., Beck, S., Chen, Y., Schier, A. F., and Constam, D. B. (2005). Nodal stability determines signalling range. Curr Biol *15*, 31-36.

Lemaire, P., and Yasuo, H. (1998). Developmental signalling: a careful balancing act. Curr Biol *8*, R228-231.

Levis, G. M., Evangelatos, G. P., and Crumpton, M. J. (1976). Lipid composition of lymphocyte plasma membrane from pig mesenteric lymph node. Biochem J *156*, 103-110.

Li, S., Song, K. S., and Lisanti, M. P. (1996). Expression and characterization of recombinant caveolin. Purification by polyhistidine tagging and cholesterol-dependent incorporation into defined lipid membranes. J Biol Chem *271*, 568-573.

Liguori, G., Tucci, M., Montuori, N., Dono, R., Lago, C. T., Pacifico, F., Armenante, F., and Persico, M. G. (1996). Characterization of the mouse Tdgf1 gene and Tdgf pseudogenes. Mamm Genome *7*, 344-348.

Lin, S. J., Lerch, T. F., Cook, R. W., Jardetzky, T. S., and Woodruff, T. K. (2006). The structural basis of TGF-beta, bone morphogenetic protein, and activin ligand binding. Reproduction *132*, 179-190.

Lin, X. (2004). Functions of heparan sulfate proteoglycans in cell signalling during development. Development *131*, 6009-6021.

Lin, X., Liang, Y. Y., Sun, B., Liang, M., Shi, Y., Brunicardi, F. C., Shi, Y., and Feng, X. H. (2003). Smad6 recruits transcription corepressor CtBP to repress bone morphogenetic protein-induced transcription. Mol Cell Biol *23*, 9081-9093.

Lin, X., and Perrimon, N. (2002). Developmental roles of heparan sulfate proteoglycans in Drosophila. Glycoconj J *19*, 363-368.

Lu, C. C., Brennan, J., and Robertson, E. J. (2001). From fertilization to gastrulation: axis formation in the mouse embryo. Curr Opin Genet Dev *11*, 384-392.

Malkus, P., Jiang, F., and Schekman, R. (2002). Concentrative sorting of secretory cargo proteins into COPII-coated vesicles. J Cell Biol *159*, 915-921.

Mallet, W. G., and Maxfield, F. R. (1999). Chimeric forms of furin and TGN38 are transported with the plasma membrane in the trans-Golgi network via distinct endosomal pathways. J Cell Biol *146*, 345-359.

Manders, E. M., Stap, J., Brakenhoff, G. J., van Driel, R., and Aten, J. A. (1992). Dynamics of three-dimensional replication patterns during the S-phase, analysed by double labelling of DNA and confocal microscopy. J Cell Sci *103 (Pt 3)*, 857-862.

Marcus, J., and Popko, B. (2002). Galactolipids are molecular determinants of myelin development and axo-glial organization. Biochim Biophys Acta *1573*, 406-413.

Massague, J., Blain, S. W., and Lo, R. S. (2000). TGFbeta signalling in growth control, cancer, and heritable disorders. Cell *103*, 295-309.

Massague, J., Cheifetz, S., Ignotz, R. A., and Boyd, F. T. (1987). Multiple type-beta transforming growth factors and their receptors. J Cell Physiol Suppl *Suppl 5*, 43-47.

Massague, J., and Wotton, D. (2000). Transcriptional control by the TGF-beta/Smad signalling system. Embo J *19*, 1745-1754.

Mayor, S., and Pagano, R. E. (2007). Pathways of clathrin-independent endocytosis. Nat Rev Mol Cell Biol *8*, 603-612.

Mayor, S., and Riezman, H. (2004). Sorting GPI-anchored proteins. Nat Rev Mol Cell Biol *5*, 110-120.

Mayor, S., Sabharanjak, S., and Maxfield, F. R. (1998). Cholesterol-dependent retention of GPI-anchored proteins in endosomes. Embo J *17*, 4626-4638.

McDonald, N. Q., and Hendrickson, W. A. (1993). A structural superfamily of growth factors containing a cystine knot motif. Cell *73*, 421-424.

McDowell, N., and Gurdon, J. B. (1999). Activin as a morphogen in Xenopus mesoderm induction. Semin Cell Dev Biol *10*, 311-317.

Mellman, I., and Steinman, R. M. (2001). Dendritic cells: specialized and regulated antigen processing machines. Cell *106*, 255-258.

Mesnard, D., Guzman-Ayala, M., and Constam, D. B. (2006). Nodal specifies embryonic visceral endoderm and sustains pluripotent cells in the epiblast before overt axial patterning. Development *133*, 2497-2505.

Miaczynska, M., Christoforidis, S., Giner, A., Shevchenko, A., Uttenweiler-Joseph, S., Habermann, B., Wilm, M., Parton, R. G., and Zerial, M. (2004). APPL proteins link Rab5 to nuclear signal transduction via an endosomal compartment. Cell *116*, 445-456.

Miaczynska, M., and Zerial, M. (2002). Mosaic organization of the endocytic pathway. Exp Cell Res *272*, 8-14.

Micchelli, C. A., The, I., Selva, E., Mogila, V., and Perrimon, N. (2002). Rasp, a putative transmembrane acyltransferase, is required for Hedgehog signalling. Development *129*, 843-851.

Miller, E., Antonny, B., Hamamoto, S., and Schekman, R. (2002). Cargo selection into COPII vesicles is driven by the Sec24p subunit. Embo J *21*, 6105-6113.

Minchiotti, G., Manco, G., Parisi, S., Lago, C. T., Rosa, F., and Persico, M. G. (2001). Structure-function analysis of the EGF-CFC family member Cripto identifies residues essential for nodal signalling. Development *128*, 4501-4510.

Minchiotti, G., Parisi, S., Liguori, G., Signore, M., Lania, G., Adamson, E. D., Lago, C. T., and Persico, M. G. (2000). Membrane-anchorage of Cripto protein by glycosylphosphatidylinositol and its distribution during early mouse development. Mech Dev *90*, 133-142.

Miura, S., Takeshita, T., Asao, H., Kimura, Y., Murata, K., Sasaki, Y., Hanai, J. I., Beppu, H., Tsukazaki, T., Wrana, J. L.*, et al.* (2000). Hgs (Hrs), a FYVE domain protein, is involved in Smad signalling through cooperation with SARA. Mol Cell Biol *20*, 9346-9355.

112

Miyazawa, K., Shinozaki, M., Hara, T., Furuya, T., and Miyazono, K. (2002). Two major Smad pathways in TGF-beta superfamily signalling. Genes Cells *7*, 1191-1204.

Miyazono, K., ten Dijke, P., and Heldin, C. H. (2000). TGF-beta signalling by Smad proteins. Adv Immunol *75*, 115-157.

Molloy, S. S., Thomas, L., VanSlyke, J. K., Stenberg, P. E., and Thomas, G. (1994). Intracellular trafficking and activation of the furin proprotein convertase: localization to the TGN and recycling from the cell surface. Embo J *13*, 18-33.

Morkel, M., Huelsken, J., Wakamiya, M., Ding, J., van de Wetering, M., Clevers, H., Taketo, M. M., Behringer, R. R., Shen, M. M., and Birchmeier, W. (2003). Beta-catenin regulates Cripto- and Wnt3-dependent gene expression programs in mouse axis and mesoderm formation. Development *130*, 6283-6294.

Morrow, I. C., Rea, S., Martin, S., Prior, I. A., Prohaska, R., Hancock, J. F., James, D. E., and Parton, R. G. (2002). Flotillin-1/reggie-2 traffics to surface raft domains via a novel golgi-independent pathway. Identification of a novel membrane targeting domain and a role for palmitoylation. J Biol Chem *277*, 48834-48841.

Mukherjee, S., and Maxfield, F. R. (2000). Role of membrane organization and membrane domains in endocytic lipid trafficking. Traffic *1*, 203-211.

Mullor, J. L., and Ruiz i Altaba, A. (2002). Growth, hedgehog and the price of GAS. Bioessays *24*, 22-26.

Muniz, M., Morsomme, P., and Riezman, H. (2001). Protein sorting upon exit from the endoplasmic reticulum. Cell *104*, 313-320.

Nabi, I. R., and Le, P. U. (2003). Caveolae/raft-dependent endocytosis. J Cell Biol *161*, 673-677.

Nakato, H., Futch, T. A., and Selleck, S. B. (1995). The division abnormally delayed (dally) gene: a putative integral membrane proteoglycan required for cell division patterning during postembryonic development of the nervous system in Drosophila. Development *121*, 3687-3702.

Naslavsky, N., Weigert, R., and Donaldson, J. G. (2003). Convergence of non-clathrin- and clathrin-derived endosomes involves Arf6 inactivation and changes in phosphoinositides. Mol Biol Cell *14*, 417-431.

Naslavsky, N., Weigert, R., and Donaldson, J. G. (2004). Characterization of a nonclathrin endocytic pathway: membrane cargo and lipid requirements. Mol Biol Cell *15*, 3542-3552.

Nebenfuhr, A., Ritzenthaler, C., and Robinson, D. G. (2002). Brefeldin A: deciphering an enigmatic inhibitor of secretion. Plant Physiol *130*, 1102-1108.

Neptune, E. R., Frischmeyer, P. A., Arking, D. E., Myers, L., Bunton, T. E., Gayraud, B., Ramirez, F., Sakai, L. Y., and Dietz, H. C. (2003). Dysregulation of TGF-beta activation contributes to pathogenesis in Marfan syndrome. Nat Genet *33*, 407-411.

Nichols, B. (2003). Caveosomes and endocytosis of lipid rafts. J Cell Sci *116*, 4707-4714.

Nohe, A., Keating, E., Fivaz, M., van der Goot, F. G., and Petersen, N. O. (2006). Dynamics of GPI-anchored proteins on the surface of living cells. Nanomedicine *2*, 1-7.

Normanno, N., De Luca, A., Bianco, C., Maiello, M. R., Carriero, M. V., Rehman, A., Wechselberger, C., Arra, C., Strizzi, L., Sanicola, M., and Salomon, D. S. (2004). Cripto-1 overexpression leads to

enhanced invasiveness and resistance to anoikis in human MCF-7 breast cancer cells. J Cell Physiol *198*, 31-39.

Norris, D. P., Brennan, J., Bikoff, E. K., and Robertson, E. J. (2002). The Foxh1-dependent autoregulatory enhancer controls the level of Nodal signals in the mouse embryo. Development *129*, 3455-3468.

Nybakken, K., and Perrimon, N. (2002). Heparan sulfate proteoglycan modulation of developmental signalling in Drosophila. Biochim Biophys Acta *1573*, 280-291.

Ohkawara, B., Yamamoto, T. S., Tada, M., and Ueno, N. (2003). Role of glypican 4 in the regulation of convergent extension movements during gastrulation in Xenopus laevis. Development *130*, 2129-2138.

Oki, S., Hashimoto, R., Okui, Y., Shen, M. M., Mekada, E., Otani, H., Saijoh, Y., and Hamada, H. (2007). Sulfated glycosaminoglycans are necessary for Nodal signal transmission from the node to the left lateral plate in the mouse embryo. Development *134*, 3893-3904.

Padgett, R. W., St Johnston, R. D., and Gelbart, W. M. (1987). A transcript from a Drosophila pattern gene predicts a protein homologous to the transforming growth factor-beta family. Nature *325*, 81-84.

Panakova, D., Sprong, H., Marois, E., Thiele, C., and Eaton, S. (2005). Lipoprotein particles are required for Hedgehog and Wingless signalling. Nature *435*, 58-65.

Panopoulou, E., Gillooly, D. J., Wrana, J. L., Zerial, M., Stenmark, H., Murphy, C., and Fotsis, T. (2002). Early endosomal regulation of Smad-dependent signalling in endothelial cells. J Biol Chem *277*, 18046-18052.

Papaioannou, V. E. (1982). Lineage analysis of inner cell mass and trophectoderm using microsurgically reconstituted mouse blastocysts. J Embryol Exp Morphol *68*, 199-209.

Parisi, S., D'Andrea, D., Lago, C. T., Adamson, E. D., Persico, M. G., and Minchiotti, G. (2003). Nodal-dependent Cripto signalling promotes cardiomyogenesis and redirects the neural fate of embryonic stem cells. J Cell Biol *163*, 303-314.

Parton, R. G. (1996). Caveolae and caveolins. Curr Opin Cell Biol *8*, 542-548.

Parton, R. G. (2003). Caveolae--from ultrastructure to molecular mechanisms. Nat Rev Mol Cell Biol *4*, 162-167.

Pearse, B. M., Smith, C. J., and Owen, D. J. (2000). Clathrin coat construction in endocytosis. Curr Opin Struct Biol *10*, 220-228.

Pedersen, R. A., and Spindle, A. I. (1980). Role of the blastocoele microenvironment in early mouse embryo differentiation. Nature *284*, 550-552.

Pelkmans, L., Burli, T., Zerial, M., and Helenius, A. (2004). Caveolin-stabilized membrane domains as multifunctional transport and sorting devices in endocytic membrane traffic. Cell *118*, 767-780.

Pelkmans, L., and Helenius, A. (2002). Endocytosis via caveolae. Traffic *3*, 311-320.

Pelkmans, L., Kartenbeck, J., and Helenius, A. (2001). Caveolar endocytosis of simian virus 40 reveals a new two-step vesicular-transport pathway to the ER. Nat Cell Biol *3*, 473-483.

Pelton, T. A., Bettess, M. D., Lake, J., Rathjen, J., and Rathjen, P. D. (1998). Developmental complexity of early mammalian pluripotent cell populations in vivo and in vitro. Reprod Fertil Dev *10*, 535-549.

Penheiter, S. G., Mitchell, H., Garamszegi, N., Edens, M., Dore, J. J., Jr., and Leof, E. B. (2002). Internalization-dependent and -independent requirements for transforming growth factor beta receptor signalling via the Smad pathway. Mol Cell Biol *22*, 4750-4759.

Perea-Gomez, A., Rhinn, M., and Ang, S. L. (2001). Role of the anterior visceral endoderm in restricting posterior signals in the mouse embryo. Int J Dev Biol *45*, 311-320.

Persico, M. G., Liguori, G. L., Parisi, S., D'Andrea, D., Salomon, D. S., and Minchiotti, G. (2001). Cripto in tumors and embryo development. Biochim Biophys Acta *1552*, 87-93.

Piccolo, S., Agius, E., Leyns, L., Bhattacharyya, S., Grunz, H., Bouwmeester, T., and De Robertis, E. M. (1999). The head inducer Cerberus is a multifunctional antagonist of Nodal, BMP and Wnt signals. Nature *397*, 707-710.

Pickart, C. M. (2001). Mechanisms underlying ubiquitination. Annu Rev Biochem *70*, 503-533.

Pratt, H. P., Ziomek, C. A., Reeve, W. J., and Johnson, M. H. (1982). Compaction of the mouse embryo: an analysis of its components. J Embryol Exp Morphol *70*, 113-132.

Puri, V., Watanabe, R., Dominguez, M., Sun, X., Wheatley, C. L., Marks, D. L., and Pagano, R. E. (1999). Cholesterol modulates membrane traffic along the endocytic pathway in sphingolipid-storage diseases. Nat Cell Biol *1*, 386-388.

Raftery, L. A., and Sutherland, D. J. (1999). TGF-beta family signal transduction in Drosophila development: from Mad to Smads. Dev Biol *210*, 251-268.

Raiborg, C., Bremnes, B., Mehlum, A., Gillooly, D. J., D'Arrigo, A., Stang, E., and Stenmark, H. (2001). FYVE and coiled-coil domains determine the specific localisation of Hrs to early endosomes. J Cell Sci *114*, 2255-2263.

Raiborg, C., Rusten, T. E., and Stenmark, H. (2003). Protein sorting into multivesicular endosomes. Curr Opin Cell Biol *15*, 446-455.

Raiborg, C., and Stenmark, H. (2002). Hrs and endocytic sorting of ubiquitinated membrane proteins. Cell Struct Funct *27*, 403-408.

Rajendran, L., and Simons, K. (2005). Lipid rafts and membrane dynamics. J Cell Sci *118*, 1099-1102.

Ramis, J. M., Collart, C., and Smith, J. C. (2007). Xnrs and activin regulate distinct genes during xenopus development: activin regulates cell division. PLoS ONE *2*, e213.

Razani, B., Engelman, J. A., Wang, X. B., Schubert, W., Zhang, X. L., Marks, C. B., Macaluso, F., Russell, R. G., Li, M., Pestell, R. G., *et al.* (2001a). Caveolin-1 null mice are viable but show evidence of hyperproliferative and vascular abnormalities. J Biol Chem *276*, 38121-38138.

Razani, B., Schlegel, A., Liu, J., and Lisanti, M. P. (2001b). Caveolin-1, a putative tumour suppressor gene. Biochem Soc Trans *29*, 494-499.

Razani, B., Woodman, S. E., and Lisanti, M. P. (2002). Caveolae: from cell biology to animal physiology. Pharmacol Rev *54*, 431-467.

Reissmann, E., Jornvall, H., Blokzijl, A., Andersson, O., Chang, C., Minchiotti, G., Persico, M. G., Ibanez, C. F., and Brivanlou, A. H. (2001). The orphan receptor ALK7 and the Activin receptor ALK4 mediate signalling by Nodal proteins during vertebrate development. Genes Dev *15*, 2010-2022.

Renkonen, O., Kaarainen, L., Simons, K., and Gahmberg, C. G. (1971). The lipid class composition of Semliki forest virus and plasma membranes of the host cells. Virology *46*, 318-326.

Ridley, A. J. (2006). Rho GTPases and actin dynamics in membrane protrusions and vesicle trafficking. Trends Cell Biol *16*, 522-529.

Risbridger, G. P., Schmitt, J. F., and Robertson, D. M. (2001). Activins and inhibins in endocrine and other tumors. Endocr Rev *22*, 836-858.

Robinson, M. S. (2004). Adaptable adaptors for coated vesicles. Trends Cell Biol *14*, 167-174.

Sabharanjak, S., Sharma, P., Parton, R. G., and Mayor, S. (2002). GPI-anchored proteins are delivered to recycling endosomes via a distinct cdc42-regulated, clathrin-independent pinocytic pathway. Dev Cell *2*, 411-423.

Saijoh, Y., Oki, S., Tanaka, C., Nakamura, T., Adachi, H., Yan, Y. T., Shen, M. M., and Hamada, H. (2005). Two nodal-responsive enhancers control left-right asymmetric expression of Nodal. Dev Dyn *232*, 1031-1036.

Sakuma, R., Ohnishi Yi, Y., Meno, C., Fujii, H., Juan, H., Takeuchi, J., Ogura, T., Li, E., Miyazono, K., and Hamada, H. (2002). Inhibition of Nodal signalling by Lefty mediated through interaction with common receptors and efficient diffusion. Genes Cells *7*, 401-412.

Sallusto, F., Cella, M., Danieli, C., and Lanzavecchia, A. (1995). Dendritic cells use macropinocytosis and the mannose receptor to concentrate macromolecules in the major histocompatibility complex class II compartment: downregulation by cytokines and bacterial products. J Exp Med *182*, 389-400.

Saloman, D. S., Bianco, C., Ebert, A. D., Khan, N. I., De Santis, M., Normanno, N., Wechselberger, C., Seno, M., Williams, K., Sanicola, M.*, et al.* (2000). The EGF-CFC family: novel epidermal growth factor-related proteins in development and cancer. Endocr Relat Cancer *7*, 199-226.

Salomon, D. S., Bianco, C., and De Santis, M. (1999). Cripto: a novel epidermal growth factor (EGF)-related peptide in mammary gland development and neoplasia. Bioessays *21*, 61-70.

Salzer, J. L., Lovejoy, L., Linder, M. C., and Rosen, C. (1998). Ran-2, a glial lineage marker, is a GPI-anchored form of ceruloplasmin. J Neurosci Res *54*, 147-157.

Satow, R., Kurisaki, A., Chan, T. C., Hamazaki, T. S., and Asashima, M. (2006). Dullard promotes degradation and dephosphorylation of BMP receptors and is required for neural induction. Dev Cell *11*, 763-774.

Schapiro, F. B., Soe, T. T., Mallet, W. G., and Maxfield, F. R. (2004). Role of cytoplasmic domain serines in intracellular trafficking of furin. Mol Biol Cell *15*, 2884-2894.

Schier, A. F. (2003). Nodal signalling in vertebrate development. Annu Rev Cell Dev Biol *19*, 589-621.

Schier, A. F., and Shen, M. M. (2000). Nodal signalling in vertebrate development. Nature *403*, 385-389.

Schiffer, S. G., Foley, S., Kaffashan, A., Hronowski, X., Zichittella, A. E., Yeo, C. Y., Miatkowski, K., Adkins, H. B., Damon, B., Whitman, M., *et al.* (2001). Fucosylation of Cripto is required for its ability to facilitate nodal signalling. J Biol Chem *276*, 37769-37778.

Schlunegger, M. P., and Grutter, M. G. (1992). An unusual feature revealed by the crystal structure at 2.2 A resolution of human transforming growth factor-beta 2. Nature *358*, 430-434.

Schmid, S. L. (1997). Clathrin-coated vesicle formation and protein sorting: an integrated process. Annu Rev Biochem *66*, 511-548.

Schmierer, B., and Hill, C. S. (2007). TGFbeta-SMAD signal transduction: molecular specificity and functional flexibility. Nat Rev Mol Cell Biol *8*, 970-982.

Schuck, S., Honsho, M., Ekroos, K., Shevchenko, A., and Simons, K. (2003). Resistance of cell membranes to different detergents. Proc Natl Acad Sci U S A *100*, 5795-5800.

Schuck, S., and Simons, K. (2004). Polarized sorting in epithelial cells: raft clustering and the biogenesis of the apical membrane. J Cell Sci *117*, 5955-5964.

Searle, R. F., Sellens, M. H., Elson, J., Jenkinson, E. J., and Billington, W. D. (1976). Detection of alloantigens during preimplantation development and early trophoblast differentiation in the mouse by immunoperoxidase labeling. J Exp Med *143*, 348-359.

Shao, Y., Akmentin, W., Toledo-Aral, J. J., Rosenbaum, J., Valdez, G., Cabot, J. B., Hilbush, B. S., and Halegoua, S. (2002). Pincher, a pinocytic chaperone for nerve growth factor/TrkA signalling endosomes. J Cell Biol *157*, 679-691.

Shen, M. M. (2007). Nodal signalling: developmental roles and regulation. Development *134*, 1023-1034.

Shen, M. M., Wang, H., and Leder, P. (1997). A differential display strategy identifies Cryptic, a novel EGF-related gene expressed in the axial and lateral mesoderm during mouse gastrulation. Development *124*, 429-442.

Shi, S., Ge, C., Luo, Y., Hou, X., Haltiwanger, R. S., and Stanley, P. (2007). The threonine that carries fucose, but not fucose, is required for Cripto to facilitate Nodal signalling. J Biol Chem *282*, 20133-20141.

Shi, W., Sun, C., He, B., Xiong, W., Shi, X., Yao, D., and Cao, X. (2004). GADD34-PP1c recruited by Smad7 dephosphorylates TGFbeta type I receptor. J Cell Biol *164*, 291-300.

Shi, Y., and Massague, J. (2003). Mechanisms of TGF-beta signalling from cell membrane to the nucleus. Cell *113*, 685-700.

Shim, J. H., Xiao, C., Hayden, M. S., Lee, K. Y., Trombetta, E. S., Pypaert, M., Nara, A., Yoshimori, T., Wilm, B., Erdjument-Bromage, H., *et al.* (2006). CHMP5 is essential for late endosome function and down-regulation of receptor signalling during mouse embryogenesis. J Cell Biol *172*, 1045-1056.

Sigismund, S., Woelk, T., Puri, C., Maspero, E., Tacchetti, C., Transidico, P., Di Fiore, P. P., and Polo, S. (2005). Clathrin-independent endocytosis of ubiquitinated cargos. Proc Natl Acad Sci U S A *102*, 2760-2765.

Simons, K., and Ikonen, E. (1997). Functional rafts in cell membranes. Nature *387*, 569-572.

Simons, K., and Toomre, D. (2000). Lipid rafts and signal transduction. Nat Rev Mol Cell Biol *1*, 31-39.

Simons, K., and van Meer, G. (1988). Lipid sorting in epithelial cells. Biochemistry *27*, 6197-6202.

Sinha, S., Nevett, C., Shuttleworth, C. A., and Kielty, C. M. (1998). Cellular and extracellular biology of the latent transforming growth factor-beta binding proteins. Matrix Biol *17*, 529-545.

Slot, J. W., and Geuze, H. J. (2007). Cryosectioning and immunolabeling. Nat Protoc *2*, 2480-2491.

Smart, E. J., Graf, G. A., McNiven, M. A., Sessa, W. C., Engelman, J. A., Scherer, P. E., Okamoto, T., and Lisanti, M. P. (1999). Caveolins, liquid-ordered domains, and signal transduction. Mol Cell Biol *19*, 7289-7304.

Srinivas, S., Rodriguez, T., Clements, M., Smith, J. C., and Beddington, R. S. (2004). Active cell migration drives the unilateral movements of the anterior visceral endoderm. Development *131*, 1157-1164.

Strizzi, L., Bianco, C., Normanno, N., Seno, M., Wechselberger, C., Wallace-Jones, B., Khan, N. I., Hirota, M., Sun, Y., Sanicola, M., and Salomon, D. S. (2004). Epithelial mesenchymal transition is a characteristic of hyperplasias and tumors in mammary gland from MMTV-Cripto-1 transgenic mice. J Cell Physiol *201*, 266-276.

Sun, P. D., and Davies, D. R. (1995). The cystine-knot growth-factor superfamily. Annu Rev Biophys Biomol Struct *24*, 269-291.

Takahashi, S., Nakagawa, T., Kasai, K., Banno, T., Duguay, S. J., Van de Ven, W. J., Murakami, K., and Nakayama, K. (1995). A second mutant allele of furin in the processing-incompetent cell line, LoVo. Evidence for involvement of the homo B domain in autocatalytic activation. J Biol Chem *270*, 26565-26569.

Tam, P. P., and Beddington, R. S. (1987). The formation of mesodermal tissues in the mouse embryo during gastrulation and early organogenesis. Development *99*, 109-126.

Tam, P. P., and Loebel, D. A. (2007). Gene function in mouse embryogenesis: get set for gastrulation. Nat Rev Genet *8*, 368-381.

Tam, P. P., Steiner, K. A., Zhou, S. X., and Quinlan, G. A. (1997). Lineage and functional analyses of the mouse organizer. Cold Spring Harb Symp Quant Biol *62*, 135-144.

Tansey, M. G., Baloh, R. H., Milbrandt, J., and Johnson, E. M., Jr. (2000). GFRalpha-mediated localization of RET to lipid rafts is required for effective downstream signalling, differentiation, and neuronal survival. Neuron *25*, 611-623.

Tao, Q., Yokota, C., Puck, H., Kofron, M., Birsoy, B., Yan, D., Asashima, M., Wylie, C. C., Lin, X., and Heasman, J. (2005). Maternal wnt11 activates the canonical wnt signalling pathway required for axis formation in Xenopus embryos. Cell *120*, 857-871.

ten Dijke, P., Miyazono, K., and Heldin, C. H. (1996). Signalling via hetero-oligomeric complexes of type I and type II serine/threonine kinase receptors. Curr Opin Cell Biol *8*, 139-145.

Thiery, J. P., and Sleeman, J. P. (2006). Complex networks orchestrate epithelial-mesenchymal transitions. Nat Rev Mol Cell Biol *7*, 131-142.

Thomas, G. (2002). Furin at the cutting edge: from protein traffic to embryogenesis and disease. Nat Rev Mol Cell Biol *3*, 753-766.

Thomas, P., and Beddington, R. (1996). Anterior primitive endoderm may be responsible for patterning the anterior neural plate in the mouse embryo. Curr Biol *6*, 1487-1496.

Tooze, S. A., and Huttner, W. B. (1990). Cell-free protein sorting to the regulated and constitutive secretory pathways. Cell *60*, 837-847.

Topczewska, J. M., Postovit, L. M., Margaryan, N. V., Sam, A., Hess, A. R., Wheaton, W. W., Nickoloff, B. J., Topczewski, J., and Hendrix, M. J. (2006). Embryonic and tumorigenic pathways converge via Nodal signalling: role in melanoma aggressiveness. Nat Med *12*, 925-932.

Tsuda, M., Kamimura, K., Nakato, H., Archer, M., Staatz, W., Fox, B., Humphrey, M., Olson, S., Futch, T., Kaluza, V., *et al.* (1999). The cell-surface proteoglycan Dally regulates Wingless signalling in Drosophila. Nature *400*, 276-280.

Tsukazaki, T., Chiang, T. A., Davison, A. F., Attisano, L., and Wrana, J. L. (1998). SARA, a FYVE domain protein that recruits Smad2 to the TGFbeta receptor. Cell *95*, 779-791.

Tsukita, S., Furuse, M., and Itoh, M. (2001). Multifunctional strands in tight junctions. Nat Rev Mol Cell Biol *2*, 285-293.

Udenfriend, S., and Kodukula, K. (1995). How glycosylphosphatidylinositol-anchored membrane proteins are made. Annu Rev Biochem *64*, 563-591.

Valdez, G., Akmentin, W., Philippidou, P., Kuruvilla, R., Ginty, D. D., and Halegoua, S. (2005). Pincher-mediated macroendocytosis underlies retrograde signalling by neurotrophin receptors. J Neurosci *25*, 5236-5247.

Valdez, G., Philippidou, P., Rosenbaum, J., Akmentin, W., Shao, Y., and Halegoua, S. (2007). Trk-signalling endosomes are generated by Rac-dependent macroendocytosis. Proc Natl Acad Sci U S A *104*, 12270-12275.

Vallier, L., Reynolds, D., and Pedersen, R. A. (2004). Nodal inhibits differentiation of human embryonic stem cells along the neuroectodermal default pathway. Dev Biol *275*, 403-421.

van der Goot, F. G., and Gruenberg, J. (2006). Intra-endosomal membrane traffic. Trends Cell Biol *16*, 514-521.

van der Goot, F. G., and Harder, T. (2001). Raft membrane domains: from a liquid-ordered membrane phase to a site of pathogen attack. Semin Immunol *13*, 89-97.

van der Sluijs, P., Hull, M., Webster, P., Male, P., Goud, B., and Mellman, I. (1992). The small GTP-binding protein rab4 controls an early sorting event on the endocytic pathway. Cell *70*, 729-740.

Varlet, I., Collignon, J., and Robertson, E. J. (1997). nodal expression in the primitive endoderm is required for specification of the anterior axis during mouse gastrulation. Development *124*, 1033-1044.

Varma, R., and Mayor, S. (1998). GPI-anchored proteins are organized in submicron domains at the cell surface. Nature *394*, 798-801.

Varsano, T., Dong, M. Q., Niesman, I., Gacula, H., Lou, X., Ma, T., Testa, J. R., Yates, J. R., 3rd, and Farquhar, M. G. (2006). GIPC is recruited by APPL to peripheral TrkA endosomes and regulates TrkA trafficking and signalling. Mol Cell Biol *26*, 8942-8952.

Vey, M., Schafer, W., Berghofer, S., Klenk, H. D., and Garten, W. (1994). Maturation of the trans-Golgi network protease furin: compartmentalization of propeptide removal, substrate cleavage, and COOH-terminal truncation. J Cell Biol *127*, 1829-1842.

Viola, A., Schroeder, S., Sakakibara, Y., and Lanzavecchia, A. (1999). T lymphocyte costimulation mediated by reorganization of membrane microdomains. Science *283*, 680-682.

Vogel, U., Sandvig, K., and van Deurs, B. (1998). Expression of caveolin-1 and polarized formation of invaginated caveolae in Caco-2 and MDCK II cells. J Cell Sci *111 (Pt 6)*, 825-832.

Volonte, D., Galbiati, F., Li, S., Nishiyama, K., Okamoto, T., and Lisanti, M. P. (1999). Flotillins/cavatellins are differentially expressed in cells and tissues and form a hetero-oligomeric complex with caveolins in vivo. Characterization and epitope-mapping of a novel flotillin-1 monoclonal antibody probe. J Biol Chem *274*, 12702-12709.

Wakefield, L. M., and Roberts, A. B. (2002). TGF-beta signalling: positive and negative effects on tumorigenesis. Curr Opin Genet Dev *12*, 22-29.

Wang, H., and Tsang, B. K. (2007). Nodal signalling and apoptosis. Reproduction *133*, 847-853.

Warga, R. M., and Kane, D. A. (2003). One-eyed pinhead regulates cell motility independent of Squint/Cyclops signalling. Dev Biol *261*, 391-411.

Watanabe, K., Hamada, S., Bianco, C., Mancino, M., Nagaoka, T., Gonzales, M., Bailly, V., Strizzi, L., and Salomon, D. S. (2007). Requirement of glycosylphosphatidylinositol anchor of cripto-1 for 'trans' activity as a nodal co-receptor. J Biol Chem.

White, I. J., Bailey, L. M., Aghakhani, M. R., Moss, S. E., and Futter, C. E. (2006). EGF stimulates annexin 1-dependent inward vesiculation in a multivesicular endosome subpopulation. Embo J *25*, 1-12.

Willert, K., Brown, J. D., Danenberg, E., Duncan, A. W., Weissman, I. L., Reya, T., Yates, J. R., 3rd, and Nusse, R. (2003). Wnt proteins are lipid-modified and can act as stem cell growth factors. Nature *423*, 448-452.

Williams, P. H., Hagemann, A., Gonzalez-Gaitan, M., and Smith, J. C. (2004). Visualizing long-range movement of the morphogen Xnr2 in the Xenopus embryo. Curr Biol *14*, 1916-1923.

Williams, R. L., and Urbe, S. (2007). The emerging shape of the ESCRT machinery. Nat Rev Mol Cell Biol *8*, 355-368.

Wozney, J. M., Rosen, V., Celeste, A. J., Mitsock, L. M., Whitters, M. J., Kriz, R. W., Hewick, R. M., and Wang, E. A. (1988). Novel regulators of bone formation: molecular clones and activities. Science *242*, 1528-1534.

Wrana, J. L., Attisano, L., Wieser, R., Ventura, F., and Massague, J. (1994). Mechanism of activation of the TGF-beta receptor. Nature *370*, 341-347.

Xu, C., Liguori, G., Persico, M. G., and Adamson, E. D. (1999). Abrogation of the Cripto gene in mouse leads to failure of postgastrulation morphogenesis and lack of differentiation of cardiomyocytes. Development *126*, 483-494.

Yan, Y. T., Gritsman, K., Ding, J., Burdine, R. D., Corrales, J. D., Price, S. M., Talbot, W. S., Schier, A. F., and Shen, M. M. (1999). Conserved requirement for EGF-CFC genes in vertebrate left-right axis formation. Genes Dev *13*, 2527-2537.

Yan, Y. T., Liu, J. J., Luo, Y., E, C., Haltiwanger, R. S., Abate-Shen, C., and Shen, M. M. (2002). Dual roles of Cripto as a ligand and coreceptor in the nodal signalling pathway. Mol Cell Biol *22*, 4439-4449.

Ye, H., Kuruvilla, R., Zweifel, L. S., and Ginty, D. D. (2003). Evidence in support of signalling endosome-based retrograde survival of sympathetic neurons. Neuron *39*, 57-68.

Yeo, C.-Y., and Whitman, M. (2001a). Nodal Signals to Smads through Cripto-Dependent and Cripto-Independent Mechanisms. Mol Cell *7*, 949-957.

Yeo, C., and Whitman, M. (2001b). Nodal signals to Smads through Cripto-dependent and Cripto-independent mechanisms. Mol Cell *7*, 949-957.

Yu, J. K., Holland, L. Z., and Holland, N. D. (2002). An amphioxus nodal gene (AmphiNodal) with early symmetrical expression in the organizer and mesoderm and later asymmetrical expression associated with left-right axis formation. Evol Dev *4*, 418-425.

Zerial, M., and McBride, H. (2001). Rab proteins as membrane organizers. Nat Rev Mol Cell Biol *2*, 107-117.

Zernicka-Goetz, M. (2002). Patterning of the embryo: the first spatial decisions in the life of a mouse. Development *129*, 815-829.

Zhang, J., Talbot, W. S., and Schier, A. F. (1998). Positional cloning identifies zebrafish one-eyed pinhead as a permissive EGF-related ligand required during gastrulation. Cell *92*, 241-251.

Zhou, X., Sasaki, H., Lowe, L., Hogan, B. L., and Kuehn, M. R. (1993). Nodal is a novel TGF-beta-like gene expressed in the mouse node during gastrulation. Nature *361*, 543-547.